Seasonality in Zebrafish

Jessica Olsen

Thesis submitted for the
degree of Doctor of Philosophy (Ph.D.)

Cell and Developmental Biology
Division of Biosciences
University College London

I, Jessica Olsen, confirm that the work presented in this thesis is my own. Where information has been derived from other sources, I confirm that this has been indicated in the thesis.

ACKNOWLEDGEMENTS

I would like to thank a number of supporters who have helped with much needed guidance throughout the life of this project.

Academic support has been provided by my primary thesis supervisor, Professor David Whitmore, whose efforts have been instrumental in getting this work over the finish line. I am extremely grateful to Dr. Elodie Peyric for her extended supervision both during the experimental stages of the project and the writing of this thesis. Her skills and help have been invaluable.

Thanks also go out to the other members of the Whitmore lab (2006-2010), including Veronica Ferrer, Lucy Young, Peter Cormie, Helen Moore, Andrew Beale, and Catherine Cox, who all worked with me on the bench and in the office.

Additional guidance was provided by our departmental central lab manager, Mary Rahman, and consumables and deliveries organized by Ian Blaney and his team in the CDB stores office.

The work done to support this thesis was generously funded by the BBSRC.

Finally, thanks to my friends, co-workers and colleagues, most especially Kepmen Lee, for his incredible patience and optimism over the course of this project.

ABSTRACT

Annual rhythms of seasonal daylength act as powerful cues for seasonal fertility and physiology. As seasonal daylength changes, nocturnal melatonin secretion is altered, providing the organism an internal representation of daylength through melatonin exposure and duration. Melatonin has been linked with various neuroendocrine and gonadal changes. By altering external light/dark phase durations I expected an increase in zebrafish growth and fertility, mediated by changes in the hypothalamic-pituitary-gonad axis. These results confirm zebrafish photoperiodic responsively through physiological measures of growth and reproduction, neural gene expression in the hypothalamus and pituitary, and circadian gene expression profiles from clonal cells and tissue explants.

Long-term entrainment of adult zebrafish to long day (16h/8h light dark) photoperiods stimulated growth (length and weight), while short day (8h/16h light dark) groups had delayed and inhibited growth rates throughout life. Long day entrainment increased gonadal weight in females only, while male testis showed no response to photoperiod differences. Zebrafish fecundity and fertility were stimulated by long day entrainment, coupled with dramatic inhibition of spawning immediately after exposure to short day conditions.

Neuroendocrine targets showed a number of tissue and subtype specific differences in circadian and photoperiodic expression, including a 3-fold increase in melatonin receptor expression in the zebrafish pituitary over the hypothalamus, with circadian expression of melatonin receptor 1 and photoperiodic modulation of melatonin receptor 2, a pattern repeated in the circadian expression of hypothalamic diodinases enzyme Dio2 and the seasonal expression of Dio3.

Zebrafish cells, tissues contain functional circadian clocks and are directly light responsive. Using transgenic clonal cell lines (Per1:luc and Cry1a:luc) and tissues (Per3:luc) the effect of light duration vs. pulse entrainment was monitored *in vitro* using skeleton photoperiod exposure. In all cases, circadian gene expression entrained to the first light pulse after the longest period of darkness, regardless of

the time or phase of the exposure, thus selectively oscillating to the shortest daylength. Per3 expression in the hypothalamus showed a direct light responsive profile, not seen in pituitary or pineal tissue explants. The current work presents novel physiological, endocrine and cellular evidence supporting the hypothesis that zebrafish are responsive to changes in seasonal photoperiods.

TABLE OF CONTENTS

LIST OF FIGURES

Chapter 1

Chapter 2

Chapter 3

Chapter 4

LIST OF ABBREVIATIONS

General

aaNAT	aralkylamine n-acetyltransferase
Dio1	iodothyronine deiodinase (type 1)
Dio2	iodothyronine deiodinase (type 2)
Dio3	iodothyronine deiodinase (type 3)
DNA	deoxyribonucleic acid
EC	External Coincidence Model of Photoperiodism
FSH	follicle stimulating hormone
GH	growth hormone
GHRH	growth hormone releasing hormone
cGnRH-II	gonadotrophin releasing hormone 2 – in ZF midbrain (chicken derived)
GnRH	gonadotrophin releasing hormone
sGnRH	gonadotrophin releasing hormone - in ZF hypothalamus (salmon derived)
HPG	hypothalamic-pituitary-gonadal axis (of reproductive physiology)
IC	Internal Coincidence Model of Photoperiodism
LD	long day photoperiod (16h/8h) light dark cycle
LDsk	long day skeleton photoperiod (2h-12h-2h/8h) light pulse cycle
LED	light emitting diode
LH	luteinizing hormone
MBH	medial basal hypothalamus
MT1	melatonin receptor (type 1)
MT2	melatonin receptor (type 2)
Mel 1c	melatonin receptor (type 3 – fish only)
mRNA	messenger ribonucleic acid
PD	pars distalis
PI	pars intermedia
PRL	prolactin hormone
PT	pars tuberalis
RNA	ribonucleic acid
SCN	suprachiasmatic nucleus (of hypothalamus)
SD	short day photoperiod (8h/16h) light dark cycle

SDsk	short day skeleton photoperiod (2h-6h-2h/12h) light pulse cycle
SEM	standard error of the mean (statistical measure)
T_3	triiodothyronine (low abundance form of thyroid hormone)
rT_3	reverse T_3 (triiodothyronine; inactive form)
T_4	thyroxine (high abundance form of thyroid hormone)
TH	thyroid hormone
TH-RH	thyroid hormone stimulating hormone
TSH	thyroid stimulating hormone
TSH	thyroid stimulating hormone (heterodimer)
Vtg	vitellogenin
ZT	zeitgeber time (ZT 0 defined as lights on)

Genes

Clk	clock gene (on the negative limb of the circadian clock)
Bmal	brain and muscle aryl hydrocarbon receptor nuclear translocator (ARNT)-like gene (positive limb of the circadian clock)
Cry1a	cryptochrome gene (cry; on the positive limb of the circadian clock)
Cry1a-luc	cryptochrome gene mutation with luciferase
Per	period gene (on the positive limb of the circadian clock)
Per-luc	period gene mutation with luciferase

LIST OF SPECIES NAMES

Betta splendens	Siamese fighting fish
Calendula officinalis	Marigolds
Carassius auratus	Goldfish
Catla catla	Indian carp
Coturnix japonica	Japanese Quail
Danio Rerio	Zebrafish
Dicentrarchus labrax	European Sea Bass
Drosophila pseudo-obscura	Fruit fly
Esox lucius	Pike
Gadus morhua	Atlantic Cod
Gasterosteus aculeatus	Stickleback
Glycine max	Soya Bean
Heteropneustes fossilis	Catfish
Ipomoea nil	Japanese Morning Glory
Megoura viciae	Green Vetch Aphid
Mesocricetus auratus	Syrian Hamster
Mimosa pudica	Mimosa
Mugil cephalus	Grey Mullet
Nicotiana tabacum	Tobacco
Oncorhynchus masou	Masu Salmon
Oncorhynchus mykiss	Rainbow Trout
Oreochromis aureus x Oreochromis niloticus	Tilapia (hybrid)
Oryzias latipes	Japanese Medaka
Ovis aries	Soay Sheep
Paralichthys oliaceus	Japanese Flounder
Passer domesticus	House Sparrow
Passer montanus	Tree Sparrow
Perca fluviatilis	Eurasian Perch
Phaseolus coccineus	Runner Bean
Phodopus sungorus	Siberian Hamster
Salmo salar	Atlantic Salmon
Siganus guttatus	Golden Rabbitfish
Sparus aurata	Sea Bream
Sturnus vulgaris	Starling

CHAPTER 1 – GENERAL INTRODUCTION

1.1 What is Photoperiodism?

Biological imperatives in a seasonal environment

Growing up on a rotating planet can be a tricky business. Most organisms have evolved in a dynamic environment where daily and seasonal changes are the norm. Due to the 23.43^{o} vertical tilt of the earth's axis, our annual planetary rotation around the sun leads to the cycle of seasons in an antiphasic relationship between the northern hemisphere and southern hemispheres (Bradshaw & Holzapfel, 2007).

In a seasonal environment, evolutionary fitness must include the ability to cope with these changing seasons, optimizing periods of fertility and growth with cycles of food and energy abundance. Organisms that reproduce too late in the autumn risk exposing their offspring to the extremes of winter weather and those that begin an early migration or become dormant too soon miss additional reproductive opportunities and resources (Bradshaw & Holzapfel, 2007). By synchronizing fertility to seasonal photoperiod (length of the daily light-dark cycle), organisms increase their reproductive success, ensuring their offspring develop during periods of optimal environmental conditions (Hazlerigg & Wagner, 2006). These seasonal changes must be endured and even exploited for animals to survive and thrive.

Most living things anticipate the predictable seasonal changes in the weather and behave accordingly. Some animals migrate thousands of kilometers to more moderate climates, others build up fat stores for dormancy, grow thick winter covers of fur or feathers, or simply lower their metabolic rates and wait for the return of the sun (Callaghan et al., 2004). Photoperiodism has been noted in organisms such as rotifers, annelids, mollusks, bony fish, frogs, turtles, lizards, birds, and mammals (Bradshaw & Holzapfel, 2007). In vertebrates, the light/dark cycle synchronizes numerous circadian rhythms such as locomotor activity, food intake, growth and reproductive states. Other factors, such as temperature, food

availability and salinity (in fish) also influence these rhythms, but were not tested in the current work (Koger et al., 1999). Examples of photoperiod-influenced physiological changes include annual cycles of coat color (pelage) change in Siberian and Syrian hamsters (*Phodopus sungorus* and *Mesocricetus auratus)* (Paul et al., 2007), the annual cycles of reproduction, molting, and migration in Tree Sparrows (*Passer montanus*) (Dixit & Singh, 2011), and rates of smoltification (movement from fresh to salt water) in Atlantic salmon (*Salmo salar*) (Bjornsson et al., 2000).

1.2 A role for the biological clock in photoperiodism

1.2.1 What is a circadian clock?

The self-sustained circadian (approximately 24-hours) rhythms regulating daily activities are often referred to as "the biological clock". Almost all organisms display circadian rhythms with similar basic properties – the rhythm is synchronized to environmental cues (predominantly light), is maintained in the absence of such cues, and is displayed in constant periodicity over a wide temperature range (Fukada, 2003).

In mammals the "master clock" controlling circadian rhythms is located in the small region of the hypothalamus called the superchiasmatic nucleus (SCN). Experiments have shown that the SCN transmits daily hormonal and electrical signals in keeping with the day/night cycle (Morris et al., 2012). For many years the SCN was considered the exclusive site for biological timekeeping in mammals. This was in contrast to several other vertebrates, where clocks were known to be present in peripheral tissues such as the pineal gland and eye (Granados-Fuentes & Herzog, 2013). Peripheral clocks have now been described in a number of mammalian and non-mammalian tissues including the oesophagus, lungs, liver, pancreas, spleen, thymus, and skin (Yamazaki et al., 2000). Work on zebrafish cells (*in vivo* and *in vitro*) suggests that the vertebrate circadian timing system may be highly distributed, with a majority of cells containing a clock (Whitmore et al., 1998a).

The genetic basis of circadian rhythms was established through the identification of mutant circadian patterns, and in the polymorphisms within clock genes themselves (Konopka & Benzer, 1971). Underlying a majority of overt rhythms is a feedback loop composed of cycling gene products, which influence their own synthesis and degradation (Takahashi, 1995). Post-translational modification, protein dimerization and nuclear transport are all essential features of how these biological clocks tick (Takahashi, 1995). The role of specific circadian genes within seasonal photoperiodism will be discussed further in Chapter 4.

1.2.2 How is photoperiodic time measured?

In exploring the role of photoperiodism in biological timekeeping, it is important to define the 3 main models of circadian timing. These models form the basis of modern circadian testing regimes and give a context for the work presented here; describing how peripheral and central circadian oscillators function and how light perception can be translated into biological clocks and calendars.

Some of the first explorations of seasonal rhythmicity were based on experiments on plants such as soya bean (*Glycine max*), mimosa (*Mimosa pudica*) and tobacco (*Nicotiana tabacum*) (Garner & Allard, 1927; Nanda & Hamner, 1958; Parker et al., 1945). In the early 18th century the French scientist, Jacques de Mairan noticed mimosa leaves would droop and stiffen in time with the daily periods of dark and light, and these rhythmic leaf movements would persist in periods of extended darkness, stiffening during the plant's "subjective day" and dropping during the "subjective night". This crucial observation wasn't revisited again till the early 1920s, with the work of two US plant physiologists, H.A. Allard and W.W Garner. Their work focused on a mutant strain of tobacco, called the "Maryland Mammoth" which continued to grow throughout the year, not setting seed till late December, when the winter frost would kill the plant ending any chance for reproduction (Garner & Allard, 1927). Previous observations suggested that light intensity, wavelength and duration of light exposure were all critical in the control of plant flowering as reviewed by (Lumsden, 2002). Using these cues, Allard and Garner extended the plants "subjective night" by physically moving them into a darkened room in the early evenings, causing the tobacco to flower three months early

(Garner & Allard, 1927). This clearly established the length of the night (and conversely day-length) as a critical factor in the timing of plant flowering, a phenomenon they called *photoperiodism*. This finding suggested that plants use light as both an energy source in photosynthetic reactions, and as a cue for seasonal timing. By tracking the expanding and contracting night (and day) lengths, plants are able to mark the passage of the seasons, effectively keeping an internal "calendar", enabling them to anticipate seasonal change and regulate their reproduction and growth accordingly (Jackson, 2009).

In 1938, Karl Hamner and James Bonner suggested that the photoperiodic signal for plant "flowering" was a diffusible substance, and by exposing plants to long or short periods of darkness, they confirmed that flowering is primarily a response to the dark portion of the photoperiod (Hamner & Bonner, 1938). For many plants there is a species-specific critical daylength that controls these states of development, as in short-day plants like marigolds (*Calendula officinalis*), which flower when the days are no longer than 6.5h short-day and long-day plants such as the Japanese morning glory (*Ipomoea nil*) which flower in daylengths of 16h or longer (Jackson, 2009). Night-length control of photoperiodic events leads to the formulation of the first theoretical model of circadian timing, the Hourglass Theory. Three early models of seasonal timing have been proposed for light-induced photoperiodic responses, (1) the Hourglass Timer, (2) the External Coincidence model and (3) the Internal Coincidence model.

The Hourglass model of timing (as shown in fig 1.1) was first described by Erwin Bunning in the early 1930s. As with the mimosa experiments by Jacques de Mairan, Bunning found the leaves of the common runner bean (*Phaseolus coccineus*) were elevated during the day and lowered at night (Bunning, 1932). By wiring the plant's leaves to a rotating drum, he was able to record their cyclic movements and found they oscillated with an average period of 24.4h (Bunning, 1932). Bunning suggested the phase of this internal 24h rhythm was synchronized by light exposure at dawn and dusk. He suggested that the timing mechanism behind the photoperiodic response had two alternating phases, approximately 12 hours each; one light-loving (photophilic) and the other dark-loving (scotophilic)

(Bunning, 1960). This model suggests the presence of a substance damaged or removed by light, which accumulates over the course of the night, only to be eliminated in the morning sun (Aschoff, 1960). A certain quantity of this substance is necessary to trigger a physiological response (such as flowering in plants, or growth of gonads in mammals). As winter nights become longer this "night-substance" accumulates till an internal threshold is reached, initiating a given photoperiodic response such as maturation of the reproductive system (Aschoff, 1960). This model argues against the participation of an inner circadian clock, as the hourglass lacks any endogenous rhythmicity and must be reset or 'turned over' by the light cycle each day (Aschoff, 1960).

Evidence for this form of timekeeping came from experiments with light regulation of reproduction in the green vetch aphid (*Megoura viciae)* (Lees, 1952). During summer (LD photoperiods) this insect reproduces asexually, and begins sexual reproduction during autumn and winter (SD photoperiods). Lees found that exposing LD-entrained aphids to prolonged LD light regimes extended their asexual phases, while exposure to SD photoperiods led to a switch from asexual to sexual reproduction and egg laying (Lees, 1952). Later work found inconsistencies with the hourglass theory, as the actual conversion rate of this "night substance" took far less time than predicted by the critical dark periods observed in the species tested (Vaz Nunes & Saunders, 1999).

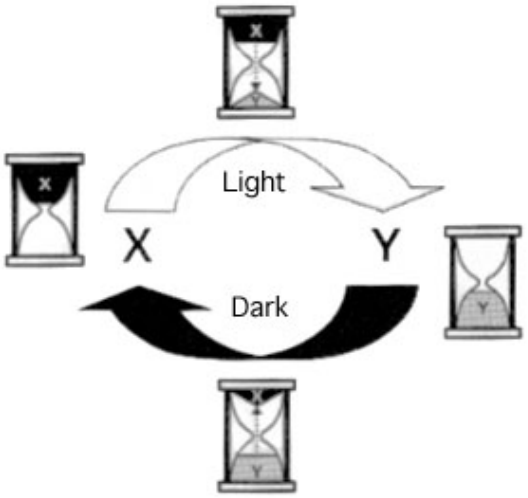

Figure 1.1 - The "hourglass" model of photoperiodic timing. In the light, substance X is converted to substance Y. In the dark, substance Y is converted back to substance X. The duration of the light and dark periods determine the ratio of X to Y. This ratio can be used to measure day/night length and therefore the seasonal photoperiod. Adapted from Foster and Kreitzman, 2004.

The second major model of photoperiodic time keeping, the External Coincidence (EC) Theory of Photoperiodism expands on the hourglass model, giving a greater emphasis on the entrainment of endogenous phases of light sensitivity and insensitivity. This model proposes the existence of a circadian rhythm of photoperiodic photosensitivity where the majority of the night-phase is sensitive to light, while the day-phase is photo-insensitive. As daylength increases in spring, light exposure during the photosensitive phase would stimulate photoperiodic behaviour, while light exposure during the photo-*in*sensitive period would inhibit it, as shown in fig. 1.2 (Pittendrigh, 1966). According to this model, as nights get shorter (in LD or summer), the dawn light of the daily photophase extends "backward," eventually illuminating a critical period (φ) in the late (subjective) night (Pittendrigh, 1966).

Evidence for this model was first found in the pupal eclosion of fruit fly (*Drosophila pseudo-obscura)* (Pittendrigh, 1966). Light pulses falling early in the night caused phase delays in the underlying circadian oscillation (of pupal eclosion), while those falling late in the night caused phase advances in these rhythms (Pittendrigh, 1966). The External Coincidence model suggests a dual role for light in setting the internal clock; (1) light could entrain the circadian clock, setting the "time" for the rhythmic changes of photosensitivity (between the photophil and scotophil periods) and (2) light could stimulate or inhibit photoperiodic behaviour, depending on the current phase of the organism (Pittendrigh, 1966). In the EC model, it is not the total duration of light or dark that matters, but the organism's photoperiodic phase when light exposure begins at dawn.

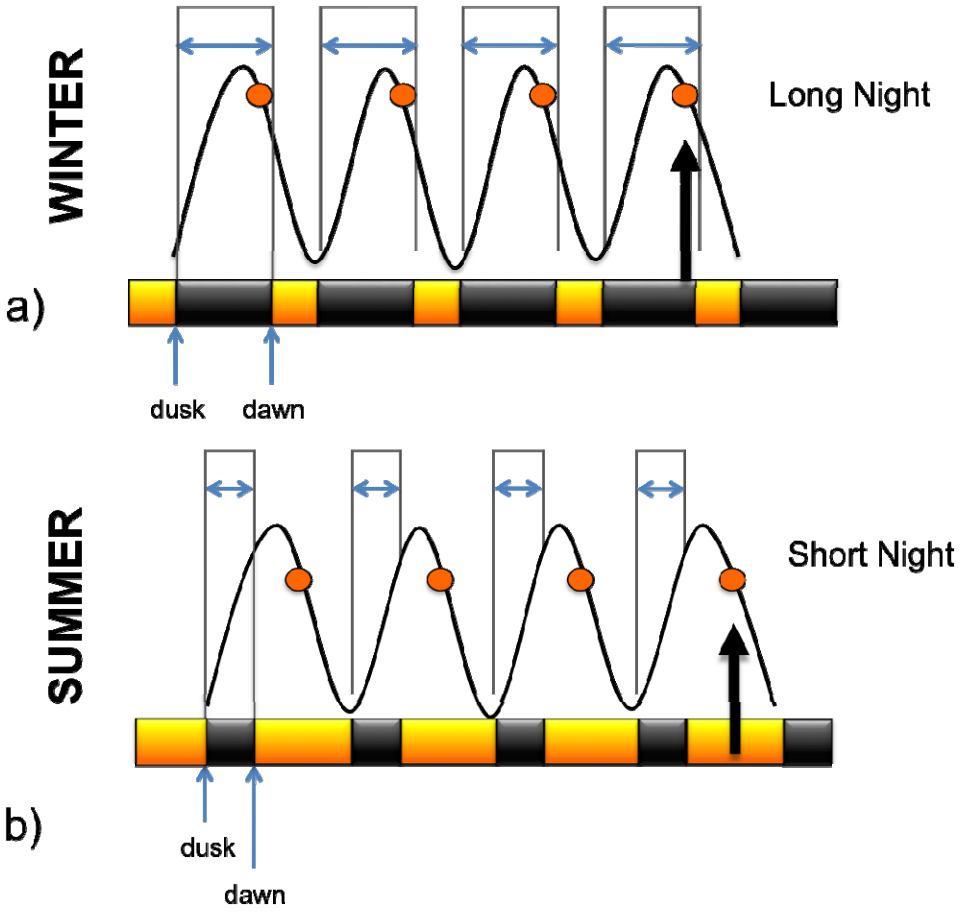

Figure 1.2 - The External Coincidence model of Photoperiodism. a) An internal circadian oscillator tracks day/night length annually. During winter (long nights) the photoinducible phase (orange dot) is not exposed to light, but in (b) summer (short nights) this sensitive phase does encounter light, triggering a photoperiodic response. Light influences both photoperiodic physiology and sets the phase of the daily oscillator.

Similar to the External Coincidence model, the alternative Internal Coincidence (IC) model of photoperiodism links photoperiod with an internal circadian rhythm (Pittendrigh, 1972). This model emphasizes a singular role for light, solely as a cue for endogenous rhythm entrainment and suggests the photoperiodic clock is based on two oscillators; one entrained to dawn and one to dusk (Pittendrigh, 1972). As the annual daylength changes, the coincident phase between the two oscillators is altered providing a signal encoding seasonal daylength. By the late 1950s evidence showed that multicellular organisms house more than one circadian pacemaker, each with their own cycles and phase relationships (Pittendrigh et al., 1958). Pittendrigh proposed that altering the prevailing photoperiod may modify these internal phase-relationships, causing particular physiological pathways to become

synchronized or desynchronized, such that the secretion of a hormone would coincide with the availability of its receptor(s) at the target tissue (Pittendrigh et al., 1958). In this model (shown in fig 1.3), light has a single entrainment role, setting the period of a pair of downstream oscillators whose synchronized phasing leads to circadian and seasonal gene expression (Pittendrigh, 1972).

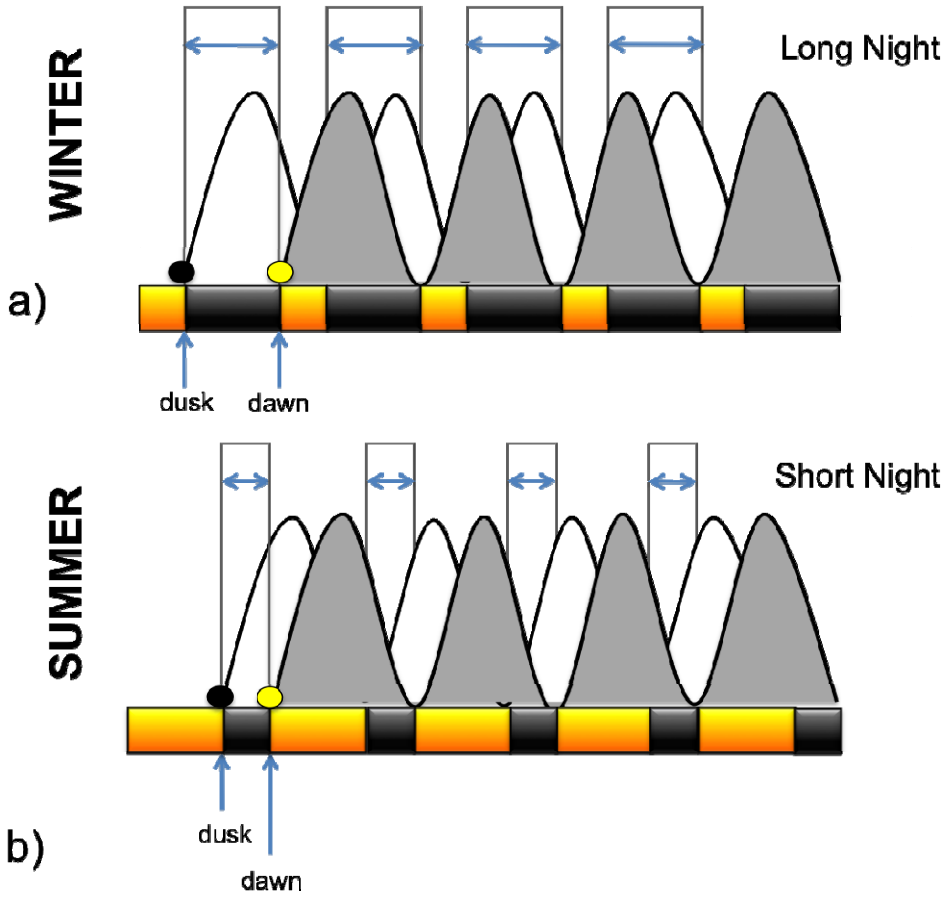

Figure 1.3 - A representation of the Internal Coincidence model of photoperiodism. By measuring the relative proximity and synchronization of two independent circadian clock elements, an organism is able to monitor the changes in the external photoperiod, enabling expression of later photoperiodic signaling cascades, turning the circadian clock into a seasonal calendar.

1.2.3 Evidence of a circadian clock underlying photoperiodism

Several experimental protocols have been developed testing the underlying mechanisms of circadian rhymicity, and confirm the involvement of the circadian system in photoperiodic time measurement (Vaz Nunes & Saunders, 1999). These protocols involve the use of night-break light pulses, such as resonance light cycles, non-24h cycles (T-cycles) and skeleton photoperiods of light and dark.

The Nanda-Hamner or Resonance protocol has become one of the main techniques used to determine an organism's circadian and seasonal timing. This regime is structured with a basic circadian period (tau or T) of 12 hours, or multiples of 12 hours (e.g., LD 6h:18h, LD 6h:30h, LD 6h:42h, etc.). Normally the main light period is 6h-12h with a dark period extending the overall period length to 18h–72h (Nanda & Hamner, 1958). It would be expected that photoperiodic induction would be most effective when the circadian system is in resonance (or harmony) with the photic environment, such that photoperiodic induction is normal seen in organisms when tau approximates 24h, 48h and/or 72 hours and non-24h light/dark periods such as 36h and 60h "days" are normally non-inductive (Nanda & Hamner, 1958). Positive Nanda-Hamner experiments support the use of an endogenous circadian clock, as specific gating of induction to periods of 24h would be unlikely in a simple timer system such as an hourglass timer.

Extending from Nanda-Hamner regimes, skeleton photoperiods and complex night interruption experiments were developed. In T-cycle experiments, the main light phase is 6h-12h, with an extended dark period systematically interrupted by a short light pulse at later and later points in each cycle (Vaz Nunes & Saunders, 1999). Skeleton photoperiods mimic full photoperiods, by exposing subjects to light at both dawn and dusk, with no light exposure between these points. This protocol limits the subjects' total daily light exposure, but maintains the entraining signal of light during the photosensitive periods of dawn and dusk. By varying the time of the second (dusk) pulse, it is possible to pinpoint the window of a photosensitive phase in the subjective night (Pittendrigh, 1964). A good example of a simple skeleton photoperiodic regime is shown in figure 1.5, using avian gonadal growth as an outcome of skeleton photoperiod exposure.

1.3 Circadian and Photoperiodism in Mammals, Birds and Fish

Animals time reproduction to fit closely with the change of seasons, ensuring that their young are born at peak of food availability. In the northern hemisphere, the breeding of long gestating animals like bears, deer, and herd cattle is triggered by the decreasing daylengths of autumn (thus SD breeders), allowing their offspring to be born the following spring or early summer (Bradshaw & Holzapfel, 2007). Animals with short gestating times such as birds and small mammals like hamsters mate in the lengthening days of early spring (LD breeders), giving birth a few weeks later (Karsch et al., 1984). The ability to translate the prevailing photoperiod into circadian and seasonal hormonal signalling has been a strong research focus in vertebrates of all kinds (see Bradshaw, 2007 for review). The circadian models of internal and external coincidence timing suggest a role of the circadian clock in performing the functions of a long-term timer or calendar (Lincoln et al., 2003). In vertebrates, the response to photoperiod is based on both the absolute day length, and the previous photoperiodic history of the animal (Malpaux et al., 2001).

1.3.1 Mammalian circadian systems

The linear mammalian light-reception pathway is based on electrical activity of the retinal afferents of the eye, which act as circadian inputs to the hypothalamus, entraining clock gene expression and electrical activity of the SCN neurons (Sumova et al., 1995). In mammals, the electrical activity of the SCN is high during the day, and low at night; a circadian pattern which continues under constant conditions (Hazlerigg & Wagner, 2006). Low electrical pulses in the SCN at night stimulate the release of noradrenaline from its sympathetic nerve terminals to the pineal gland (Granados-Fuentes & Herzog, 2013), leading to a cascade of calcium signalling which causes the activation of the enzyme arylalkylamine N-acetyl transferase (AA-NAT), the rate-limiting enzyme controlling the conversion of serotonin to melatonin in the pineal (Granados-Fuentes & Herzog, 2013). Direct control of melatonin release is also possible, through the light-associated inhibition of AA-NAT by the local pinealocytes (Malpaux et al., 2001). This pineal-derived melatonin then targets cells in the basal hypothalamus and pituitary gland

controlling the release of reproductive and growth hormones which are released into the systemic circulation for downstream effects in various tissues throughout the body (Hazlerigg & Wagner, 2006). The SCN controls pineal activity, thereby modulating the nocturnal production of melatonin and removal of the pineal prevents photoperiodic responsiveness (Granados-Fuentes & Herzog, 2013).

Melatonin, considered the "night hormone", is secreted into the blood by the pineal gland during periods of darkness in both day-active (diurnal) and night-active (nocturnal) animals (Morris et al., 2012). It is also produced by the retina and gut in significant amounts (Damian, 1977), although the roles of these tissues in central timekeeping is still under scrutiny (Huether, 1993). Pineal melatonin production begins on or soon after dusk and ends before dawn (Falcon et al., 1989). As seasonal daylength changes, nocturnal melatonin secretion changes, providing vertebrates an internal representation of daylength through melatonin exposure and duration (Morris et al., 2012).

In mammals, photoperiodic control of reproduction and growth has been clearly demonstrated in a series of ablation experiments. Disruption of the SCN inhibits photoperiodic responses and blocks the regulation of reproduction through annual photoperiodic signals (Klein et al., 1983; Reppert et al., 1981). Previous work in Syrian hamsters (*M. auratus*), demonstrated that pinealectomy prevented photoperiodic gonad regression and gonadotrophin secretion normally initiated by a short day (winter) photoperiod, and subsequent melatonin injections reversed the effect (Reiter, 1975). Working with pinealectomized ewes, Fred Karsh and colleagues demonstrated that a short-day melatonin injection profile stimulated reproduction, while a long day injection profile left the animals under gonadal regression (Wayne et al., 1988). Exposing these sheep to a short-night or "spring" photoperiod while injecting them with a "winter" melatonin profile (and *vice versa*) demonstrated a clear insensitivity to the prevailing photoperiod – the principal response was timed to injected melatonin profile (Roche et al., 1970; Wayne et al., 1988). Photoperiodic reproduction in mammals is determined by the duration of melatonin exposure thereby encoding night length, rather than light exposure during a photoinducible phase, as earlier believed (Malpaux et al.,

2001), thereby negating the role of the previously postulated Hourglass and External Coincidence models of photoperiodism.

1.3.2 Avian circadian systems

In birds, both the eye and pineal gland act as paired, autonomous circadian oscillators each having light sensitive photoreceptors, and rhythmically secreting melatonin (Piesiewicz et al., 2012). Ocular-ablation studies have shown that birds without eyes can still entrain to circadian photoperiods, indicating a non-ocular photoreceptor system unlike the linear retinal-hypothalamic-pineal system used by mammals (Menaker, 1968), as shown in figure 1.4.

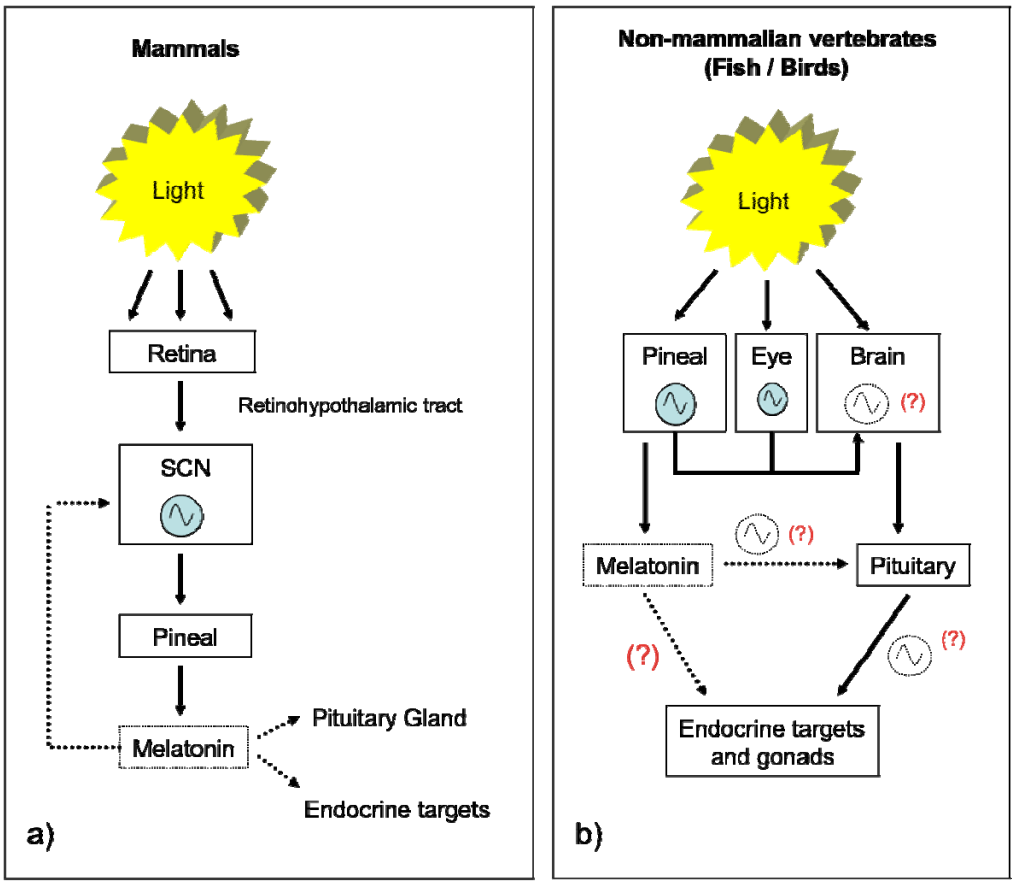

Figure 1.4 - a) Photoperiodism in mammals. Light stimulation via the retina and SCN to the pineal, which secretes melatonin, acting on the brain, pituitary gland and other downstream targets; b) a proposed model for photoperiodism, where light acts directly on central and peripheral tissues, including the eye, brain and pineal gland. Melatonin is secreted in response to photoperiod, and its effects on the fish pituitary may be modulated by seasonal melatonin receptor expression. Melatonin exposure may gate pituitary hormone expression, leading to seasonal hormone secretion to the gonads and downstream tissues.

In the avian circadian system both the eye and pineal gland are semi-independent circadian oscillators (Dawson & Goldsmith, 1983), having light sensitive photoreceptors (Takahashi et al., 1984), and rhythmically secrete melatonin (Piesiewicz et al., 2012). Working with the common house sparrow (*Passer domesticus*), Mike Menaker demonstrated that sparrows with no eyes could still entrain to circadian photoperiods, indicating a non-ocular photoreceptor system in use (Menaker, 1968), quite unlike the linear retinal-hypothalamic-pineal system used by mammals. Using thin fibre optics, a small set of neurons were isolated in medial basal hypothalamus (MBH) of the Japanese quail (*Coturnix japonica*) which respond directly to light and house a set of body clock genes that oscillate approximately every 24 hours (Foster & Soni, 1998). These deep-brain photosensitive neurons detect changes in light at dawn and dusk and respond to annual changes in photoperiod (Foster & Soni, 1998), as predicted by the Internal Coincidence model of photoperiodism.

Work in young chicks has demonstrated a nocturnal peak in pineal aaNAT, which is modulated by LD/SD conditions (Majewski et al., 2005). Levels of aaNAT, its enzymatic activity, and pineal melatonin content changed during postembryonic development, depending on the season of hatching; SD hatched birds showed no changes in the pattern and amplitude of diurnal rhythmicity over age while in LD hatched birds, age-related changes were noted over time (Piesiewicz et al., 2012).

As an independent oscillator, the avian pineal releases melatonin during periods of darkness and can maintain its entrained circadian oscillations *in vitro*, yet pineal removal has little effect on the seasonal reproduction of the birds (Zimmerman & Menaker, 1979). Transplantation of an entrained pineal to an arrhythmic host restored the appropriate circadian profile, but ablation of the pineal did not completely block circadian activity (Zimmerman & Menaker, 1979). Although melatonin reflects the length of the dark period, it does not seem to be the only form of seasonal timing in bird neurobiology (Yoshimura, 2010). The role of the bird SCN was found to act as a damped oscillator – not able to initiate a self-sustaining circadian oscillation itself, but crucial to behavioural rhythms (Takahashi & Menaker, 1982). SCN ablation in the sparrow led to arrhythmic

behaviour, regardless of pineal condition, suggesting that both the pineal and SCN are important for proper circadian rhythmicity in avian brains (Takahashi & Menaker, 1982)

Working with Japanese quail (*C. japonica*), Brian Follett exposed subjects to a set of "skeleton photoperiods"; photoperiods with graduating pulses of light set later and later within the dark phase of the light/dark cycle (Sharp & Follett, 1969). As shown in fig 1.5, only birds exposed to a light pulse between 12h-16h after dawn were stimulated to breed, indicating a clear photoinducible phase of reproductive sensitivity as predicted by the External Coincidence theory (Sharp & Follett, 1969).

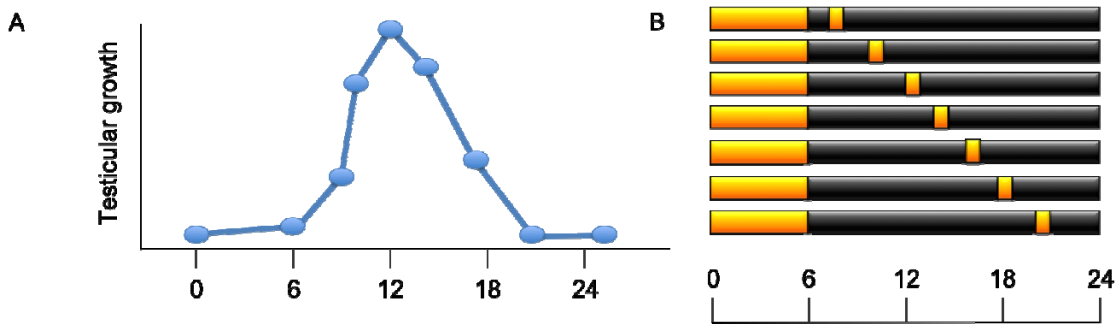

Figure 1.5 - a) Testicular growth in Japanese quail maintained under a 6h light/dark cycle with a skeleton photoperiod, circles indicate time of 15min light pulse; b) structure of the skeleton photoperiod and light pulse regime. Adapted from Sharp & Follett, 1969.

The precise timing of a given photoinducible phase varies from species to species. For birds in temperate climates, the longer nights of winter led to the photoinducible phase falling during the dark period. As the days lengthen, the photoinducible phase is exposed to dawn light, and reproduction is triggered (Hastings & Follett, 2001). Experiments using skeleton photoperiods have been performed on isolated tissues and zebrafish cell cultures and are discussed in detail in chapter 4.

1.3.3 Refractory outputs in response to extended photoperiods

Countering this stimulatory photoperiodic system is a built-in block to on-going reproduction throughout the rest of the year. Single-brood birds, such as the starling (*Sturnus vulgaris*) become insensitive or "refractory" to long days

approximately 6 weeks after initial stimulation (Dawson & Goldsmith, 1983). This refractoriness is reversed by exposure to the shortening daylengths of late summer and fall, allowing them to respond to stimulatory photoperiods again the following spring. In contrast with birds, mammalian refractoriness is based on insensitivity to the previous inhibitory daylength (i.e. ignoring the block to reproduction). Small mammals like hamsters regress their reproductive systems in the autumn as a direct response to the decreasing daylength, and spontaneously redevelop their reproductive systems in spring (Rudeen & Reiter, 1980). The opposite is true in sheep, a short-day breeder, as reproduction is inhibited by the long daylengths of summer until they become insensitive/refractory to the inhibitory effect of long daylengths and resume photoperiodic fertility (Almeida & Lincoln, 1984).

1.3.4 Fish circadian system

Several circadian core clock genes have been identified in fish, which act as transcriptional activators and/or repressors, modulating protein stability and nuclear translocation. In zebrafish, the molecular mechanism of circadian rhythmicity is based on a set of interacting positive (stimulatory) and negative (inhibitory) feedback loops (Whitmore et al., 2000). The positive loop is formed by the heterodimerization of CLOCK and BMAL1 proteins, activating transcription of three p*eriod* (*mPer1*, *mPer2* and *mPer3*) and two c*ryptochrome* (*mCry1* and *mCry2*) genes. The negative feedback loop involves the translocation of PER:CRY heterodimers to the nucleus to repress their own transcription by inhibiting the activity of the CLOCK:BMAL1 complexes (Cahill, 2002a).

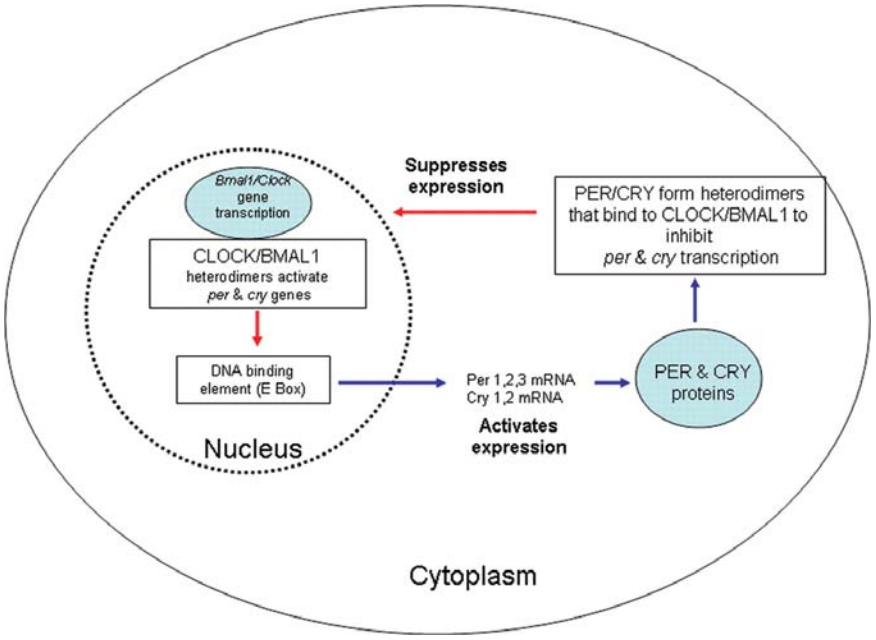

Figure 1.6: A simplified diagram of the autoregulatory feedback mechanisms involved in the regulation of the circadian clock. The interactions between a negative feedback loop repressing *per* and *cry* gene transcription (blue lines) and a positive feedback loop promoting *Bmal* and *Clock* transcription (red lines) acts to maintain circadian rhythmicity.

Transcripts for most zebrafish clock genes are rhythmically expressed in tissues throughout the body and in embryonic cell lines, and can entrained to exogenous LD cycles (Whitmore et al., 2000). Interestingly, zebrafish clock genes are rhythmically expressed in both the classical central circadian pacemaker regions (such as the SCN) and in almost all peripheral tissues tested (Whitmore et al., 1998b). Experiments monitoring the expression of zebrafish circadian clock genes in cell and tissue explant cultures are described in detail in chapter 4.

1.3.5 Photoperiodism in fish

The light/dark cycle modulates behavioural processes in fish such as migration, skin pigmentation, O_2 consumption, and food intake (Migaud et al., 2010). Fish have adapted to annual changes in environmental cues, so that physiological functions such as growth and reproduction are also seasonal (Falcon et al., 2007).

Early photoperiodic work on fish has shown that exposure to seasonal light cycles compressed into periods shorter that 1 year caused rainbow trout (*Oncorhynchus*

mykiss) to spawn 3mo-4mo earlier than control fish under ambient condition (Hoover, 1937). Similar light regimes have also been shown to alter the spawning timing in Medaka (*Oryzias latipes*) (Koger et al., 1999) and European Sea Bass (*Dicentrarchus labrax*) (Rodriguez et al., 2004), among others.

Photoperiodism is fish has been studied primarily in farmed and commercial stocks, where it is regarded as a key environmental cue for the timing of seasonal reproduction and growth (Taranger et al., 2010). Previous studies have shown that artificial light regimes may increase growth rates up to 25% in farmed trout (*O. mykiss*) (Taylor et al., 2006) and can advance gonadal maturation in Indian carp (*Catla catla*) (Bhattacharyya et al., 2005).

In salmonids such as rainbow trout, photoperiod provides the cue for smoltification (fresh/salt water transition) and initiation of gonadal maturation and spawning (Bromage & Duston, 1986). Results suggest that exposure to LD (long day) during normally SD (short day) environmental conditions (such as the winter months) significantly alter reproductive entrainment cycles (Randall & Bromage, 1998). In cases of prolonged LD or continuous light exposure (LL), a significant increases in puberty rates has been shown in salmon (*S. salar*) (Oppedal et al., 1999), while LL can have inhibitory maturational effects in Atlantic cod (*Gadus morhua)*, depending of the season during which the regime is applied (Hansen et al., 2001).

Interestingly, in species such as the grey mullet (*Mugil cephalus*), both continuous light (LL) and continuous darkness (DD) inhibit gonad maturation (O'Donovan-Lockard et al., 1987). These inhibitory effects of constant photoperiod exposure may depend on the photophase duration; in Eurasian perch (*Perca fluviatilis*) reproductive inhibition was observed under a constant long photoperiod (17h L:7h D), while only a partial inhibition was observed under a shorter constant photoperiod (12h L:12h D) (Migaud et al., 2004).

A final aspect of photoperiodic influence may depend on the direction of photoperiodic change. In European sea bass *(D. labrax)*, there is evidence that the

absolute duration of the photoperiod exposure is less important that the direction of change (i.e. from long to short day conditions) in determining the onset of gonadal maturation (Carrillo et al., 2009). These effects are likely gated, such that if a particular size or physical threshold is not reached during a critical circannual phase, then the maturational event may be delayed till the next cycle (Bjornsson et al., 1994). Once a threshold is reached, photoperiod determines the initiation of sexual maturation, while timing of spawning is more affected by environmental conditions locally (Davies, 2002).

1.3.6 Melatonin in fish

Early work on the circadian system in vertebrates like zebrafish focused primarily on the retina and pineal gland (two organs of common diencephalic origin) as centres of circadian clock control (Cahill, 1996; Falcon et al., 2003b). Both tissues are known to regulate the rhythmic release of melatonin, in a number of teleost species (Bolliet et al., 1996; Falcon et al., 1989). These melatonin rhythms persisted in culture, under constant conditions (Cahill, 1996), and reflected similar profiles seen in mammals (Falcon et al., 2010). Plasma melatonin was higher at night than during the day and the shape of these oscillations changed with the season (Gern et al., 1978) being of short duration and high amplitude in the summer, and low amplitude, long duration in the winter (Underwood, 1990).

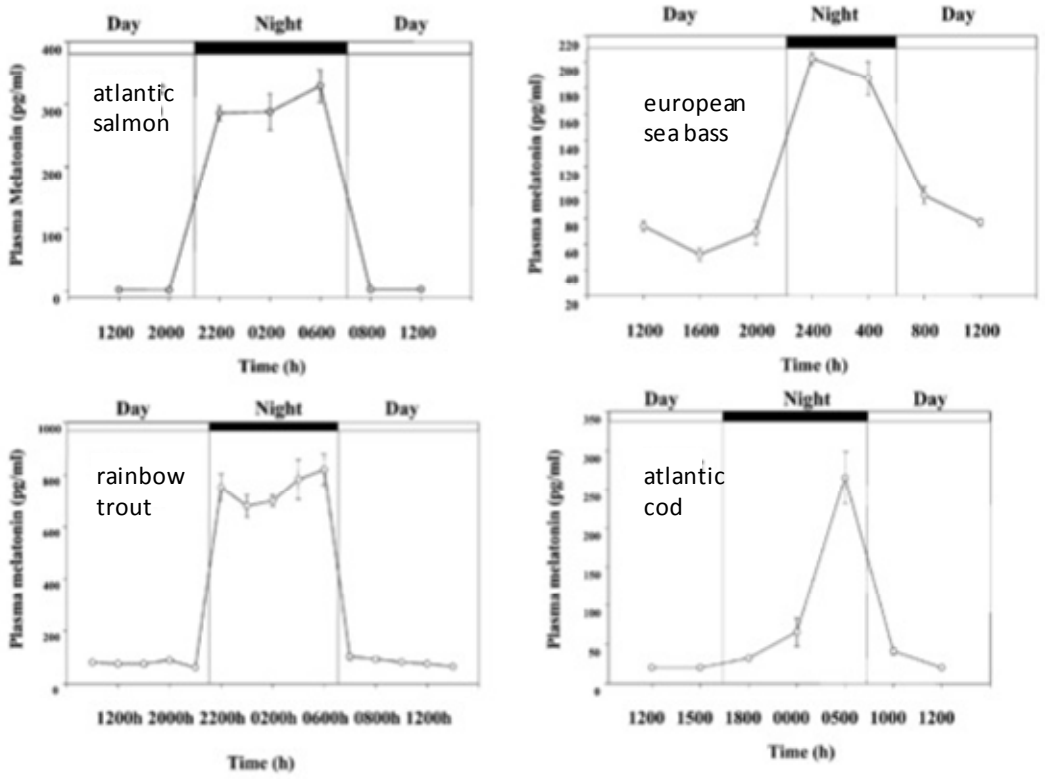

Figure 1.7: Daily plasma melatonin levels (Mean ± SEM; pg/ml) in atlantic salmon, rainbow trout, european sea bass and atlantic cod. Plasma melatonin is increased at night and drops quickly in the early morning in all 4 species, reminescent of findings in mammalian models. Figure adapted from Bromage and Randall, 2001.

Figure 1.7 shows the daily change of plasma melatonin in 4 teleost species. Overall, the duration of the nocturnal melatonin expression is directly proportional to night length. Similar daily patterns of melatonin expression have been seen in Goldfish (*Carassius auratus*) (Iigo et al., 1994), Pike (*Esox lucius*) (Falcon et al., 1989) and Stickleback (*Gasterosteus aculeatus*) (Mayer et al., 1997), among others. These findings suggested the plasma melatonin profile is an indicator of both day length and season, and led to the proposal of melatonin as a time-keeping molecule in teleost fish (Bolliet et al., 1996; Falcon et al., 2007).

Experiments using exogenous melatonin administration in fish are problematic, as injections have a short half-life of 8min-9min and cause transitory spikes of plasma melatonin (Skliar et al., 2006). Melatonin implants provide long-term delivery, but only at constant levels which don't produce the expected reproductive response in other vertebrate models (Bartness et al., 1993). As zebrafish are too small to provide regular blood samples, accurate measurement of

plasma melatonin is problematic. Researchers often turn to mRNA expression of secondary targets such as hypothalamic and pituitary hormones which are known to be linked to melatonin activity in order to study the effect of photoperiod on teleost reproduction (Bayarri et al., 2004). Photoperiodic advancement and delay experiments have shown significant changes in GnRH, FSH and LH expression following photoperiodic maturation in Rainbow Trout (*O. mykiss*) (Davies et al., 1999).

In zebrafish, pineal melatonin is used as a systemic signal for circadian and seasonal light/dark cycles (Cahill, 1996). Melatonin is circulated through the cerebrospinal fluid and blood, acting on targets throughout the body, through tissue-specific expression on melatonin receptors (Vatine et al., 2011). Specific photoperiodic effects on growth and reproduction may be determined by melatonin modulation of control centres such as the pituitary, hypothalamus and the gonads themselves (Hazlerigg & Wagner, 2006). The photoperiodic expression of melatonin receptors in a range of target tissues has been explored in detail in the current work and will be discussed in detail in chapter 2.

1.4 Photoperiodism reinvented: TH and DIO expression

Increasingly evidence suggests that thyroid hormone (TH) is crucial for the expression of seasonal rhythms in vertebrates (Barrett et al., 2007). TH expression is controlled by hypothalamic neurosecretory cells releasing thyroid-stimulating hormone-releasing hormone (TSH-RH). This releasing hormone targets the thyrotroph cells of the anterior pituitary, increasing the release of thyroid-stimulating hormone (TSH), which stimulates the production of thyroxine (T_4) from the thyroid gland (Nakao et al., 2008b).

Vertebrate thyroid hormones have two isoforms; thyroxine (T_4) is circulated systemically, with a low biological activity; and the more biologically potent form, triiodothyronine (T_3), is created in target tissues through the local conversion of T_4 by deiodinase enzymes (Hazlerigg & Wagner, 2006). As shown in figure 1.8, the two principal deiodinase enzymes found in local tissues are type 2 deiodinase (Dio2) and type 3 deiodinase (Dio3) (Hazlerigg & Wagner, 2006). Dio2 catalyzes

the conversion of T_4 to the active T_3 form, while Dio3 converts T_3 to inactive reverse-T_3 (rT_3) form. The relative expression and activity of Dio2 and Dio3 determine the levels of biologically active T_3 in the brain (Nakao et al., 2008b).

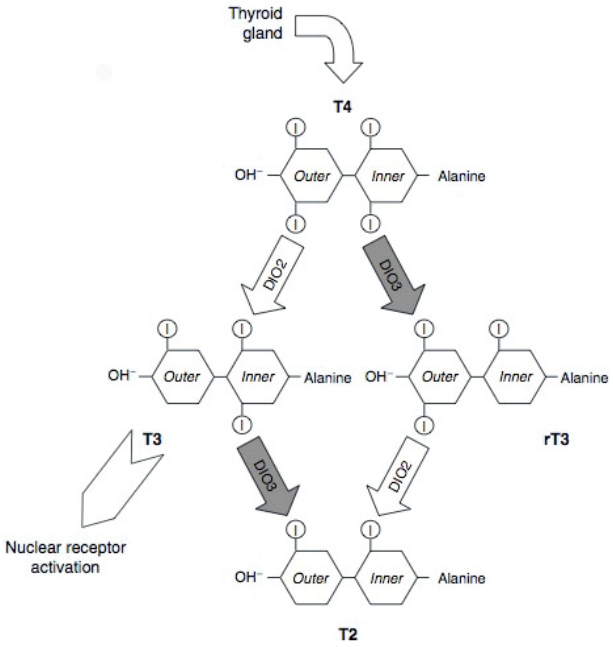

Figure 1.8 - Thyroid hormone (TH) processing by local deiodinase enzymes. The main form of circulating thyroid hormone, T4 is converted to T3 in tissues expressing type 2 deiodinase (Dio2). T4 can also be converted to an inactive form, reverse T3 (rT3) by type 3 deiodinase (Dio3). Both rT3 and T3 can be processed into T2. Figure from Hazlerigg and Loudon, 2008.

Using autumn-breeding mammals such as sheep, Fred Karsh and colleagues have shown that thyroidectomy removes the seasonal (or photo-refractory) inhibition of reproductive behavior normally expressed in spring (Billings et al., 2002). Injections of T_4 in these thyroidectomised animals restores endogenous springtime reproductive inhibition, but has only a weak effect on the onset of photoperiodic reproduction in autumn (Billings et al., 2002). These inhibitory springtime T_4 effects have been shown to be maximally effective within the basal hypothalamus of thyroidectomised ewes (Anderson et al., 2003). Experiments using microinjection mapping have shown the ependymal cells of the ventral hypothalamus as the site of the greatest photoperiodic induced Dio2/Dio3 activity in both long and short day breeding mammals (Hanon et al., 2008). This ependymal cell layer is composed of tanycyte cells surrounding the 3rd ventricle which act as regulatory cells for the transport of solutes in/out of the brain (Hazlerigg & Loudon, 2008). These tanycyte cells project to the pars tuberalis of the anterior pituitary, and may regulate the hypothalamic-pituitary hormone relay system (Nakao et al., 2008b).

Figure 1.9 gives a schematic drawing illustrating the differences between mammalian and non-mammalian (vertebrate) light reception systems, and a model of the connection between the hypothalamus and pituitary gland specifically.

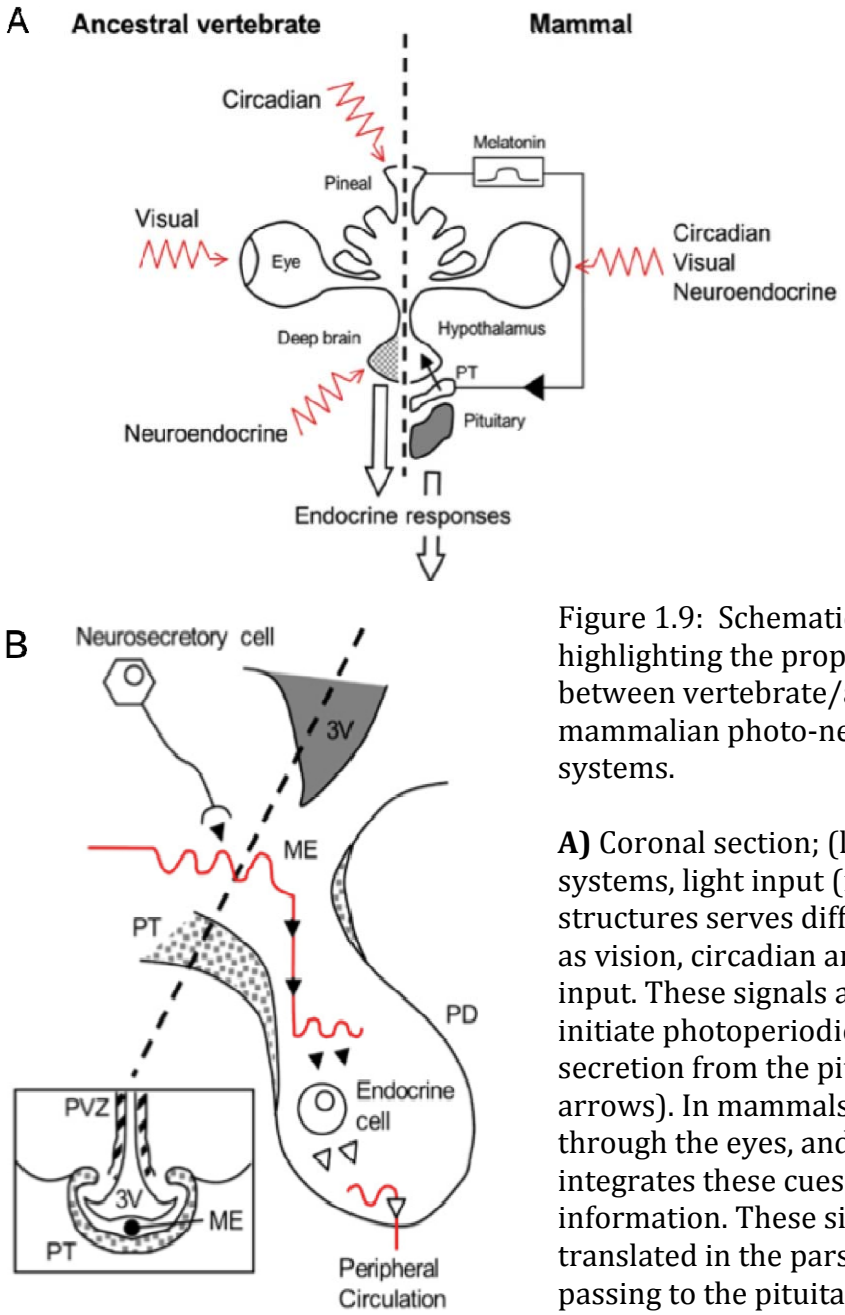

Figure 1.9: Schematic drawing highlighting the proposed differences between vertebrate/avian and mammalian photo-neuroendocrine systems.

A) Coronal section; (left) in ancestral systems, light input (red) to different structures serves different functions such as vision, circadian and photoperiodic input. These signals are integrated and initiate photoperiodic-linked endocrine secretion from the pituitary (open arrows). In mammals (right), light input is through the eyes, and the hypothalamus integrates these cues into photoperiodic information. These signals may be translated in the pars tuberalis, before passing to the pituitary gland where endocrine output is initiated.

B) Schematic of the hypothalamic-pituitary portal system. Hypothalamic neurosecretory cells release signals into median eminence (ME) capillaries, which drain into portal vessels (red) to the pituitary endocrine cells, whose hormones are secreted into peripheral circulation. The dashed line indicates the plane of section of the inset, a coronal view of the ME ventral to the third ventricle (3V); cells surrounding the 3V form the paraventricular zone (PVZ), extending to the ME. The pituitary pars tuberalis (PT) lies adjacent to the ME. Figures from Hanon et al., 2008.

Working with Japanese quail (*C. japonica*), Brian Follett and others have shown that thyroidectomy inhibits seasonal responses to photoperiod, such as gonad growth, and this response can be restored by T_4 injections (Follett & Nicholls, 1985). T_4 levels in the hypothalamus increase during the lengthening days of spring, and drop in autumn, reflecting the stimulating long day photoperiod of the species (Yoshimura et al., 2003). When the quail were exposed to stimulatory long photoperiods, Dio2 was significantly up regulated in the hypothalamus, synthesizing more active T_3 (Yasuo et al., 2005). Exposure to inhibitory short photoperiods suppressed Dio2 while increasing Dio3 expression, effectively limiting T_3 availability in a seasonal manner (Nakao et al., 2008b). T_3 targets include the GnRH cells of the median eminence (in the ventral hypothalamus), which release GnRH pulses into the portal blood supply, managing the subsequent release of downstream pituitary hormones such as LH and FSH (Nakao et al., 2008b).

Experiments in mammalian models with both long and short day breeders suggest that T_4/T_3 expression by local Dio enzymes conversion governs seasonal reproduction (Hazlerigg & Loudon, 2008) and the seasonal photoperiod regulates the expression of these deiodinase enzymes within the basal hypothalamus (Nakao et al., 2008b).

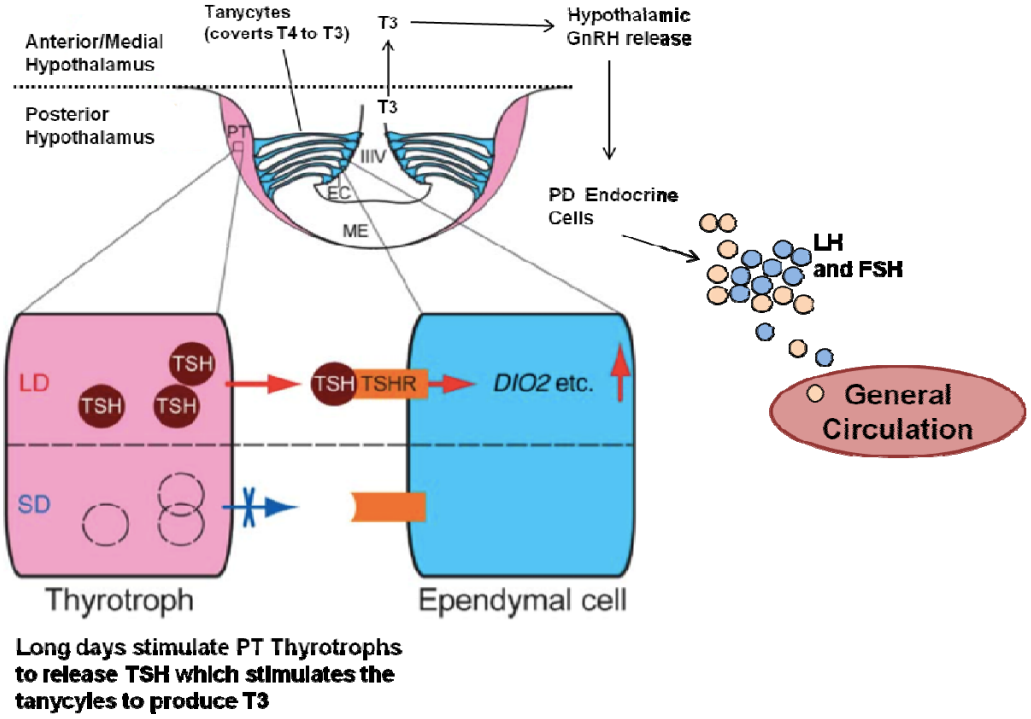

Figure 1.10: Schematic drawing of the proposed photoperiodic regulation of thyroid hormones in avian ependymal cells. Light received by deep brain photoreceptors induces TSH expression in the pituitary pars tuberalis (PT; pink). Long-day expression of TSH leads to the formation of TSH in the PT, acting on TSH receptors (TSHR) expressed by ependymal cells (blue); leading to seasonal changes in hypothalamic Dio1-2-3 expression. Tanycytes convert T_4 into bio-active T_3, stimulating the release of hypothalamic GnRH. GnRH is carried to the pituitary (pars distalis; PD) by portal blood vessels, modulating release of LH and FSH from the anterior pituitary into general circulation. Figure adapted from Nakao et al., 2008.

The principal components making up the thyroid axis are conserved across vertebrates, including teleost fish (Power et al., 2001). As with mammalian and avian models, thyroid hormones play crucial roles in regulating development, differentiation and metabolism and species are unable to grow and mature normally without them (Porterfield & Hendrich, 1993). Much of the past TH fish-specific literature has highlighted the importance of THs during metamorphosis, early development and growth (Power et al., 2001). Thyroid hormone receptors (TR) have been isolated from several teleosts such as Japanese flounder (*Paralichthys oliaceus*), sea bream (*Sparus aurata*) and zebrafish (*D. rerio*) (Power et al., 2001).

In Atlantic cod (*G. morhua*) photoperiod alterations affect cyclic patterns of sex steroids, thyroid hormones, and the timing of spawning (Norberg et al., 2004). In this species, plasma T_3 levels are highest from mid-summer to fall, coinciding with the highest annual growth rate (Norberg et al., 2004). Both plasma T_3 and T_4 levels exhibit a strong seasonal rhythm in teleosts and are associated with the uptake of thyroid hormones by developing eggs from circulating plasma levels, accounting for significant declines in plasma T_3 seen prior to spawning (Tagawa & Brown, 2001). Previous data suggested temperature acted as a major regulator of TH expression, but modern studies have focused on photoperiod as a primary entrainer of thyroid hormone secretion (Comeau et al., 2000). Thyroid hormones also act as growth inducers in fish (Donaldson et al., 1979), stimulating growth hormone secretion (Ebbesson et al., 1998). Up till now there has been no literature available regarding the seasonal photoperiodic T_4/T_3 expression by local Dio enzymes within the basal hypothalamus in light entrained zebrafish and the work presented here (Chapter 3; figures 3.1 and 3.3) is the first of its kind.

1.5 Photoperiodism and Reproductive Endocrinology

The coordination of photoperiodic reproduction and physiology is controlled by neuroendocrine signaling, which integrates signals of reproductive, nutritional, and health conditions with environmental cues (Gan & Quinton, 2010). The hypothalamic-pituitary-gonadal axis (HPG) stimulates the release of hormones such as gonadotrophin-releasing hormone (GnRH), luteinizing hormone (LH) and follicle-stimulating hormone (FSH) (Sharp & Follett, 1969). In mammals, the hypothalamus receives input regarding the day length, environmental conditions and internal physiological states, while the pituitary secretes trophic hormones which act downstream controlling sexual maturation and reproduction in vertebrates (Gan & Quinton, 2010).

The vertebrate pituitary gland has two lobes, the anterior (adenohypophysis) and posterior (hypophysis), with the anterior pituitary further divided into three distinct regions known as the pars tuberalis (PT), pars intermedia (PI) and the pars distalis (PD) (Romer & Parsons, 1977). The main function of the anterior

pituitary is the synthesis and release of a number of related hormones. In fish, the pituitary houses six different cell types, characterized by the hormones they secrete, such as lactotrophes generating prolactin (PRL); somatotrophs, growth hormone (GH); thyrotrophs, thyroid-stimulating hormone (TSH); corticotrophs, adenocorticotrophic hormone (ATCH), and gonadotropes, follicle-stimulating hormone (FSH) and luteinizing hormone (LH) (Romer & Parsons, 1977).

1.5.1 GnRH forms in zebrafish

Gonadotrophin-releasing hormone (GnRH) released from the ventral telencephalon-preoptic region and hypothalamus induces gonadal development and maturation of fish through the secretion of gonadotrophins such as LH and FSH from the pituitary gland (Zohar et al., 1995). Non-mammalian vertebrates express two to three forms of GnRH. Zebrafish have two forms; GnRH-2 (cGnRH-II), expressed in the midbrain, and GnRH3 (sGnRH), a hypothalamic form used in hypothalamic-pituitary signaling (Kuo et al., 2005) and is illustrated in fig 1.11. In zebrafish, GnRH3 (in forebrain and diencephalon) is expressed three to four fold higher than GnRH-2 (in the midbrain) and have four different GnRH receptors which are expressed in a variety of tissues (Tello et al., 2008).The variation in structure, location, and response strength to GnRH forms indicates that these four receptors may have novel functions (Tello et al., 2008).In some fish, the fibers entering the pituitary come from cells expressing other forms of GnRH, whose roles are still unknown (Lethimonier et al., 2004).

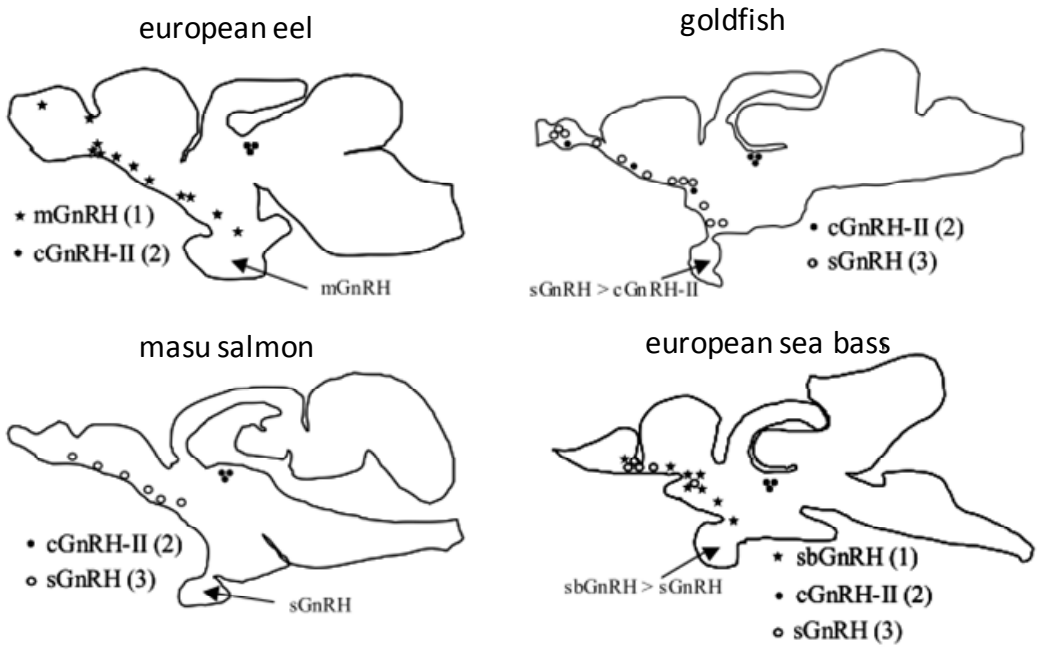

Figure 1.11: Comparative teleost GnRH systems, with expression of both GnRH-2 (cGnRH-II) and GnRH (sGnRH3). Examples of expression of these GnRH subtypes in the midbrain and pituitary in different teleost species. Figure adapted from Lethimonier et al., 2004. c= chicken, m= mammalian, s= salmon, sb= sea bream

1.5.2 Seasonal expression of Prolactin

In mammals, Prolactin (PRL) is released from the anterior pituitary (from the pars distalis) and is linked with melatonin signalling in this region (Lincoln, 1999). PRL regulates milk production and is associated with seasonal changes such as food intake, metabolic rate and winter coat (pelage) growth in sheep (Lincoln et al., 2003). The possibility of a paracrine role of PRL has been postulated heavily in mammalian circannual research (Johnston, 2004). Anterior pituitary (pars tuberalis) cells express melatonin receptors in a seasonal manner and are thought to regulate PRL secretion (from the lactotrophes of the pars distalis) by producing "tuberalin", a PRL releasing factor not yet fully characterized (Johnston, 2004). This hypothesis suggests photoperiodic melatonin secretion (and melatonin receptor expression) entrains PRL cycling independently from other pituitary hormones, regulating a number of key phases of sexual maturation (Bachelot & Binart, 2007).

In fish, PRL has over 300 different functions grouped into 5 categories: (1) osmoregulation, (2) growth and development, (3) endocrinology and metabolism, (4) brain and behavior, and (5) reproduction (Bole-Feysot et al., 1998). PRL expression has been found in the pituitary, liver, intestine, and gonads of the sea bream (*S. aurata*) (Santos et al., 2001) and in the pituitary, liver, kidney, spleen, gill, muscle, gonads, and brain of goldfish (*C. auratus*) (Tse et al., 2000). The almost ubiquitous expression of PRL throughout fish tissues may build evidence for presence of multiple, separate seasonal timers, which respond to a common melatonin signal or indicate a wholly independent role of PRL in fish. This hypothesis is beyond the scope of the current work, but is an excellent direction for future research.

1.5.3 Seasonal LH and FSH expression

In avian models, the gonadotrophs, controlled by GnRH, release luteinizing hormone (LH) and follicle-stimulating hormone (FSH); in certain cases, GnRH itself can directly affect gonads, altering the functioning of the ovaries and testes downstream (Sharp, 1996). In females, FSH promotes gonadal maturation, follicular selection and regulates progesterone secretion by granulosa cells of the developing follicles while LH regulates estrogen production by maturing ovarian follicles (Sharp, 1996). In males, FSH stimulates gonadal growth and estrogen secretion by Sertoli cells while LH controls the productions of androgens by Leydig cells (Sharp, 1996).

Like other vertebrates, gonadal development in teleost fish is stimulated by LH and FSH. Recent work on the responsiveness of teleost reproductive system to seasonal photoperiods has been demonstrated in the male stickleback (*G. aculeatus*). Fish kept in LD (16h/8h) showed increased pituitary LH and FSH expression and maturation over SD (8h/16h) entrained fish (Shao et al., 2013). Seasonal expression in these hormones has also been noted, with LH expression peaking in late spring (long day) and FSH peaking in mid-winter (short day) (Hellqvist et al., 2006). Samples of FSH from isolated pituitary glands of rainbow trout (*O. mykiss*) also demonstrated comparable seasonal profiles (Santos et al., 2001). Both LH and FSH receptors are strongly expressed in zebrafish gonads, and

are present in kidney and liver tissues also (Chen & Ge, 2012). Experiments suggest that FSH signalling is limited in sexually immature female gonads, but plays a significant role in zebrafish ovarian follicle development later in life (Kwok et al., 2005).

1.5.4 Seasonal GH expression

In mammals, GH is released in nocturnal pulses from the pituitary gland, linked to the body's circadian cycle (Norris et al., 2003). GH has a number of downstream effects, including the stimulation of bone and muscle growth (Sam & Frohman, 2008).

While GH samples taken from goldfish maintained under naturally alternating seasonal photoperiods showed no clear daily rhythms in expression, they were closely correlated to seasonal changes in daylength, with the highest mean daily serum GH levels found in spring/summer (LD) and the lowest in early winter (SD) (Marchant & Peter, 1986). In adult salmon and sea bream, plasma GH levels increase with increasing photoperiod, i.e. from April to June (Boeuf, 1993). Conversely, decreasing daylength in winter season suppressed GH levels, whereas fish kept under long photoperiod during the same period of time did maintain high plasma GH levels (Bjornsson et al., 2000).

The release of teleost GH is also affected by melatonin, in a variable manner. Experiments using cultured adult trout pituitaries showed a bi-modal change in GH release, with picomolar concentrations of melatonin inducing a reduction in GH release, and higher (nanomolar range) concentrations resulting in the stimulation of GH secretion (Falcon et al., 2003b). Further evidence of melatonin modulation of GH secretion comes from pituitary culture experiments where the addition of luzindol (a melatonin receptor blocker) prevents both inhibitory and stimulatory responses of GH to melatonin concentration (Falcon et al., 2003b). Circulating melatonin is expected to decrease in LD conditions, while SD melatonin expression is expected to increase (Kezuka et al., 1988). The bimodal effects of melatonin on GH release, and the annual variations in the sensitivity to melatonin, may be an underlying factor in the management of biological resources for either

reproduction or growth in sexually mature fish. The seasonal expression of GH in zebrafish is reported in detail in Chapter 2, while measures of growth are given in Chapter 1.

1.6 Zebrafish as a circadian model

Key discoveries in circadian biology have been made through large-scale genetic mutant screens, using model organisms such as *Drosophila* and mouse (Reppert & Weaver, 2002). A popular alternative vertebrate model system to mouse is the zebrafish (*D. rerio*), a member of the largest group of vertebrates known, the teleost super-order, which comprises more than 90% of the total number of described fish species (Pitcher, 1986). Zebrafish (*D. rerio*) are small, free spawning teleost fish with a wide distribution extending from India into Burma (Engeszer et al., 2007). These fish are ideal for reproductive studies, as they spawn regularly, ovulating approximately every 4-5 days, they are highly fecund, providing between 100-500 eggs at each laying and their eggs are fertilized outside the body, developing in a transparent chorion (Westerfield, 1995). The eggs are non-adherent, transparent and have a developmental period from fertilization to hatching of 96h at 26°C (Laale, 1977). All juveniles are hermaphroditic during early development (Takahashi, 1977). Sex differentiation begins at 23–25 days, where ovaries may degenerate and transform into testes in males (Takahashi, 1977). The process of sex differentiation is completed by 40 days post-hatch and gonadal maturation is completed by 60 days (Takahashi, 1977). As spawning time and clutch sizes have been shown to increase with age (Spence et al., 2008), the experiments described here began no earlier than 90 days post-hatch, to ensure sexual maturity in all specimens.

As a tropical and sub-tropical native, zebrafish (*D. rerio*) are subject to minimal changes in seasonal light, as compared to species in temperate regions such as northern Europe (stickleback, *G. aculeatus*) and Japan (medaka, *O. latipes*) (Wittbrodt et al., 2002). Recent work has demonstrated the importance of temperature in zebrafish swimming behaviour (Condon et al., 2010), but did not investigate the physiology of reproductive seasonality, a wide-ranging

phenomenon of seasonal teleost biology. The authors suggested that photoperiod may be a secondary cue of seasonal change in animals living in tropical latitudes (Condon et al., 2010), making the results presented here particularly novel (see Chap 2).

In mammals, the SCN was thought to act as the principle circadian pacemaker, entraining its activity to light-dark cycles and coordinating damped oscillations in numerous dependent tissues (Granados-Fuentes & Herzog, 2013). This circadian model was overturned in fish, in 1998-2000, when David Whitmore and others found isolated, cultured fish organs possess endogenous circadian pacemakers (Whitmore et al., 2000; Whitmore et al., 1998a). In zebrafish and other non-mammalian vertebrates, the photo-neuroendocrine system is organized as a network of semi-independent, light-sensitive oscillating units particularly in the retina, pineal gland, and hypothalamus (Whitmore et al., 2000). Cells displaying both photosensitive and circadian oscillations have been described in numerous peripheral tissues and in cell culture (Vatine et al., 2011). In most zebrafish tissues examined there is a functional circadian clock and these cellular circadian clocks can be directly entrained to a rhythmic light-dark cycle (Whitmore et al., 2000). The presence of light-sensitive oscillators in peripheral tissues suggests the zebrafish circadian system is based on distributed pacemakers, independently entrained by light exposure (Vatine et al., 2011). This has led to a long debate over the role of melatonin and other central circadian cues in models with clearly defined peripheral clock oscillators and photoreceptors such as zebrafish (Cahill, 2002b; Falcon et al., 2010).

In 1996, studies of the zebrafish clock were published by Greg Cahill's group, using a video analysis system to monitor larval zebrafish circadian activity, as a form of fish mutant screen (Cahill et al., 1998). Cahill's lab found evidence of a functional circadian pacemaker with a population average period of 25.6 hours, and a variance of 30min to 1 hour (Cahill, 1996). Many of the genes involved in the mammalian circadian clock have zebrafish homologues and transcripts for most of these genes are rhythmically expressed in multiple tissues (Vatine et al., 2011).

Historically, it was believed that photoperiodic timing was transmitted to the reproductive axis by daily and season changes in melatonin (Sundararaj & Sehgal, 1970). More recently, the effect of thyroid hormone activity and tissue-specific diodinase enzyme expression has been highlighted as a possible signaling pathway in seasonal photoperiodic reproduction (Nakao et al., 2008b). Although the circadian clock is now being extensively explored in zebrafish, to date there has been no analysis of photoperiodism and seasonality in this species. Given the lack of evidence for seasonal responsiveness in this model of choice, I hypothesize increases in zebrafish growth and fertility when housed and entrained in long day photoperiodic conditions. These increases are likely mediated through a number of pathways, including:

- Changes in growth (length and weight) over the zebrafish lifespan
- Seasonal fertility and fecundity in light entrained populations
- Pituitary hormone expression (GH, LH, FSH and TSH)
- Melatonin receptor expression in the hypothalamus and pituitary
- Dio enzyme expression in the hypothalamus

Each set of experiments listed above is reviewed in the following chapters 2 - 4.

CHAPTER 2 - PHOTOPERIOD ON FERTILITY AND GROWTH

2.1 Introduction

While there are many environmental cues used to determine seasonal change (such as light, temperature and food availability) the present chapter focuses on the effect of photoperiod on the reproductive capacity of the popular model organism, zebrafish (*D. rerio*). Zebrafish are diurnal (active during daylight hours) and synchronise to external light/dark cycles (Spence et al., 2008). Their first activity period begins immediately after lights on, with other high activity periods in the early afternoon and the last hour of light. Zebrafish can grow up to 65mm in the wild, normally reaching a maximum of 40mm in captivity and have a life-span of 24-36mo (Spence et al., 2008); the zebrafish sampled in this study were monitored between 3mo to 24mo, during their peak reproductive years. There are a number of advantages to using zebrafish for reproductive experiments; reproductive capacity can be monitored in detail, with counts of clutch sizes weekly; groups can be exposed to specific lighting conditions, independent of temperature and other seasonal factors; zebrafish are small enough to enable significant samples to be housed in lab facilities, and their external fertilization allows easy monitoring of both fecundity and fertility rates (Cahill, 2002a).

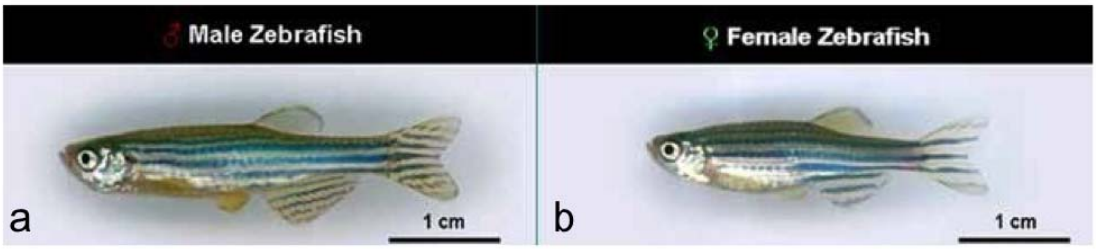

Figure 2.1 – Representative pictures of adult male and female zebrafish (15mo). Female fish generally have rounder bellies (due to distended ovaries), while males are slimmer and longer from end to end. Picture adapted from https://wiki.med.harvard.edu/SysBio (Aug 2012).

Zebrafish spawn during the first hours after illumination, beginning within minutes of light exposure and normally ovulate every 3-5 days in optimal conditions (Westerfield, 1995). In the wild, zebrafish breeding pairs spawn at irregular intervals, ranging from 1-6 days and may produce several hundred eggs

in a single clutch (Eaton & Farley, 1974). The eggs are non-adherent, transparent and have a developmental period from fertilization to hatching of 96h at 26°C (Laale, 1977). All juveniles are hermaphroditic during early development, developing ovaries at 10–12 days (Takahashi, 1977) with sex differentiation beginning at 23–25 days, when ovaries degenerate and transform into testes in males (Takahashi, 1977). The process of sex differentiation is completed by 40 days post-hatch and gonadal maturation is completed by 60 days (Takahashi, 1977). As sexual differentiation is not completed until 2mo post-hatch, the current experiments were began 90 days post-hatch, to ensure sexual maturity in all specimens.

Studies have shown that teleost fish are sensitive to photoperiod manipulation. In Atlantic salmon (*S. salar)*, continuous light exposure affects growth and sexual maturation, and night time illumination reduces plasma melatonin rhythms (Davie et al., 2009), with similar conditions impacting reproductive status in European Sea Bass (*D. labrax)* (Bayarri et al., 2004). The most established model teleost photoperiodic reproduction is the Japanese medaka (*O. latipes*), who have a natural breeding season from April to September (LD) and whose daily rhythms of early morning egg laying follows photoperiodic cues (Wittbrodt et al., 2002). Experiments of photoperiodic factors on reproductive parameters in this species indicate oocyte atresia and lower clutch sizes over time, when fish were moved from LD (16h/8h) to SD (8h/16h) (Koger et al., 1999).

By manipulating photoperiod regimes under controlled conditions, I aim to describe the links between seasonal light responsiveness, growth and reproduction in zebrafish. As noted in other teleost species, LD conditions are associated with increases in both reproduction and body growth, and I hypothesize similar stimulatory effect in LD entrained zebrafish (as compared to SD cohorts). The following data describes the effects of different photoperiodic light regimes on physiological measures, such as average body weight and length, and reproductive parameters such as clutch sizes and fertilization rates.

2.2 Methods and materials

The following experiments were performed within the UCL fish facility. Zebrafish were bred from a stock of wild-type samples (Ab tup), raised by the fish facility staff in a fish nursery under standard conditions until 90 days post-hatch. From 3mo onwards, zebrafish were housed in specially designed metal cabinets fitted with LED light arrays. Each cabinet houses 12 x 1.5 litre tanks, or 6 x 3 litre tanks, with up to 50 fish per tank. Each LED array was timer controlled, set to LD (16h/8h), SD (8h/16h) or control (14h/10h) lighting profiles (400–700 nm at 2,500 μW/cm^2). Cabinet-housed fish were fed twice daily, housed on an open-water circuit, with individual tanks cleaned once a week. Figure 2.2 illustrates the light-tight cabinets used and the LED systems used.

Figure 2.2 – Pictures of the UCL fish facility where the zebrafish used in these experiments were raised and housed throughout the experiments. Left: some light-tight metal cabinets shown closed; Right: a single cabinet housing a number of fish tanks, opened.

2.2.1 Zebrafish breeding

Trials of photoperiodic breeding, fertility and fecundity were performed with long and short day entrained zebrafish, in two experiments. Adult fish were given 12 -

40 days of pre-test breeding, in control lighting (14h/10h light/dark) in the main breeding room, and bred every 4 days to adapt them to semi-continuous egg laying, as per Westerfield (1995). These fish were moved to LD or SD cabinets for 2 days of acclimatization, represented by grey divisions in figures 2.5 - 2.8. Water quality, air and water temperature, food availability, and pH all conformed to UCL Fish Facility standards. All adults were housed at 1 male: 3 females for optimal breeding as per UCL fish facility recommendations and per Westerfield (1995). Fish were age-matched siblings, either 3.5mo old (fig 2.5; newly mature) or 10mo (fig 2.6: established breeders) at the start of testing. All eggs were collected 2 to 4 hours after lights on (ZT 2-4) and washed twice with a 0.5% bleach solution before counting began, to minimize bacterial infection between samples.

Statistical testing was performed with Kolmogorov-Smirnov tests, normally used for comparison between two non-normally distributed groups with *cumulative* differences over time. Analysis was performed using an external web-based stats calculator (Kirkman, 1996), accessed Nov. 2010. D-values give a measure of the cumulative difference between two groups; the closer to 1, the higher the significant cumulative difference between datasets.

2.2.2 Lighting conditions

All data shown are based on differences between LD (16h/8h) and SD (8h/16h) conditions. Control conditions, are based on the regular light cycle of the UCL fish facility (14h/10h).

Points defined as "ZT" refer to zeitgeber time, a standard of time based on the point of lights on (or dawn; usually defined as ZT 0). This is opposed to "CT" time (circadian time) which refers to the point of the internal circadian cycle entrained to external ZT times, in such cases CT O represents ZT 0 in conditions of full darkness. Figure 2.3 illustrates the entrainment lighting conditions used.

Figure 2.3 - Schematic of light entrainment conditions. Long day (LD) refers to 16 hours of light, 8 hours of dark per 24h day; Short day (SD) refers to 8 hours of light, 16 hours of dark per 24h day. Zeitgeber time (ZT) refers to hours after dawn, or lights on.

2.2.3 Measures of body length and weight; gonad weight

All zebrafish growth data for length and weight are based on standard methods of anatomical measurement. Zebrafish length was recorded from the tip of the snout to the tip of the caudal fin. It is a straight-line measure, not measured over the curve of the body, using a standard 12-inch ruler, with mm increments. Zebrafish weight was recorded on intact samples, blotted dry before recording. Whole body weights were recorded to 3 significant figures, using a standard lab analytical balance (Sartorius, London, UK).

Whole gonad (ovary and testis) weights were recorded directly after a midline dissection, blotted dry and recorded to 3 significant figures, using a standard lab analytical balance (Sartorius). Ovary weights included all mature and/or immature oocytes present.

2.2.4 Egg Collection

To avoid adult consumption of eggs, a set of rectangular nested dishes were used to promote and catch eggs at the bottom of each tank. The base dish is clear plexiglass (4”x10”x4”), with a second (slightly smaller; 3.8”x9.8”x3.8”) dish nested within it, with a fine mesh bottom (blocking direct access to the eggs, as they drop into the base dish). Marbles are then placed in the dish (mess bottom), to simulate rocks/riverbed debris, where zebrafish lay their eggs in protected niches. These nested dish sets are placed in the bottom of the breeding tanks 10h-12h before anticipated ovulation, no earlier than 4 days after the previous breeding cycle. This allowed the deposited eggs to sink between the marbles, minimizing consumption and egg loss. These breeding dishes (with marbles) were collected

the following morning, and the eggs were removed with a hand-pipette and counted one-by-one under the microscope. Overall clutch numbers, regardless of condition were recorded as a measure of fecundity. The resulting egg clutches were also examined for fertilization and further development, as a measure of fertility.

2.3 Results

2.3.1 Length / Weight of adult zebrafish in different photoperiods

Adult zebrafish body length and weight are significantly affected by exposure to long and short day photoperiods. Adults were tested at 6-30 months, having spent all their lives in LD or SD, from 3 months onwards. Data for both males and females are pooled, and are shown in figure 2.4.

Adult body weights were significantly greater in LD over SD raised fish at the majority of ages measured (fig 2.4 - left axis; bar graph); 11mo and 15mo, (both $p<0.001$); and 20mo and 30mo (both $p<0.01$), while measures taken at 6mo and 24mo failed to reach significance.

Differences in adult body length (fig 2.4 - right axis, line graph) were significant between LD and SD fish at 11mo, 15mo, 20mo and 30mo (each $p<0.001$); while 6mo and 24mo samples were not significantly different between conditions ($p>0.05$).

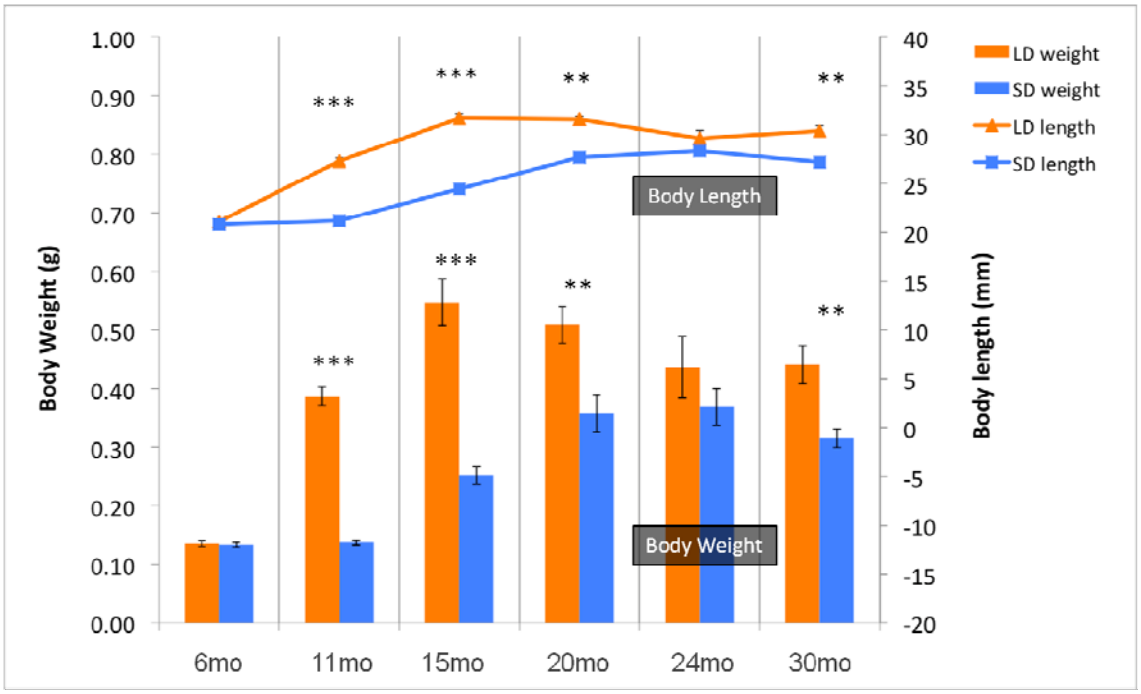

Figure 2.4 - Body weight is greater in LD compared with SD raised fish from 6mo-30mo of age (bar graph, left axis); 11mo and 15mo ($p<0.001$); 20mo and 30mo ($p<0.01$); 6mo and 24mo ($p>0.05$). Whole body length is higher in LD versus SD from 6mo to 30mo of age. (Line graph, right axis); 11mo, 15mo ($p<0.001$) and 20mo and 30mo ($p<0.01$) were strongly different between conditions, while 6mo and 24mo fish were non-significantly different between conditions ($p>0.05$). N = 37-101; depending on age.

Throughout life zebrafish raised in LD (16h/8h) photoperiods grew heavier and longer as compared with their SD (8h/16h) counterparts. LD growth peaked at 15mo (sexual maturity), gradually declining thereafter (at 20mo, 24mo and 30mo). After early similarities (at 6mo), group differences between length and weight continued throughout life. SD fish showed little to no growth between 6-11mo (a strong growth period for LD fish) and moderate growth between (15-24mo). Growth rates were significantly different between groups until 24mo. Appendix A gives the t-test results for these growth comparisons and illustrates the degree of freedom for each pairing (n = 101 at 6mo, to n = 37 at 30mo).

2.3.2 Fecundity of zebrafish on short and long photoperiods

Measures of zebrafish entrained to long and short photoperiods for fertility and fecundity were performed with 2 sets of samples. Experiment 1 focused on breeding rates from young (3.5mo; newly mature) fish, over a long period (100

days consecutively) to establish a baseline for photoperiodic differences between groups. 132 fish were tested, housed at a ratio of 3 males: 9 females, in 1.5-liter tanks. Fish were pre-tested in control (fish facility) lighting conditions (14h/10h) and moved into either LD (16h/8h) or SD (8h/16h) lighting cabinets on day 42 for the duration of the study (see fig. 2.5). As these fish were newly mature, an extended pre-testing breeding period was undertaken to confirm normal breeding rates before experimental testing began.

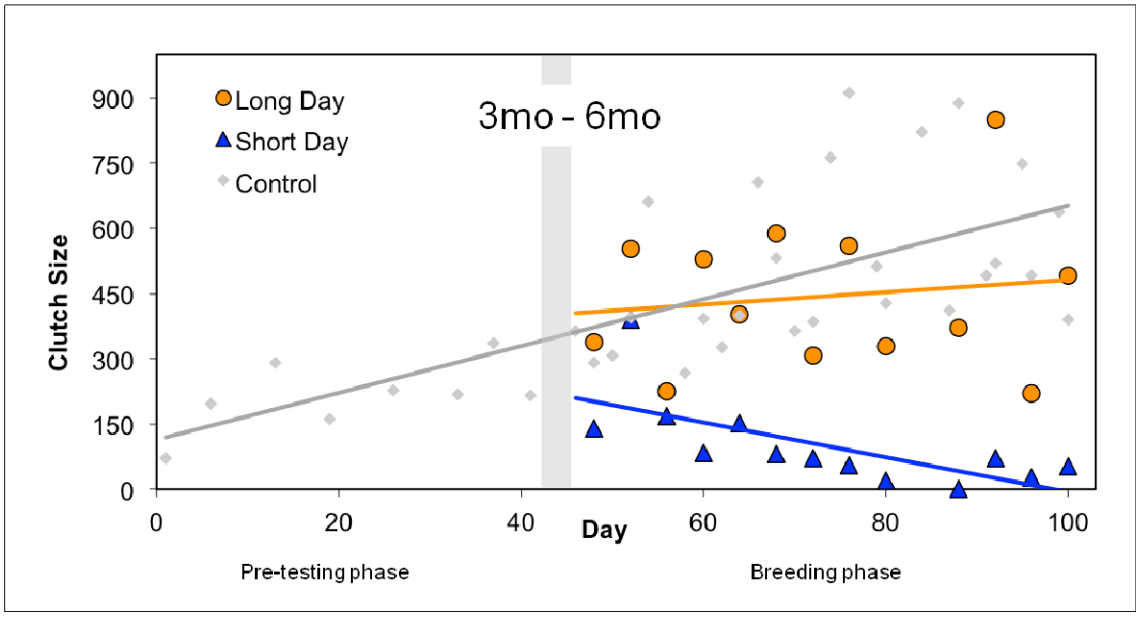

Figure 2.5 - Photoperiodic fecundity of adult zebrafish, 3mo-6mo old (experiment 1). Pre-testing in control lighting conditions on days 0 - 41, followed by breeding in LD (orange points) or SD (blue points) from day 46 - 100. Grey bar indicates the switch from control to experimental light regimes, on days 42/43. Grey points indicate clutch sizes of control fish kept in 14h/10h LD conditions.

After acclimatization, newly entrained LD and SD fish showed moderate changes in egg laying. SD fish decreased egg-laying 4 days after entrainment and maintained a low level of 50-100 eggs per clutch 30 days later. While LD fish showed a fecundity trendline lower than controls (LD slope = +1.4199, control slope = +5.3877), they significantly differed from their SD cohorts (SD slope = -4.0035), laying over 450 eggs per clutch (on average; D = 0.923; p = 0.001).

In experiment 2, fish breeding began at 10mo of age (adult; sexually mature and established breeders), for 50 days consecutively. 72 fish were tested, housed at a

ratio of 1 male: 3 females per tank. Pre-testing was performed for 12 days in control lighting (14h/10h), then tanks were moved into LD (16h/8h) or SD (8h/16h) cabinets. After 18 days, these tanks were then switched into opposite lighting cabinets – e.g. LD into SD or SD tanks into LD cabinets, to monitor the effects of acute photoperiodic changes on egg laying. This experiment had a shorter pre-testing period than experiment 1, as the sample fish were previously established breeding pairs and were sexually mature at the commencement of the testing. A 1:3 ratio of males to females was used, consistent with experiment 1, but total sample size was limited by age-matched stock available at the beginning of the study period. The goal of experiment 2 was to confirm and validate the previous pilot data (experiment 1) and to extend these findings by introducing a light-phase "switch" in the final phase of testing, as shown in figure 2.6.

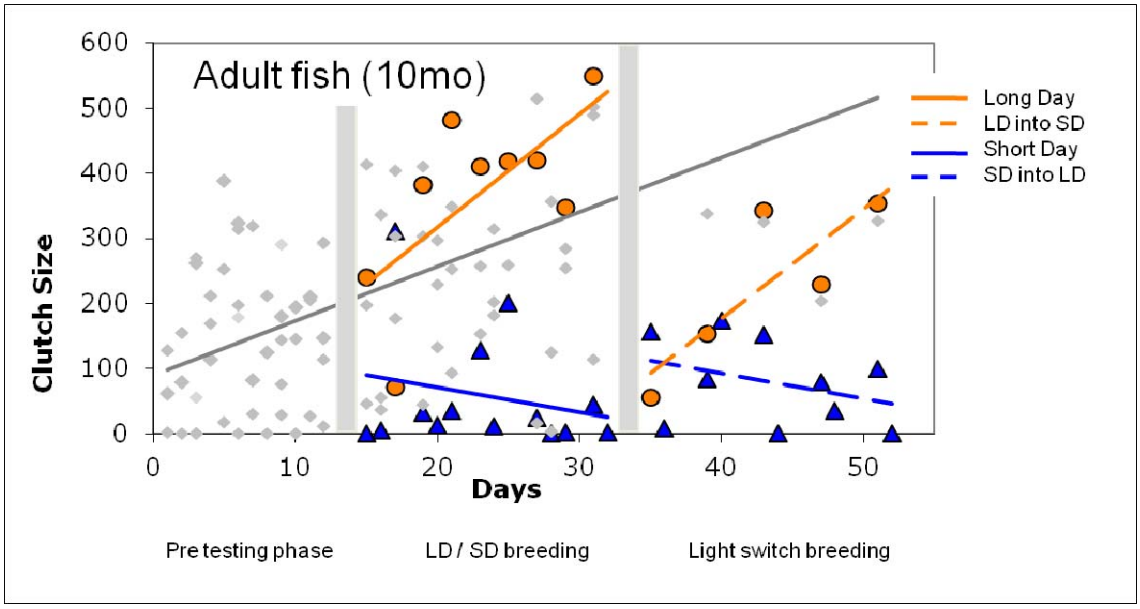

Figure 2.6 - Photoperiodic fecundity of adult 10mo-12mo zebrafish. All tanks in control light regime on days 0-12. Phase 1 (middle): tanks were moved into either LD (orange points) or SD (blue points) on days 14-32. Phase 2 (right): tanks were switched into opposite conditions (LD to SD - orange points; SD to LD – dark blue points; indicated by dotted trendlines) for the remaining testing period (days 34-52). Separator bars indicate a switch from control to experimental light regimes (on days 12/13 and 33/34), grey points indicate clutch sizes of control fish kept in 14h/10h conditions.

Experiment 2 results (shown in figure 2.6) indicate an immediate drop in clutch size in breeding pairs moved from control to SD lighting cabinets, with average

clutch sizes on day 15 significantly different between groups (control = 219, SD = 0; p=0.001); tanks moved into LD lighting displayed a small, but insignificant increase in egg laying (day 15 control = 219, vs. LD = 241; p>0.05) directly following LD light exposure. Over the course of basic light entrainment (fig 2.6, middle; pre-testing into LD or SD), significant changes in fecundity rates were measured, with LD fish increasing their clutch sizes from 241 (day 15) to 550 (day 31; overall LD slope = +17.308), and SD entrained fish dropping their clutch sizes from 0 and 6 (days 15 and 16, respectively) to 2 (day 32; SD slope = -3.7977). By the end of the regular entrainment phase (in LD or SD conditions), SD fish averaged less than 10 eggs/clutch and LD fish 400-450 eggs/clutch. The difference in photoperiodic-sensitive fecundity rates was significant different between conditions (D = 0.786; p = 0.001). Rates of egg laying by SD fish ceased completely within 18 days of entrainment (Fig 2.6, middle), 2-fold faster than younger SD entrained fish (35 days; shown in Fig 2.5, right).

Experiment 2 added an interesting twist on the basic entrainment protocol shown earlier, by moving LD or SD entrained fish into their opposite conditions after 30 days of single photoperiod exposure. Clutch sizes dropped dramatically after moving into opposing light regimes (fig 2.6, right side: LD into SD, or SD into LD; dotted trendlines). LD clutches dropped from 550 eggs/clutch to less than 100 eggs/clutch when moved in SD lighting (fig 2.6 right side, orange points). SD fish moved into LD conditions moderately increased their egg laying, from less than 30 eggs/clutch (day 32 in SD) to over 100 eggs/clutch (day 35 in LD). Egg laying trends in both groups (after light switch, phase 3) fundamentally reflected the original entrainment effects (phase 2, middle), rather than that of the new environmental conditions. This is exemplified by the synchronized slopes between LD (solid orange line; phase 2) and LD into SD (dashed orange line; phase 3), and between the SD (solid blue line; phase 2) and SD into LD (dashed blue line; phase 3) trendlines, where the slopes between the two phases are conserved, while the average clutch sizes changes in accordance with the new lighting conditions. LD entrained fish moved into SD cabinets had an acute drop in egg laying, which increased at the same rate as phase 2 levels (LD phase 2 = 17.308, phase 3 =

16.775). SD fish moved into LD cabinets had a small increase in clutch sizes that continued to decrease at a similar rate as recorded in phase 2 (SD phase 2 = -3.7977, phase 3 = -3.9488; Fig 2.6, middle). As shown in figure 2.6, the differences between LD (into SD) and SD (into LD) groups were highly significant (D = 0.3; $p<0.001$), with opposing trends mirroring the entrainment of the previous light exposure paradigm (in phase 2). Figures 2.5 and 2.6 illustrate the significant effect of photoperiod on fecundity and indicates an immediate effect of photoperiodic changes on reproductive capacity.

2.3.3 Fertility of zebrafish on short and long photoperiods

Fertility rates (viability of the gametes; live, fertilized eggs) were measured throughout the long-term experiments as described above. Embryos collected throughout these studies showed no difference in developmental abnormalities between conditions (data not shown).

Photoperiodic-sensitive fertility rates from light entrained adults were significantly different (Figure 2.7; D = 0.700, p = 0.007) between conditions. LD fish laid eggs clutches with 91% live eggs, increasing to 98% by day 100 (LD slope = 0.0743). SD fish laid clutches with an average of 88% live eggs, dropping to 81% by day 100 (SD slope = -0.1378; Fig. 2.7).

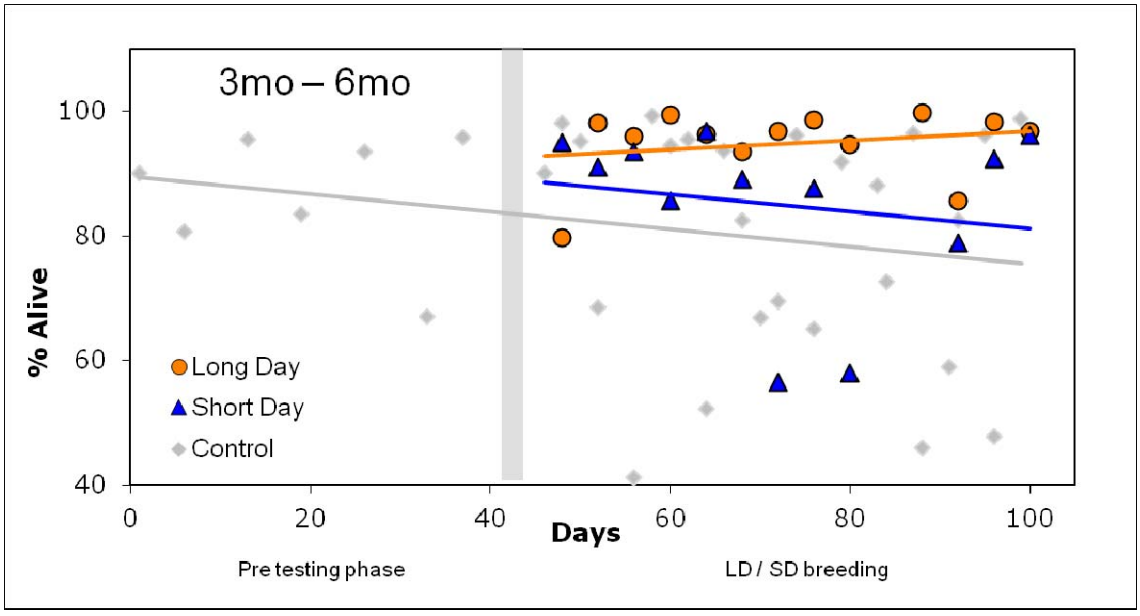

Figure 2.7 - Fertility rates (% of live eggs/clutch) between light entrained adults (3mo-6mo). Day 0-41; entrainment in control (14h/10h) lighting. Days 46-100: breeding in LD (orange points) or SD (blue points). Grey bar indicates the switch from control to experimental light regimes, on days 42/43. Grey points indicate control samples kept in 14h/10h LD conditions.

As shown in Fig 2.8 (middle), fertility rates were significantly different between conditions, with LD fish laying 65% to 79% live eggs per clutch between days 15-32 (LD phase 2 slope = 0.6635), and SD fish laying 40% to 39% live eggs in the same period (SD phase 2 slope = 0.0349; D = 0.650; p = 0.010). After a switch into opposing light conditions (LD into SD, or SD into LD; Fig 2.8, right), fertility of LD clutches dropped from 94.5% to 41.7% eggs/clutch, increasing gradually to 68.2% by day 52 (orange dotted trendline; overall LD phase 3 slope = 1.6536). SD clutch fertility immediate increased when moved to LD conditions from 39.1% (day 32) to 80.0% (day 35). After this initial increase, the "SD into LD" fertility levels dropped precipitously from 80.0% to 0.0% (blue dotted trendline; SD phase 3 slope = -4.7086; Fig 2.8, right). While trends are noted in the 3rd experimental phase (Fig 2.8, right side), data are not significantly different (D = 0.500; p=0.111).

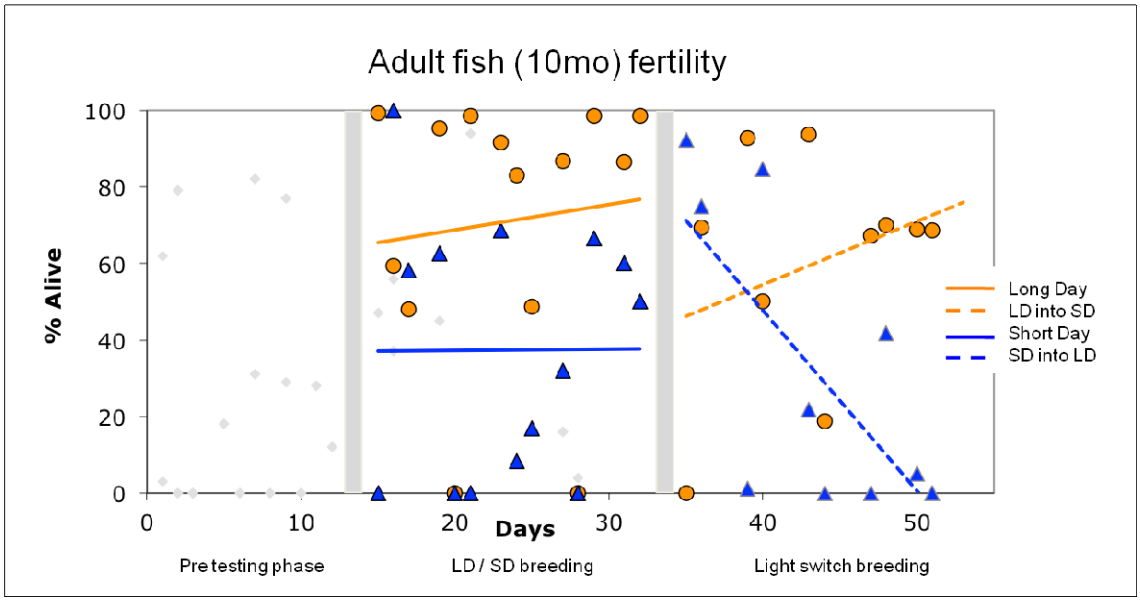

Figure 2.8 - Fertility between light entrained adult (10mo-12mo) fish. Grey bars indicates switch from control to experimental light regimes at day 13/14, and into opposite light conditions at day 33/34 (indicated by dotted trendlines). Tanks were moved into either LD (orange points) or SD (blue points) on days 14-32, and switched into opposite conditions (LD to SD - orange points; SD to LD – blue points; indicated by dotted trendlines) for the remaining testing period (days 34-52).

2.3.4 Gender-specific differences in LD and SD entrained gonad tissues

The effect of photoperiodic lighting conditions on gonad development shows a profound difference between males and females. Gonad weight is significantly different between LD and SD groups in ovaries at 6mo, 11mo, 15mo and 20mo, but not in testes at any time.

Ovary weight was higher in LD than SD entrained females from 6mo-20mo (fig 2.9, bar graph on left axis). During early-to mid life these differences significant at 6mo ($p<0.001$), 11mo ($p<0.05$), 15mo ($p<0.01$) and 20mo ($p<0.05$). Measures taken in later life (24mo and 30mo) show a loss of this LD associated gonadal increase in ovary weight ($p>0.05$, respectively). Interestingly, the difference between LD and SD entrained ovaries were measureable at 6mo, while whole body weight and length measures did not reflect difference between experimental groups until 11mo (comparing figure 2.9 with figure 2.4).

There were no significant differences in testes weight (fig 2.9; line graph on the right axis) at any age (including 30mo, $p > 0.05$), indicating a specific bias in photoperiodic lighting effect on female gonads exclusively.

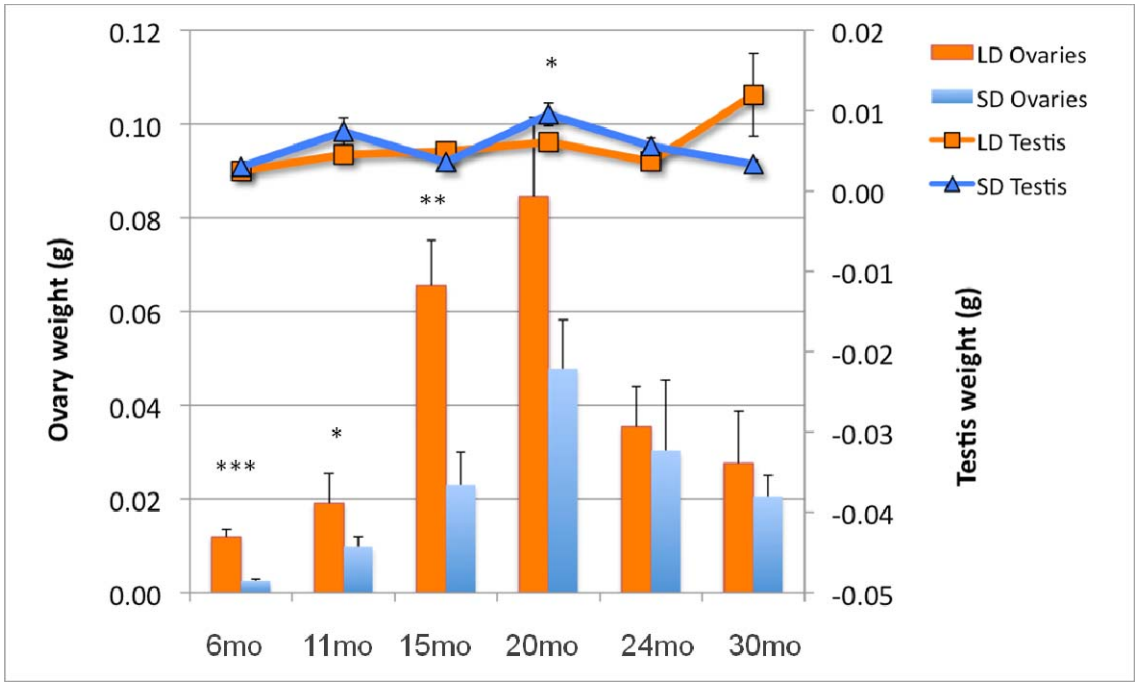

Figure 2.9 - Gonad weight is significantly different in ovaries (bar graph; left axis), LD > SD at 6mo ($p<0.001$), 11mo ($p<0.05$), 15mo ($p<0.01$) and 20mo ($p<0.05$). No differences were shown in testes weight at any age (line graph; right axis). N = 81 to 33 (6mo to 30mo, respectively).

Detailed results of statistical measures and N numbers for fish and tissues tested are provided in Appendix A.

2.4 Discussion

The data presented here clearly indicate a stimulatory effect of lengthening photoperiod on physiological measures such as growth and reproductive capacity. Previous findings have shown that teleost fish growth follows photoperiodic cycles, with long days (summer photoperiods) stimulating growth in diurnal species (Ghomi et al., 2011). These current results confirm the initial hypothesis, that long day entrained zebrafish would have increased growth and fertility (as measured by greater clutch sizes) as compared to short day entrained zebrafish.

2.4.1 Growth differences between LD and SD entrained zebrafish

The current work demonstrates a clear trend in increased body growth, in both weight and length, in LD raised zebrafish, over their SD raised cohorts (see figure 2.4). All fish used in the current studies were raised in 14h/10h lighting conditions for the first 3 months (post-hatch), and were moved to LD or SD conditions thereafter. Interestingly, there was no significant effect of photoperiod on growth at 6mo between groups, while both body length and weight were significantly different at 11mo, 15mo, 20mo and 30mo. This lack of difference at 6mo (after 3mo of light entrainment) suggests that photoperiodic control of growth and maturation may be gated by a development stage in early adulthood (6mo-11mo), when the majority of the fish are reproductively active. Samples of whole body weight and length were pooled, to include both males and females. As females showed significant increases in ovary weight at 6mo (LD over SD), it is important to note that these gonad-specific differences did not alter overall measures of weight. Measures of body weight were linked to length changes throughout the lifespan. Overall, long-day raised zebrafish grew heavier and longer as compared with their short-day counterparts, throughout their lives.

Growth rates are expected to depend on food availability, as fish are primarily visual feeders, longer daylengths are often associated with extended feeding periods. Recent work has shown that during 12h/12h LD conditions zebrafish have nocturnal feeding patterns, with 88.0% of the daily intake occurring in the last 4h of the dark phase. When food availability was restricted to the light phase, feeding activity was altered, while growth rates were maintained (del Pozo et al., 2011). It is important to note that food availability was carefully controlled in the current study, with fish in all conditions being fed twice daily during the light phase of their subjective day (ZT 1 and 6), during which time food was consumed within 5min of delivery. In addition, studies have shown that increasing light duration affects fish growth through better food conversion efficiency, and this rate is higher during increased photoperiods such as LD over SD (Taylor et al., 2006).

The effect of seasonal photoperiods has been most often recorded in smoltifying fish species (fish who move from fresh to sea water during development) such as Gilthead Sea Bream (*S. aurata*) (Mingarro et al., 2002) and Atlantic salmon (*S. salar*) (Bjornsson et al., 1995). Previous experiments have shown that salmon exposed to 7 weeks of SD photoperiods have reduced growth compared to continuously light exposed cohorts (Sigholt, 1997) and parr-smolt transition is dependent on exposure to an increasing photoperiod after short-day conditions (Bjornsson et al., 1995). Interestingly, increasing the duration of the daily photoperiod not only stimulates growth in salmon after smoltification, but also triggers early sexual maturation (Le Bail, 1988).

In freshwater species such as Goldfish (*C. auratus)*, the highest rates of growth in the northern hemisphere are July (LD – summer), and the lowest in February and March (SD – winter) (Marchant & Peter, 1986). In zebrafish, the females tend to be larger than males in both domesticated and wild populations, and have an annual growth and spawning season that commences just before the monsoon season (June-September), when food availability and conditions are optimal (Spence et al., 2007). Researchers have suggested that reproductive maturity is related to body size in zebrafish (Spence et al., 2008), and domesticated zebrafish can reach maturity by 75 days (post-hatch), when zebrafish were 23-24mm in length (Eaton & Farley, 1974). In the samples tested here, LD fish were 21.1mm at 6mo, growing to 27.3mm by 11mo, while SD fish grew from 20.8mm (6mo) to 21.2mm (11mo) and 24.5mm (15mo); during the same time period 3mo-6mo zebrafish females had significant increases in ovary weight, mainly due to oocyte maturation; together these results suggest a link between growth and reproductive maturation, shown in the figures 2.5 – 2.8.

The current set of experiments confirmed an increase in LD-associated growth, but did not examine the role of alternating, cyclic lighting patterns (summer into winter) as would be expected in the wild. Both groups (LD and SD) showed increased growth over time, with the proportion of change being significantly higher in LD-conditioned fish throughout life.

2.4.2 Effects of photoperiod on fecundity in young and mature zebrafish

In the current study, adult zebrafish fecundity (clutch size) and fertility (number of live, successfully fertilized eggs) showed significant differences between fish housed in continuous LD or SD lighting. Two sets of experiments were performed, using young (3mo-6mo) and older (10mo-12mo). Experiment 1 (young fish: 3mo to 6mo), focused on the breeding rates of young fish exposed to different photoperiods over an extended timeline of 100 days. Interestingly, while the LD (16h/8h) group showed a significant increase in fecundity rates over the SD (8h/16h) cohort, these differences were not greater than control (14h/10h) samples. This unexpected result may be due to the same developmental/age related photoperiodic gating effect shown in the growth data of figure 2.4, where LD/SD groups housed in experimental conditions from 3mo to 6mo did not show any differences in body weight or length. While the fecundity of young (3mo-6mo) LD fish show a gradual increase in clutch sizes over time (LD slope = +1.4199; from day 43 to day 100), mature (10mo-12mo) LD fish (in experiment 2) showed significantly greater increases over time (LD slope = +17.308; fig 2.6; phase 1, middle).

In this set of experiments, both young (3mo-6mo) and older (10mo-12mo) adult zebrafish entrained to long day (summer) light conditions show increased breeding rates (Figures 2.5 and 2.6) and successfully fertilized eggs (figures 2.7 and 2.8). Yet, compared to experiment 1 (3mo-6mo) results, sexually mature breeding pairs (experiment 2) laid approximately 30% fewer eggs/clutch at their maximum (fig 2.6, phase 1, middle; approx. 550 eggs/clutch) than their younger cohorts (fig 2.5, right; 850 eggs/clutch).

Findings in Japanese Medaka (*O. latipes*) has shown embryo production drops dramatically after moving LD (16h/8h) entrained breeders into SD (8h/16h) conditions, and ceases completely after 14 days in SD (Koger et al., 1999). Return to LD lighting resumed embryo production within days, indicating a dual control of photoperiod on Medaka embryo production - inhibiting established egg laying rates and re-initiating them after cessation (Koger et al., 1999). In the current

study, SD entrained zebrafish took 100 days to cease egg laying (figure 2.5), and return to LD conditions after SD entrainment (figure 2.6) had an immediate but short-lived rescue effect, with clutch sizes increasing 10-fold, with rates then dropping at the same rate established in the initial entrainment period (Fig 2.6; middle, blue trendline).

Acute changes in photoperiodic fecundity have been noted in Medaka after light switching, with decreased clutch sizes in LD to SD groups, and *vice versa* (Koger et al., 1999). In the current study this 'acute switching' effect was not sustained; previously entrained LD fish increased fertilization rates after the initial (SD-induced) drop and past SD-entrained fish had a steep drop in fertilization rates after the initial (LD-stimulated) increase on day 35 (fig 2.6). These results indicate two time courses for light modulation of reproduction in zebrafish; an immediate effect, shown within 1-2 days and a long-term effect (14-21 days) based on the previously entrained photoperiod. The temporal differences in photoperiodic breeding responsiveness suggests two forms of photoperiodic reproductive control; local (immediate) control of egg release mediated by direct responsiveness in the ovaries and long-term control of gamete development, likely modulated by reproductive hormones such as LH and FSH expressed by the pituitary.

Fertility rates (as measured by live-fertilized vs. dead eggs) were significantly different between LD and SD groups in both young (3.5mo; Fig 2.7) and older (10mo; Fig 2.8) zebrafish populations. Recent results using Siamese fighting fish (*Betta splendens*) have also shown decreased fertility rates in SD over LD photoperiods (Giannecchini et al., 2012). Similar results have been shown in tilapia subjected to a 18h/6h photoperiod, with higher fertility rates than other photoperiods due to action of melatonin on the hypothalamic-pituitary-gonadal triggering the release of hormones responsible for gametogenesis and maturation of gametes (Campos-Mendoza et al., 2004).

When LD entrained fish were moved into SD lighting, there was an initial drop in fertility, returning to initial levels after 14-20 days (Fig 2.8, right, orange dotted trendline). This result is surprising, as this group was maintained in previously inhibitory (SD) conditions, and suggests a protective effect of LD entrainment on the reproductive system. In contrast, SD entrained fish moved to LD conditions show an immediate increase from 40% to 80% successfully fertilized eggs/clutch. This initial increase is short-lived and within 14-20 days, the fertilization rate dropped to 0 %, regardless of the stimulatory LD lighting conditions (Fig 2.8, right, blue dotted trendline). These novel results indicate the sensitivity of zebrafish fertility to photoperiod, and show the important role of parental photoperiodic history to successful breeding.

Further work with this experimental regime is recommended in order to confirm the results provided here with other amenable teleost species, such as Medaka or Goldfish, and were undertaken here as zebrafish provide a relatively rare opportunity to study these "acute photoperiodic switch" effects, due to their small size and amenable housing conditions.

2.4.3 Effects of photoperiod on zebrafish gonadal weight

Gonad weight was significantly different in ovaries entrained to LD over SD throughout adult life (6mo-20mo), but not during old age (24mo-30mo). No differences in testis weight were shown between conditions, at any age. Preliminary histological examinations of SD entrained ovaries revealed oocyte atresia, reduced levels of mature and developing oocytes (data not shown). Similar to other vertebrates, the teleost reproductive cycle has two major phases; the 1st phase controls the proliferation, differentiation and growth of the gametes (spermatogenesis and vitellogenesis), while the 2nd phase controls the maturation and preparation of the oocytes and spermatozoa for release and insemination (Mylonas et al., 2010). Reproductive dysfunctions in males include reduced sperm volume and diminished sperm quality, whereas uneven or failed oocyte maturation is commonly observed in females (Bobe & Labbe, 2010). Changes in ovary, but not testis weight suggest a gender-specific effect of photo-stimulation and reproductive capacity, such that successful oocyte development may be

dependent on long day photoperiods. This confirms similar findings in Medaka, where male gonads maintained a functional morphology, indicated by mature sperm production and large numbers of maturing germ cells in both LD and SD conditions, while female gonads displayed clear oocyte atresia under SD lighting (Koger et al., 1999). Ovarian weight in catfish (*Heteropneustes fossilis*) also increases significantly with an increased daily photoperiod from 12h to 14h, suggesting that oocyte maturation is governed by the increasing photoperiod (Sundararaj & Sehgal, 1970). In both sets of breeding experiments, moving from LD (or control) conditions into SD lighting reduced clutch sizes (fecundity) and number of fertilized eggs (fertility) (Figs 2.4 - 2.7). Coupled with the changes in age-related ovarian weight, these results suggest that females produce immature eggs or fertilization rates depended on behavioral traits not measured in the current study.

These results demonstrate the effects of photoperiod on zebrafish reproduction, by interfering with the control of gonadal maturation and preparation for reproduction, leading to extended delays or even complete inhibition of reproduction (Amano et al., 2000). As hypothesized, spawning fecundity (clutch sizes) and clutch fertility (live/dead eggs) were increased in LD over SD photoperiods, and are likely mediated by the action of melatonin on the HPG (hypothalamic-pituitary-gonadal) axis, triggering the release of hormones responsible for gametogenesis and maturation of gametes (Davies et al., 1999). While I expect increases in LD fertility and growth, the modes of controls underlying these effects are complex, involving changes in the expression and release of a cascade of reproductive hormones from the pituitary. The results shown in this chapter suggest a possible mode of action for melatonin in the maturation of oocytes, mediated by the prevailing photoperiod, working to synchronize oocyte maturation and ovulation to specific temporal windows. Further investigation into the neuroendocrine control of zebrafish photoperiodism in reviewed in chapters 3 and 4.

CHAPTER 3 – PHOTOPERIODIC HORMONE EXPRESSION

3.1 Introduction

The molecular mechanisms of the circadian clock have been extensively investigated in vertebrates (Hazlerigg, 2012). In mammals, the master circadian clock is located in the suprachiasmatic nuclei of the hypothalamus (SCN). Light signals from the retina reach the SCN directly via the retino-hypothalamic neural tract. Photoperiod duration is encoded by the electrical activity of the SCN master clock, which signals to the pineal gland, controlling the rhythmic secretion of melatonin, the main hormone associated with circadian biology. Internal representation of seasonality is therefore encoded by the presence and duration of melatonin in systemic circulation (Morris et al., 2012). Downstream targets of melatonin include the hypothalamus and pituitary gland (Morris et al., 2012). The anterior pituitary (adenohypophysis) expresses melatonin receptors and consists of several different cell types, characterized by the peptide hormones they secrete; such as the lactotropes which generate prolactin (PRL), somatotropes - growth hormone (GH), thyrotrophs - thyroid-stimulating hormone (TSH), gonadotropes, secreting follicle-stimulating hormone (FSHβ) and luteinizing hormone (LHβ) and corticotropes secreting adrenocorticotropic hormone (ACTH) (Nica et al., 2006), as shown in figure 3.1.

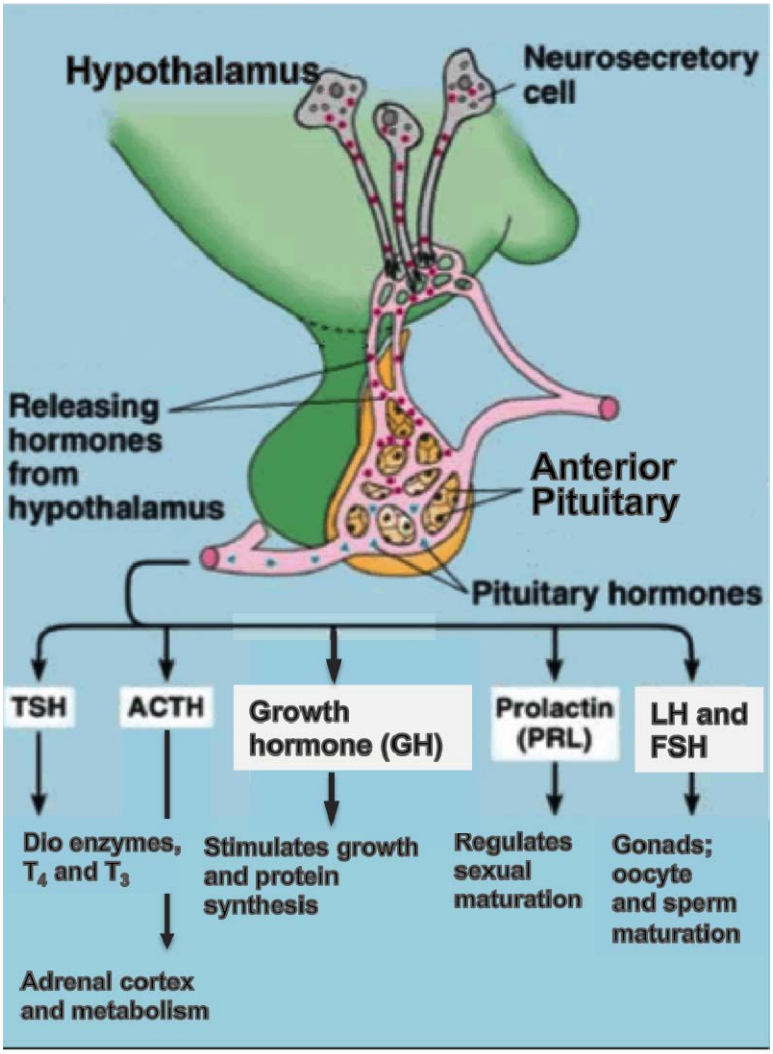

Figure 3.1: mRNA expression of hypothalamic and pituitary hormones. Releasing hormones from the hypothalamus include GHRH and GH, stimulating the expression of LH, FHS, PRL and GH in the anterior pituitary (adapted from Fox, 1984).

Seasonal differences in melatonin, melatonin receptor expression and hypothalamic/pituitary hormones may reflect both day length and season, giving cues for both circadian and annual physiological changes. For reasons discussed earlier, circulating melatonin levels were not recorded in the current work. This chapter explores the daily and lifelong differences in hormone and melatonin receptor expression in the hypothalamus and pituitary in zebrafish raised in LD or SD light regimes. While melatonin receptor expression is itself seasonal, direct measures of circulating melatonin would provide a more complete understanding of seasonal physiology and is recommended in future work. Together, measures of melatonin and tissue-specific melatonin receptors would be helpful. These data

provide evidence of the key link between photoperiodic input to seasonal fertility at the cellular and tissue levels of zebrafish physiology, expanding the role of circadian clock components from simple daily timers to short and long term time-givers, encoding information regarding seasonal and annual timing.

3.1.1 GnRH and gonadotrophin expression

Vertebrate growth and reproduction is mediated by the hypothalamic-pituitary-gonadal axis (HPG), controlling the release of a host of neuroendocrine hormones in a seasonal manner (Migaud et al., 2010). In mammals, ventral hypothalamic cells release GnRH in seasonally modulated pulses into the portal blood system, carrying it to the anterior pituitary (Chappell, 2005). These photoperiodic GnRH pulses are used as a seasonal cue for the appropriate release of LH and FSH, which target the reproductive organs, causing the release of testosterone and oestrogen; stimulating overall reproductive activity (Nett et al., 2002). In addition, teleost GnRH fibers entering the pituitary are thought to be capable of releasing GH (Marchant et al., 1989) and PRL (Weber et al., 1997). As detailed in section 1.5.1, zebrafish GnRH has 2 main forms, including GnRH3, found predominantly in the fish ventral telencephalon, preoptic and anterior hypothalamic regions. This GnRH3 isoform was selected for hypothalamic measurements in the current work, and is referred to as GnRH hereafter. The current work profiles GnRH expression in the preoptico-hypothalamus, with comparative measures of LH, FSH, TSH and PRL from the pituitary of LD and SD entrained zebrafish populations.

3.1.2 GHRH and GH expression

The classic view of anterior pituitary GH release is based on the stimulation of GHRH (growth hormone releasing hormone) from the hypothalamus, and GHRH has been shown to stimulate GH release in teleost fish (Lee et al., 2007). Tissue distribution studies have shown showed that teleost GHRH is expressed primarily in the brain, with GHRH receptors actively expressed in both the brain and pituitary (Lee et al., 2007). Recently, GHRH has been shown to stimulate GH release from pituitary cells in goldfish (*C. auratus)* (Grey & Chang, 2013). GH acts mainly to modulate postnatal growth, and contributes to regulating metabolism,

reproduction, immunity, development, and osmoregulation in different species (Gahete et al., 2009). Samples of zebrafish specific GHRH and GH were taken from hypothalamic and pituitary tissues and measured for circadian and lifespan expression in LD and SD photoperiodic conditions.

3.1.3 Melatonin receptor expression (MT1, MT2 and Mel1c)

Transduction of photoperiodic information via the retino-hypothalamic-pineal pathways leads to melatonin secretion patterns reflecting the length of the dark period (Davies et al., 1999). The expression of pineal melatonin has been linked to fish growth and reproduction, with species-specific differences (Falcon et al., 2010), and in zebrafish, administration of melatonin has recently been shown to increase egg production and maturation (Carnevali et al., 2011). Due to the wide range of receptor distribution in the teleost brain, melatonin may have a number of different physiological effects in fish (Gaildrat & Falcon, 1999).

Two melatonin receptor isoforms, MT1 and MT2 (Mel1a and Mel1b in older papers) are commonly expressed in a host of vertebrates such as mammals and birds. In mammals, MT1 is expressed in the SCN and pars tuberalis, and is thought to mediate the circadian response to melatonin, while MT2 is expressed most commonly in the retina (Reppert et al., 1994). In fish, three high affinity melatonin receptor subtypes have been identified; MT1 (Mel1a), MT2 (Mel1b) and Mel1c, which are thought to mediate various physiological functions of melatonin in the central nervous system and peripheral tissues (Reppert et al., 1996). Both MT1 and MT2 are widely distributed in the brain and retina, whereas Mel1c expression is mainly found in peripheral nervous tissue (Park et al., 2007b). Measures of Mel1c in the current study were of such low abundance that data could not be recorded consistently in the areas of interest (hypothalamus and pituitary) and were not included in the following analysis.

Seasonal expression of melatonin receptors in downstream tissues such as the gonads may allow for direct control of photoperiodic reproduction (Sauzet et al., 2008) or indirectly via the centres of neuroendocrine control such as the hypothalamus and pituitary (Gaildrat & Falcon, 1999). The data presented here

addresses the expression of melatonin receptors in the hypothalamus and pituitary, and profiles the difference in hormone expression in LD and SD entrained tissues.

3.1.4 TH, TSH and Dio expression

Thyroid hormone has been strongly linked to seasonal growth and suggested to be a circannual timing mechanism in vertebrates (Hazlerigg & Loudon, 2008). The main TH isoforms, T_4 and T_3 act in opposition to each other to activate or inhibit TH signaling in target tissues. The availability of T_4 and its conversion into the biologically potent T_3 form is governed by changes in deiodination enzyme activity in local tissues (Hazlerigg & Loudon, 2008). In the mammalian and avian hypothalamus, the local expression of type 2 deiodinase (Dio2) and type 3 deiodinase (Dio3) has been shown to change with seasonal photoperiods and likely mediates downstream neuroendocrine expression in a light-responsive manner (Lechan & Fekete, 2005). Summaries of these pathways are shown in figures 1.8 and 1.9. In mammals, pituitary derived TSH acts within the mediobasal hypothalamus to control tanycyte DIO gene expression (Hanon et al., 2008) and the majority of MT1 positive cells also express TSH, in a photoperiodic manner (Dardente et al., 2003). The current findings describe the circadian and lifespan expression of teleost TSH in the pituitary and Dio1, Dio2 and Dio3 in the zebrafish hypothalamus and suggest a link between melatonin receptors, TSH and deiodinase enzyme expression in light entrained brain tissues.

Initial experiments were performed to determine the circadian expression of these targets, allowing optimal timing of long-term tissue sampling in later phases of research. Long-term hormone profiling was taken from photo entrained (LD and SD) groups over the course of the zebrafish lifespan (6mo, 15mo, 24mo). These assays provide a profile of daily and lifelong neuroendocrine signalling in zebrafish, and establish a clear correlation between seasonal light exposure and photoperiodic hormone expression. Expanding of my initial investigations (see chapter 2), I hypothesized that reproductive and growth hormone expression from LD entrained samples would be increased throughout life, and in the light phase (ZT 3 and 9) of a given light/dark circadian cycle. Conversely, I expected SD

entrained samples to show low or inhibited growth and reproductive hormone expression throughout life. As with other models described above, expression of hypothalamic GnRH and pituitary gonadotroph mRNA levels were expected to correspond, with increased expression in LD over SD conditions. Growth hormones mRNA expression was expected to peak in the late night or early morning (ZT 21 or ZT 3), with corresponding increases in GHRH in the hypothalamus. Expression of MT1, MT2 and Mel1c in zebrafish hypothalamus and pituitary samples are novel and were monitored with the expectation of increased mRNA expression of all 3 isoforms in the dark (ZT 15 and 21), and higher expression in SD over LD entrained samples throughout life. Data regarding mRNA expression of Dio1, 2, 3 and TSH were also new in this model, but I expected increased in TSH, LH and FSH in LD pituitaries, and increased Dio2 mRNA expression in LD hypothalamic samples, as shown in figure 1.9 (chapter 1).

3.2 Methods and Materials

3.2.1 qPCR experimental sampling

Circadian target expression

The following circadian experiments focused on the periodicity of tissues over a single 24h period. Tissue samples were taken at ZT 3/9/15/21, having been entrained beforehand to a 12h/12h light dark cycle in specially designed light cabinets (see fig 2.2). Hypothalamic and pituitary samples were pooled separately (N = 5), and tested in triplicate (15 samples tested per condition, per timepoint, with 60 individual samples total). Samples were tested in triplicate on each qPCR plate. All individuals were age-matched cohorts (5mo old) and entrained for 7 days before sampling began.

Lifespan photoperiodic target expression

Fish were raised in LD (16h/8h) or SD (8h/16h) lighting cabinets from 3mo – 30mo, and were housed as described earlier (see Chapter 2 methods). Hypothalamus and pituitary samples were taken from fish at 6mo, 15mo and 24mo. All tissue samples were taken at ZT 9, the timepoint at which the majority of

the genes of interest are most abundantly expressed (see fig 3.2 and 3.3). These samples were pooled (n=5) into a single Trizol tube for RNA extraction and 5 samples of RNA were taken for analysis (n=25 fish per condition). qPCR measures were taken in triplicate, and mean values used for analysis. Samples were taken from 150 fish total, for age groups (6mo/15mo/24mo) and photoperiodic (LD and SD) conditions.

3.2.2 RT-PCR protocol

Total RNA was extracted from tissue samples using TRIzol reagent (Invitrogen, Life Technologies, Grand Island, NY) according to the manufacturer's instructions. The quality and quantity of the RNA was confirmed by NanoDrop (Thermo Fisher Scientific, Loughborough, UK). 1µg of total RNA (Hypothalamus) or 0.1µg (Pituitary) with ultrapure water up to 9.5µl, was incubated with 1µl Oligo-dT primer mix (10 µM), 1µl Random Hex primer mix (10 µM) and 1µl dNTP mix (10 µM) for 5 min at 65°C. Then, 4 µl RT buffer x5, 2 µl dTT (dithiothreitol 100 mM), 1 µl RNAse Out (40 U/µl) and 1 µl Superscript-II reverse transcriptase (Invitrogen) were added and the reaction was incubated at 25°C for 10min, 42°C for 1 hour, 70°C for 15min, held at 4°C.

3.2.3 qPCR protocol

cDNA was stored at -20°C before qPCR processing. The real time PCR was performed using a RealPlex quantitative PCR machine (Eppendorf, Cambridge, UK) and SYBR Green I kit (Invitrogen).

The PCR reaction was carried out 20µl/well, containing 2µl cDNA (1:5 dilution), 7µl of H_2O, 1µl 5' primer (10 µM), 1µl 3' primer (10 µM) and 9µl of mix (SYBR Green II). The qPCR reaction was run for 2min at 95°C, 15s at 95°C, 15s at 60°C, 15s at 68-72°C (depending on primer melting temps) for 30-40 cycles. Melting curves were analysed for specificity of the resulting PCR products and the absence of primer dimers.

3.2.4 qPCR target analysis and normalization

Extensive normalization pre-testing was performed to evaluate the rhymicity of candidate housekeeper targets, including Ubq, bActin and RPL-13 (data not shown). Ubq was confirmed to be non-circadian and non-photoperiod responsive (data not shown). The specific primers (and their GenBank accession numbers) used to amplify targets of interest are listed in Appendix B.

For each transcript, the efficiency (E) of each primer set was calculated from the slope of the standard curve using the formula: E = 10(-1/slope) -1, and only primer sets with E-values higher than 95% (where 100% = 1) were used for further long-term sampling (calculations not shown).

Gene expression was analyzed using the $2^{-\Delta\Delta Ct}$ method (Bustin, 2002), and was normalised against (Ubq) mRNA expression in the same samples and expressed as relative to a single "baseline sample" taken at ZT 21 for each target tested. For each qPCR value presented in the following graphs, the average of 3 replicate wells was taken and compared to the average of 3 replicate Ubq measures from the same tissue sample. These values were compared to get a "calibrated" value (Mean target/Mean Ubq; at a single timepoint), this calibrated number is expressed relative to the expression of a single well of the target gene taken at ZT 21 (lowest time of expression). This method allows the calibration of oscillating genes in reference to a non-oscillating control (Ubq), and gives a reference in relation to a universal fixed point in the circadian cycle (ZT 21).

3.2.5 qPCR targets

Targets of hypothalamic circadian expression included the diodinases enzymes Dio1, Dio2 and Dio3; GnRH, and GHRH. Melatonin receptors 1 and 2 were measured while Mel1c levels were not sufficient for qPCR recordings. Hypothalamic levels of circadian genes *Per1*, *Per3* and *Cry1a* were also tested, with the exclusion of Per 2, a known light-inducible gene, not suitable for circadian profile testing. Pituitary samples tested in this set of experiments include GH, LH, FSH, PRL, TSH, melatonin receptors (MT1, MT2) and the circadian genes *Per1*, *Per3* and *Cry1a*. The inclusion of *Per1*, *Per3* and *Cry1a* recordings in circadian

experiments provided positive controls, illustrating the oscillating profile and abundance of classic circadian clock mRNA targets in the tissues of interest. Tables of qPCR mean values of target expression at each timepoint (relative to samples of same target at ZT 21) are included in Appendix C.

3.2.6 Statistical testing

All samples were measured in triplicate by qPCR, and expressed as Mean ± SEM (standard error of the mean). The normality of the distribution and homogeneity of variance were tested, normally distributed data was analysed, using a 1-way Anova (between subjects) to compare multiple targets at each timepoint or condition. Post-hoc testing was conducted with the Tukey HSD (Honest Significant Difference) test, using the online stats calculators (http://www.physics.csbsju.edu/stats/ and http://web.mst.edu/~psyworld /tukeyscalculator.htm; accessed Spring 2011). The level of statistical significance was set at $p<0.05$ (significant), $p<0.01$ (highly significant), and $p<0.001$ (extremely significant). Anova and Tukey HSD results for circadian results are listed in appendices D.1 and D.2; lifespan measures are listed in appendices D.3 – D.6.

3.3 Results

3.3.1 qPCR Hypothalamic target expression over circadian timepoints

Initial circadian experiments focused on the daily cyclic expression of hormones and receptors in the zebrafish brain and is shown in fig 3.1 a-d. Overall, hormone and receptor targets showed moderate circadian oscillations, the majority of which showed single peaks at ZT 9 (late day), with up to 3-4 fold higher than base levels in Dio2, GnRH and MT1 (fig 3.1 b-d).

The classic core clock genes *Per1* and *Per3* showed highly significant expression levels during the day (ZT 3, 9 > ZT 15, 21; $p<0.001$), with early morning (ZT 3) *Per1* levels peaking 11-fold higher than baseline levels (ZT 3 > ZT 21; $p<0.001$). A distinctive peak in hypothalamic *Cry1a* mRNA levels was shown at ZT 9 as compared with all other timepoints tested (ZT 9 > ZT 3, 15, 21; $p<0.001$; fig 3.1a).

These genes were the most abundant targets tested in the zebrafish hypothalamus, with clear changes in circadian expression, up to 11 fold higher than baseline measures (at ZT 21).

Hypothalamic GnRH expression peaked at ZT 9, with highly significant differences between this and other timepoints (ZT 9> ZT 3, ZT 15, $p<0.001$; ZT 9> ZT 21; $p<0.01$; figure 3.1b). GHRH had bimodal expression peaks, at ZT 9 and ZT 21 (fig 3.1b). GHRH ZT 9 samples were significantly greater than ZT 3 and ZT 15 ($p<0.01$), while the late night peak at ZT 21 was significantly higher than ZT 3 and ZT 15 ($p<0.05$).

Circadian expression of melatonin receptors (MT1 and MT2) in the hypothalamus was distinctive, with a single, highly significant circadian peak was found in hypothalamic MT1 expression at ZT 9 ($p<0.001$), while recordings taken in the evening, night and early morning (ZT 15, 21 and 3) were stably expressed. MT2 expression was stably expressed and showed no circadian oscillations between day and night. The specificity of these melatonin receptor subtype differences is remarkable and suggests a unique role for MT1 receptors in mediating circadian information.

Hypothalamic Dio2 expression showed a specific and significant circadian peak at ZT 9 (Fig 3.1d; Dio2 ZT 9 > ZT 3, ZT 15, $p<0.01$; ZT 9 > ZT 21; $p<0.001$), while Dio3 levels were higher in the late day/evening (ZT 9, ZT 15), over early morning and late night timepoints (ZT 21, ZT 3; fig 3.1d, $p<0.01$). Interestingly, hypothalamic Dio1 expression was clearly not circadian, with stable expression levels throughout the day and night. These differences in circadian expression of Dio 1-2-3 in the hypothalamus is interesting in that there is a single distinct peak in Dio2 (ZT 9), as compared with all other Dio measures across the light/dark cycle.

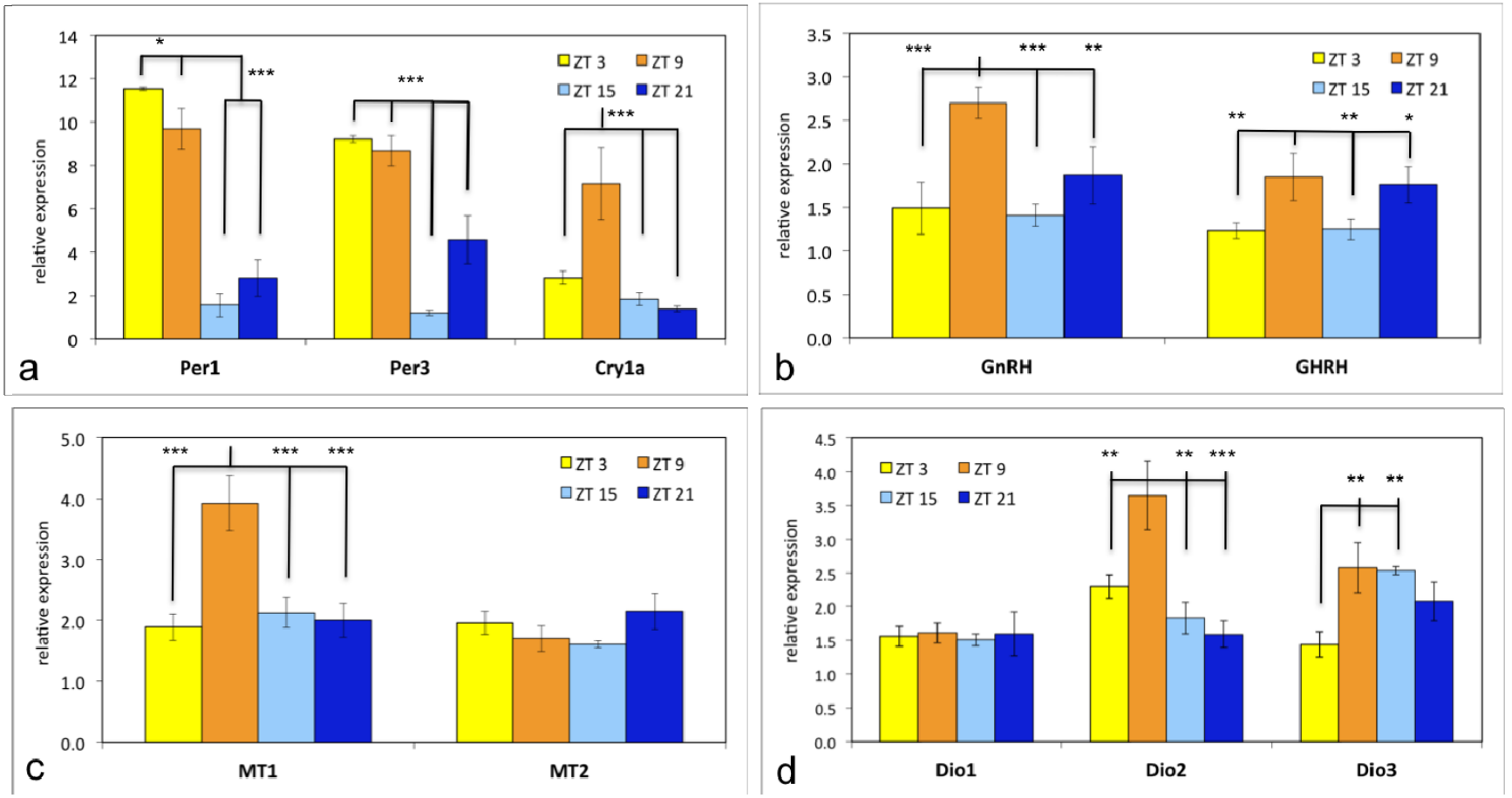

Figure 3. 2 - Circadian expression of qPCR targets in the hypothalamus. All values expressed relative to a single baseline value at ZT 21 in each target group. Error bars represent SEM; tissue samples were pooled (N = 5), and tested in triplicate (15 samples tested per condition, per timepoint, with 60 individual samples total). Significant differences between all values within a group are shown in Appendix D.

3.3.2 qPCR Pituitary target expression over circadian timepoints

Circadian expression in the pituitary *Per1*, *Per3* and *Cry1a* levels mirrored patterns found in the hypothalamus, high at ZT 3-9, and low at ZT 15-21 (see figs 3.2a and 3.3a). *Per1* expression increased significantly, 25 fold (ZT 3) and 14 fold (ZT 9) over baseline levels, dropping significantly in the dark (ZT 3>ZT 9, 15, 21; $p<0.001$; ZT 9>ZT 15, 21; $p<0.001$). *Per3* changed significantly, with early morning peaks (ZT 3), dropping thereafter (ZT 3>ZT 9, $p<0.01$; ZT 3>ZT 15, 21; $p<0.001$; ZT 9>ZT15, 21, $p<0.01$). Pituitary *Cry1a* expression had a specific and significant peak at ZT 9 (ZT 9>ZT 3, 15, 21; $p < 0.001$). *Cry1a* expression at ZT 9 was 27 fold higher than relative baseline values, demonstrating a strong circadian influence in the late afternoon. Overall, the 3 classically defined circadian targets measured in the pituitary, *Per1*, *Per3* and *Cry1a*, were expressed up to 3 fold higher than other targets (such as MT1, LH or FSH).

Daily pituitary GH expression had a distinctive (and significant) peak at dawn (ZT 3>ZT 9, 15, 21; $p<0.01$), as compared to time points tested, which were stably expressed. LH, FSH, PRL and TSH level all showed a bi-modal increases in expression at ZT 9 and ZT 21, while samples taken at dawn (ZT 3) and dusk (ZT 15) were low (fig 3.3b). LH ZT 9 and ZT 21 expression was significantly greater than ZT 3 and 15 (ZT 9, 21>ZT 3,15; $p<0.01$). FSH and PRL were similar in expression (although PRL comparisons were not statistically different), with the greatest levels of FSH at ZT 9 (ZT 9>ZT 3, 21; $p<0.05$; ZT 9>ZT 15; $p<0.01$). Pituitary TSH ZT 9 levels were significantly higher then timepoints tested (ZT 9>ZT 3, 15, 21; $p<0.001$). Overall, a trend in circadian hormone expression can be shown in figure 3.3b, where highest expression is in the late day (ZT 9), with a smaller increase at ZT 21, in the late night, just before dawn.

Melatonin receptors showed clear circadian expression in the zebrafish pituitary. MT1 expression was significantly higher at dawn (ZT 3), 8.5 fold over baseline levels (ZT 3>ZT 9, 15, 21; $p<0.001$), decreasing throughout the night, until a circadian rise at ZT 21, in anticipation of dawn. MT2 levels had a degree of circadian expression, with a single peak at dawn, 4 fold higher than baseline levels (ZT 3>ZT 9, 15, 21; $p < 0.001$). Other times showed a gradual (non-significant)

increase in expression through the night. Clearly, circadian control of melatonin receptors in the pituitary is significantly more focused in MT1 over MT2 receptors, suggesting different roles and sensitivities of these receptors to circadian (and therefore likely seasonal) photoperiods.

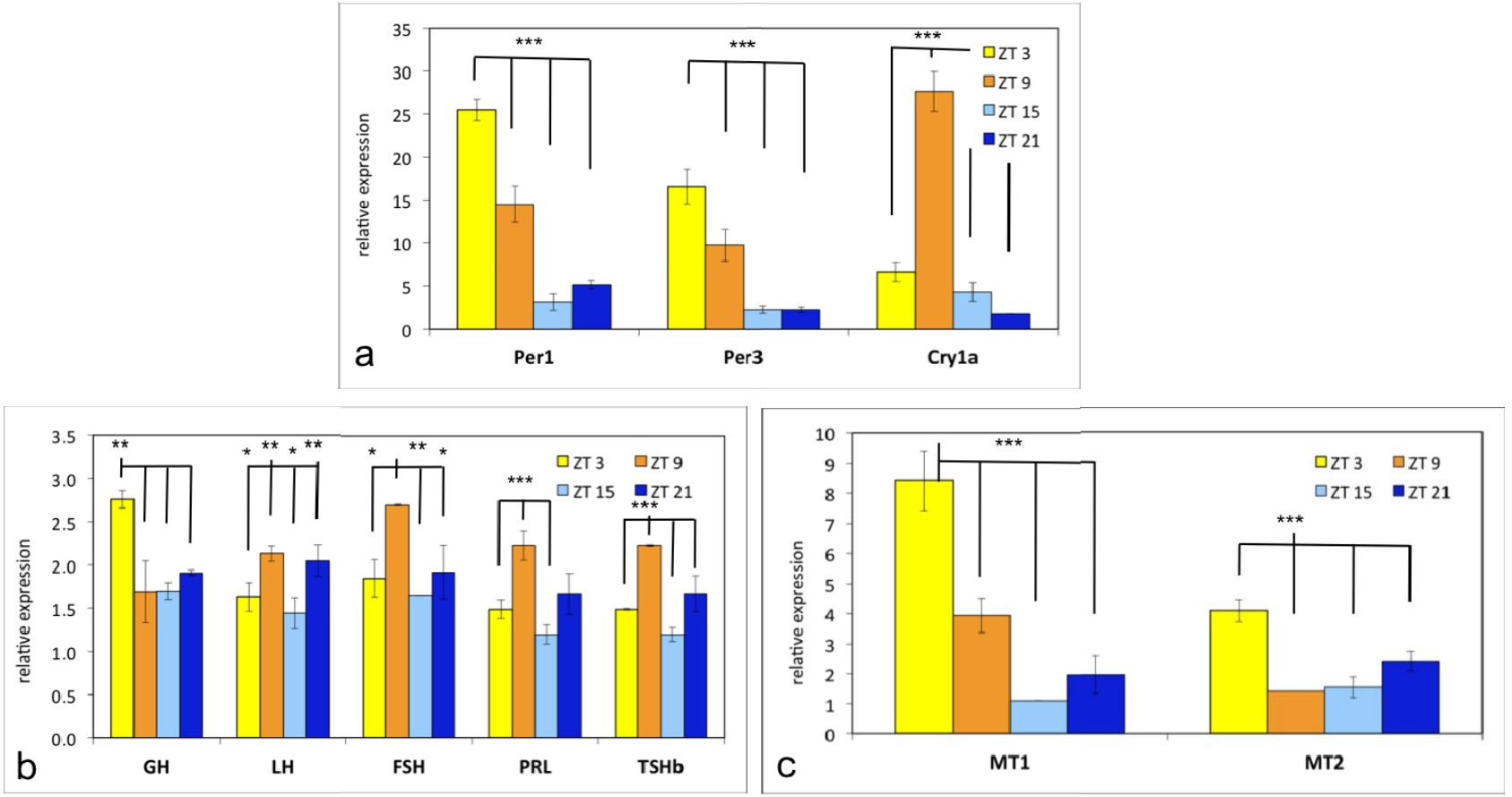

Figure 3.3 - Circadian expression of qPCR targets in the pituitary. All values expressed relative to a single baseline value at ZT 21 in each target group. Error bars represent SEM; tissue samples were pooled (N = 5), and tested in triplicate (15 samples tested per condition, per timepoint, with 60 individual samples total).

3.3.3 qPCR Hormone targets over *lifespan*

Having characterized the circadian expression of the genes of interest (section 3.3.2), it was possible to optimize DNA sampling for long-term sampling, as the majority of the genes of interest were most abundantly expressed at ZT 9 (late day). The following data and expression rates are discussed in terms of physiological links, with both hypothalamic and pituitary targets discussed together, in relation to their known biochemical inter-relationships.

3.3.3.1 qPCR GnRH and gonadotrophin hormone expression over lifespan

GnRH expression was higher in SD fish during early life (6mo-15mo), as compared to LD samples and this difference in expression was lost by old age (24mo), as shown in fig 3.4a. The clear increase in short day expression of gonadotrophin-releasing hormone is unexpected, as zebrafish breeding is clearly inhibited by long term SD exposure (see chapter 2). The age specific differences at 6mo and 15mo are synchronized, with a similar 1.9 fold increase in SD over LD measures in both samples, before aged fish lose this distinctive SD > LD expression pattern (see fig 3.4a).

The photoperiod expression of pituitary gonadotrophic hormones (LH, FSH, PRL and TSH) is significantly higher in SD over LD samples in early life (6mo). FSH samples were SD>LD throughout life (6mo, 15mo, 24mo), while TSH levels were SD>LD with decreasing differences at 15mo and 24mo. By 24mo, LH, PRL and TSH were not significantly different between LD and SD (only FSH maintained the previous SD>LD results; fig 3.4e). The 6mo peak in SD>LD pit hormones is synchronized with measures of GnRH in the hypothalamus, and may be associated with a generalized increase in pituitary hormones and hypothalamic releasing factors under short-day conditions.

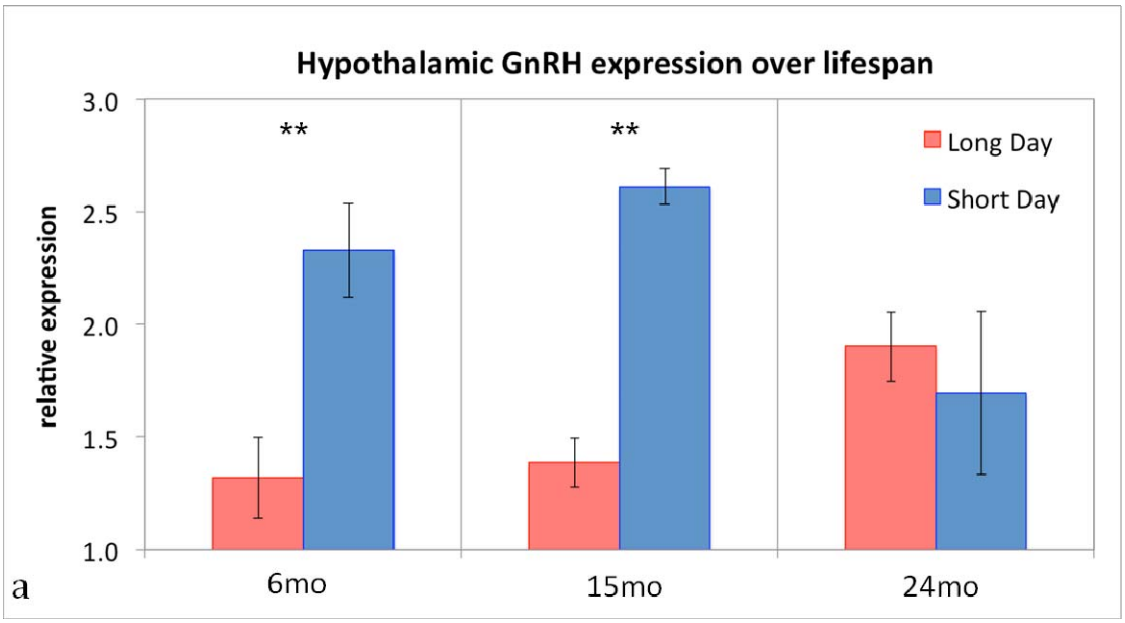

Figure 3.4 - qPCR measures of (a) Hypothalamic GnRH,

(on next page) (b) Pituitary LH, (c) FSH, (d) PRL, and (e) TSH expression in LD and SD photoperiods throughout life. Gene expression in LD samples are shown in red; SD samples in blue. Samples were taken at 6mo (left), 15mo (middle) and 24mo (right) in all figures. Error bars represent SEM; 5 sets of tissue samples were pooled into each tube, with 5 tubes tested at each timepoint and condition (N = 25). mRNA samples were tested in triplicate (75 individual samples at each timepoint).

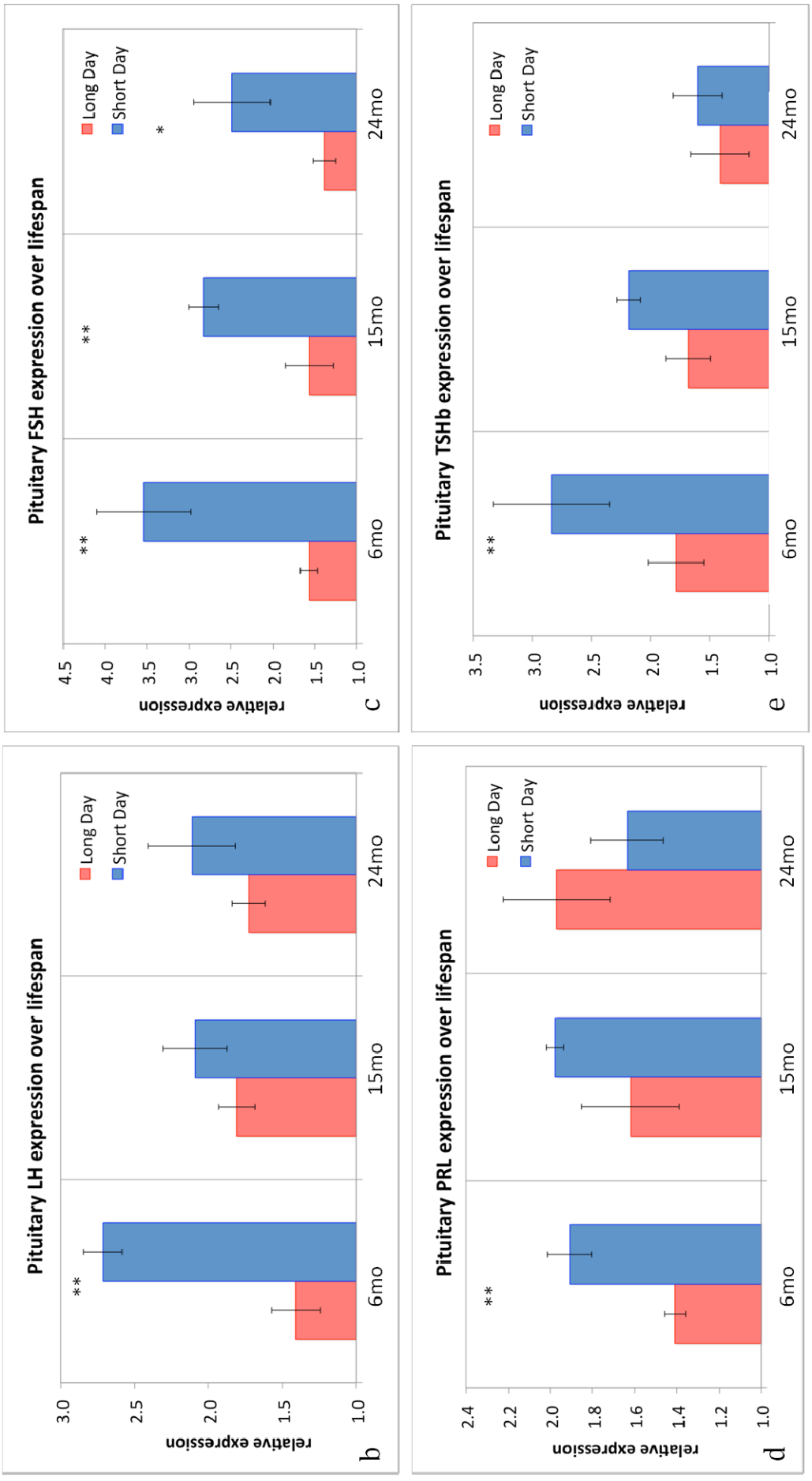
Pituitary FSH expression over lifespan
Long Day
Short Day
relative expression
4.5
4.0
3.5
3.0
2.5
2.0
1.5
1.0
**
**
*
6mo
15mo
24mo
c
Pituitary TSHb expression over lifespan
Long Day
Short Day
relative expression
3.5
3.0
2.5
2.0
1.5
1.0
**
6mo
15mo
24mo
e
Pituitary LH expression over lifespan
Long Day
Short Day
relative expression
3.0
2.5
2.0
1.5
1.0
**
6mo
15mo
24mo
b
Pituitary PRL expression over lifespan
Long Day
Short Day
relative expression
2.4
2.2
2.0
1.8
1.6
1.4
1.2
1.0
**
6mo
15mo
24mo
d

Looking at hormonal expression in detail, pituitary LH levels were significantly higher in SD over LD levels at 6mo ($p<0.01$), before equalizing (with no significant differences between SD and LD) at 15mo and 24mo (fig 3.4b). Distinctive (and significant) increases in expression of FSH in SD groups was shown throughout the lifespan (SD>LD; $p<0.01$ at 6mo, 15mo; $p<0.05$ at 24mo), with a gradual decrease in these levels overtime, while LD FSH levels remained stably expressed throughout life.

Pituitary PRL expression was significantly higher at 6mo (SD > LD; $p<0.01$), and maintained a similar pattern of expression at 15mo. Significance in SD>LD measures was lost at 15mo and 24mo, due to increased variability in LD PRL measures, with gradually increasing PRL levels in LD samples throughout life (see fig 3.4d), a trend which seems specific to PRL specifically

Echoing expression rates in FSH samples, TSH levels were significantly higher in SD over LD samples at 6mo ($p<0.01$), with a gradual decline in SD TSH over time. Similar to long day FSH levels, LD TSH expression was stably expressed throughout life, with no significant differences between age groups in this condition.

Overall, high levels of hypothalamic SD entrained GnRH expression at 6mo and 15mo are reflected in the target expression of the downstream pituitary hormones, LH, FSH, PRL and TSH; all hormonal measures indicate a greater SD over LD expression pattern at 6mo and 15mo. Lowered GnRH levels at 24mo were consistent with decreased SD hormonal expression (fig 3.4a). LD entrained GnRH expression was sustained between 6mo and 15mo, increasing at 24mo. This trend is reflected in LD PRL expression, but reversed in LD LH levels over time. LD FSH and TSH expression levels were not significantly different over lifespan and did not reflect a change in GnRH expression as shown in fig 3.4.

3.3.3.2 qPCR GHRH and GH expression over lifespan

GHRH expression in the hypothalamus was variable over the sampling ages tested, with SD>LD at 6mo ($p<0.01$), LD<SD at 15mo ($p<0.01$) and no difference between conditions at 24mo. Considering the dramatic shift in GHRH results, further testing between 6mo-15mo is recommended to further explore this result.

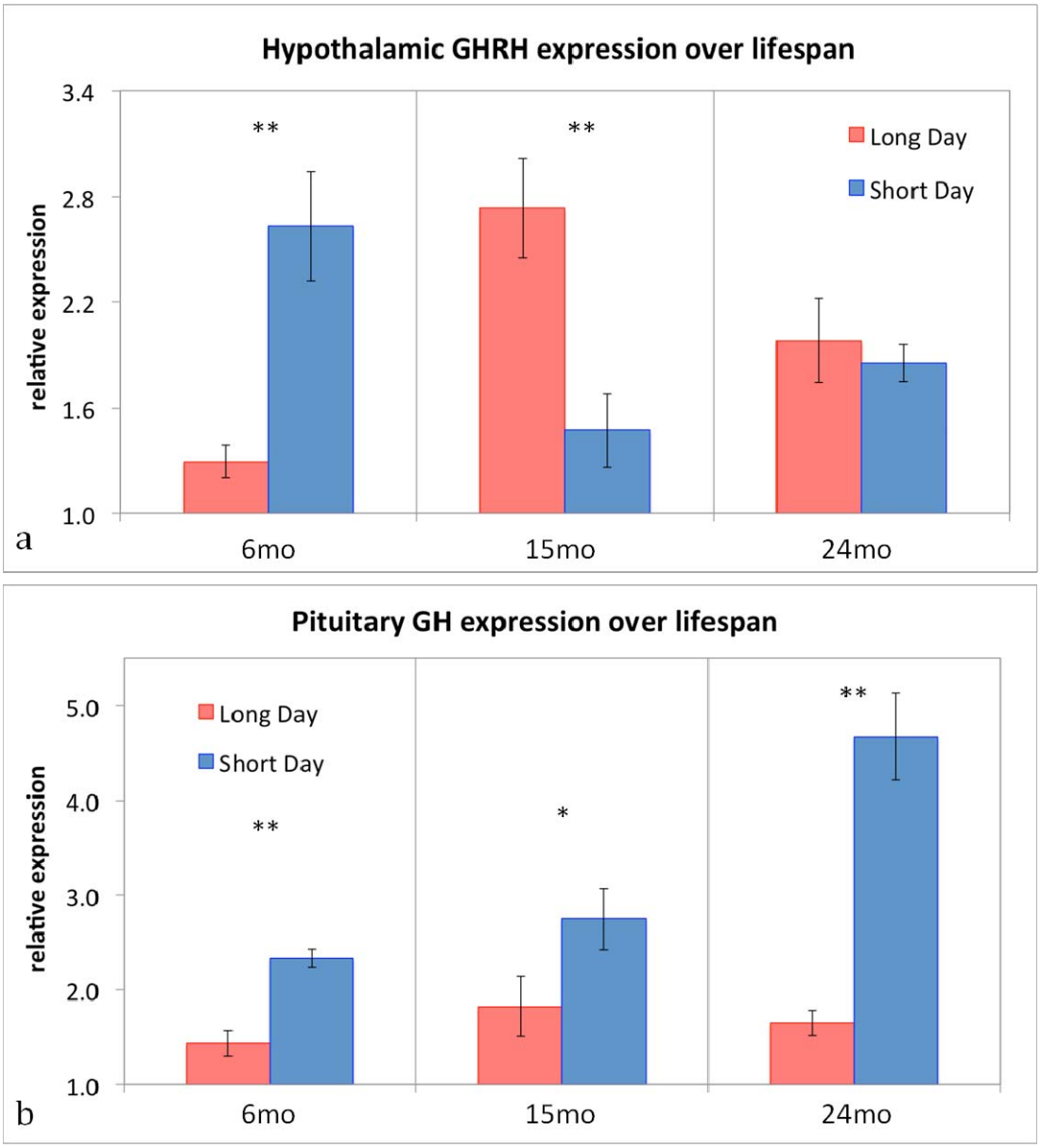

Figure 3.5 - qPCR measures of (a) Hypothalamic GHRH, and (b) Pituitary GH expression in LD and SD photoperiods throughout life. Gene expression in LD samples are shown in red; SD samples in blue. Samples were taken at 6mo (left), 15mo (middle) and 24mo (right) in all figures. Error bars represent SEM; 5 sets of tissue samples were pooled into each tube, with 5 tubes tested at each timepoint and condition (N = 25). mRNA samples were tested in triplicate (75 individual samples at each timepoint).

Interestingly, the trend in GHRH expression between groups is inverse between 6mo and 15mo , where levels are low in LD GnRH (6mo) and significantly higher at 15mo; while SD GnRH levels start high (6mo), then drop significantly at 15mo, matching LD levels at 24mo (as shown in fig 3.5a).

Levels of pituitary GH expression were significantly different between photoperiodic conditions with SD > LD at 6mo ($p<0.01$), 15mo ($p<0.05$) and 24mo ($p<0.01$). The most notable relationship in lifespan expression of GH is the significant increase in SD GH from 15mo to 24mo (approximately 60%) (fig 3.5b). Interestingly, the increased expression of GHRH in LD hypothalamic samples (at 15mo specifically) was not linked with downstream pituitary (LD) GH levels, which remained low throughout life.

3.3.3.3 qPCR MT1 and MT2 expression over lifespan

Photoperiodic expression of the melatonin receptors MT1 and MT2 were markedly different in hypothalamic and pituitary samples, over lifespan.

In the hypothalamus, MT1 expression showed no differences between LD and SD groups until 24mo, where LD MT1 showed a significant increase over SD levels ($p<0.01$, fig 3.6a). Within the pituitary, MT1 expression was significant only in late life, with SD>LD ($p<0.01$; fig 3.6b). MT1 expression in the pituitary was 43% higher than peak hypothalamic MT1 expression, as noted by the difference in axis between fig 3.6a and b. Hypothalamic LD MT1 increased in late life, but remained low in LD pituitary 24mo samples, with no change in expression of SD MT1 at 15mo-24mo, as shown in the hypothalamic samples. Interestingly this is in direct opposition to hypothalamic results for MT1 at the same age and indicates a tissue specific difference in late life MT1 expression between long day and short day exposed samples.

It is also important to note that pituitary MT1 expression at 6mo failed to reach a minimum threshold for qPCR recording (data not shown), while LD 15mo and 24mo MT1 expression were not significantly different (fig 3.6b).

Expression of MT2 in the hypothalamus was greater in LD > SD groups at 6mo ($p<0.05$), and non-significantly higher at 15mo, before dropping dramatically at 24mo. This drop in LD MT2 expression in old age was significant when compared with 6mo and 15mo levels ($p <0.01$). In the pituitary, MT2 expression reflected hypothalamic patterns, with increased MT2 levels in LD samples in early life, before a significant drop at 24mo ($p <0.01$; fig 3.6d). While pituitary LD MT2 levels dropped over lifespan, LD hypothalamic levels show sustained MT2 expression in early life, dropping significantly in old age only (fig 3.6 d vs c).

Pituitary MT2 expression in short day groups declined moderately from 6mo to 15mo, before a significant increase at 24mo over LD samples ($p<0.01$; fig 3.6d, right side). The significant increase in MT2 expression in aged SD pituitary samples was not seen in hypothalamic samples taken at the same time, as hypothalamic SD MT2 expression was maintained at low levels throughout life (see fig 3.6 c+d).

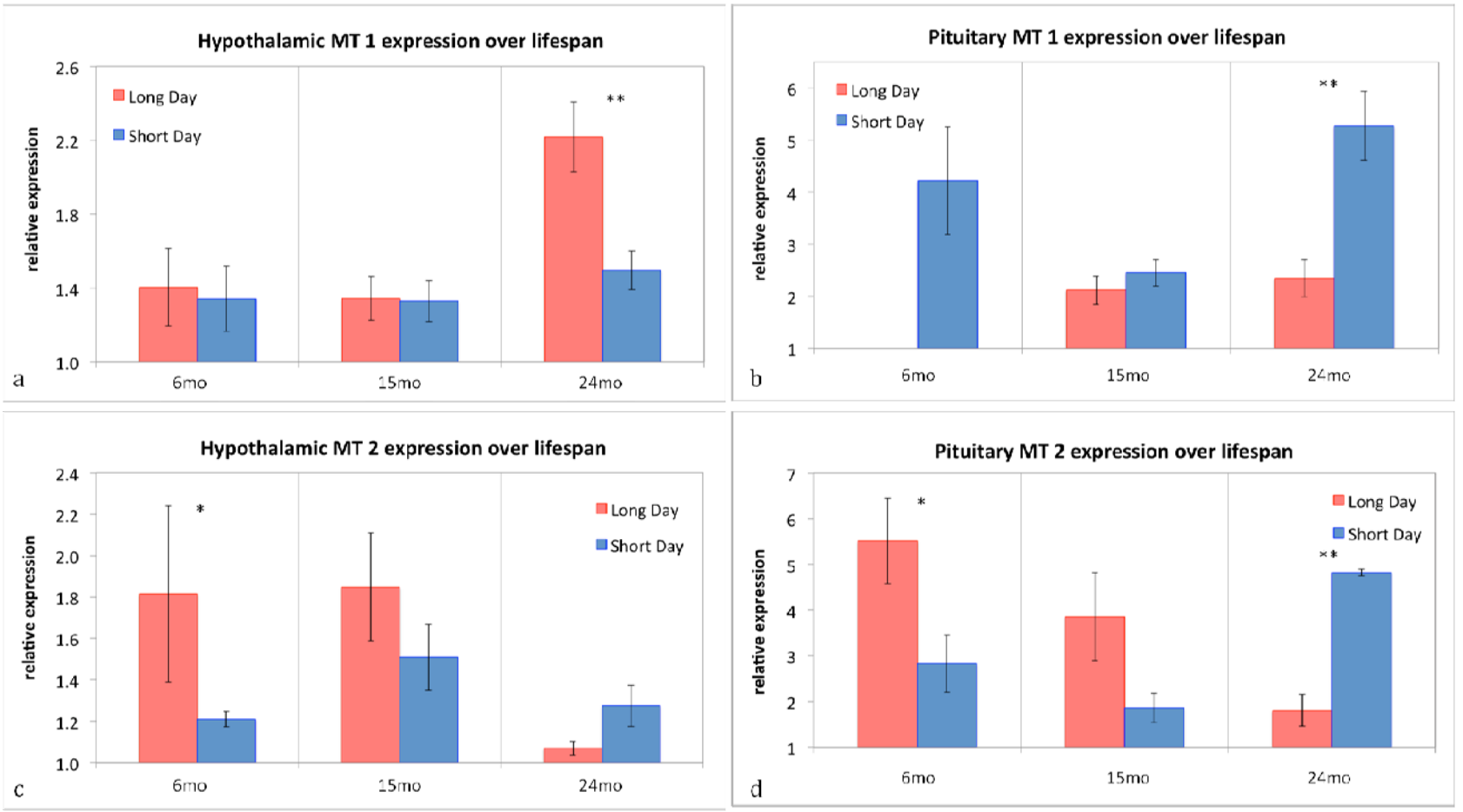

Figure 3.6 - qPCR measures of Hypothalamic MT1 (a), MT2 (c), Pituitary MT1 (b, MT2 (d) expression in LD and SD photoperiods throughout life. LD gene expression in red; SD samples in blue. Samples were taken at 6mth (left), 15mth (middle) and 24mo (right) in all figures. Error bars represent SEM; 5 sets of tissue samples were pooled into each tube, with 5 tubes tested at each timepoint and condition (N = 25). mRNA samples were tested in triplicate (75 individual

3.3.3.4 qPCR Hypothalamic Dio1-2-3 expression

Hypothalamic Dio1, Dio2 and Dio3 expression was measured by qPCR over the zebrafish lifespan (6mo, 15mo, 24mo). SD Dio1 expression was significantly greater than LD at 6mo (SD > LD; $p < 0.001$), dropping gradually to non-significant levels at the other ages tested (see fig 3.7a). Overall, SD Dio1 expression declined moderately over time, while LD Dio1 levels increased significantly from 6mo-15mo, and matched SD Dio1 expression levels in old age (thus 24mo LD and SD Dio1 levels were not significantly different).

Dio2 hypothalamic expression was closely matched between LD and SD samples throughout the ages tested (6mo, 15mo and 24mo), with no significant differences between ages and was not measurably altered by different photoperiodic light conditions (fig 3.7b).

Dio3 expression in the hypothalamus changed significantly with photoperiod. At 6mo and 24mo, LD samples were significantly higher than SD ($p<0.05$ and $p<0.01$, respectively). At 15mo, these differences were inverted, with LD Dio3 levels significantly lower than SD samples (LD<SD; $p<0.05$).

Overall, circadian expression of deiodinase enzymes in the hypothalamus is limited to Dio2 specifically, with an increased level of expression in the late day (ZT 9; figure 3.2d). When measured over the lifespan, Dio2 expression is stably expressed between LD and SD groups, with little photoperiodic effects. In direct opposition to Dio2 profiles, hypothalamic Dio1 is clearly not circadian, while photoperiodic SD > LD levels are significant increased (at 6mo; $p<0.05$). Dio3 expression in the hypothalamus was variable in both circadian and lifespan time points, with no clear patterns in expression between LD and SD conditions (fig 3.7c). These results are interesting, as overall. Dio1 and Dio2 expression are opposite in both circadian and photoperiodic trends, reflecting the complementary relationship between these targets, in a novel aspect in zebrafish.

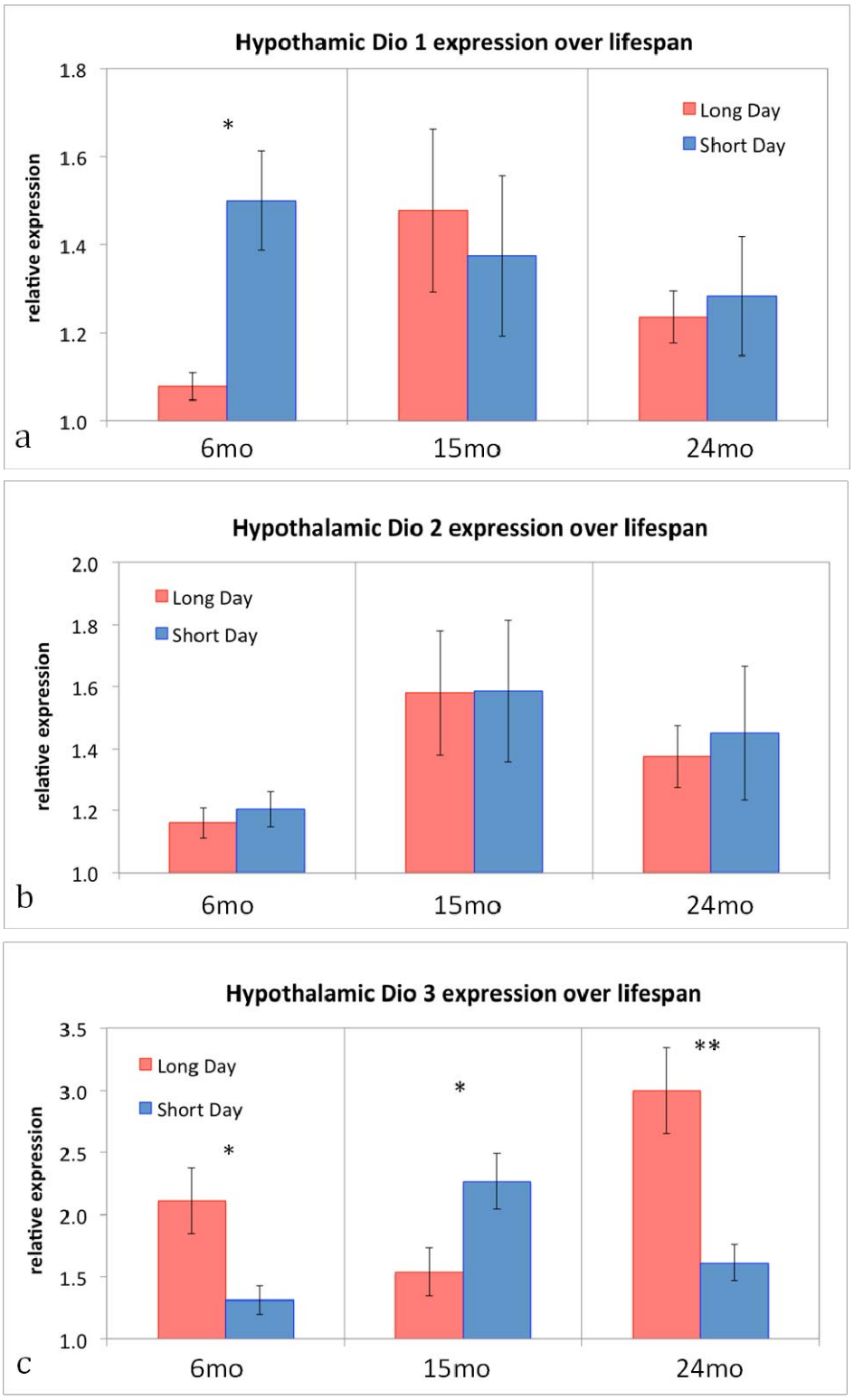

Figure 3.7- qPCR measures of Hypothalamic Dio1, Dio2 and Dio3 expression in LD and SD photoperiods throughout life. Gene expression in LD samples are shown in red; SD samples in blue. Samples were taken at 6mo (left), 15mo (middle) and 24mo (right) in all figures. Error bars represent SEM; 5 sets of tissue samples were pooled into each tube, with 5 tubes tested at each timepoint and condition (N = 25). mRNA samples were tested in triplicate (75 individual samples at each timepoint).

3.4 Discussion

Evidence of photoperiodic sensitivity has been gathered from a number of teleost species, while direct measures of light-dependent hormonal expression have been limited to larger species such as salmon and sea bass (Amano et al., 2003). The data presented here focuses on the daily and lifelong expression of a host of reproductive and growth related targets in zebrafish, including hypothalamic releasing hormones and their downstream pituitary targets. Novel findings associated with the tissue-specific expression of melatonin receptors (circadian and lifelong differences between LD and SD) and the differences between Dio1, Dio2 and Dio3 expression in the zebrafish hypothalamus are presented here for the first time. The analytical challenges of measuring hormone and receptor expression in a small model organism were overcome using quantitative PCR methods, yielding comparative measures of target expression in the nanomolar range (see methods, chapter 3). Considering differences in the seasonal expression of melatonin receptors themselves, it is important to note that photoperiodic melatonin released may be independent of the melatonin receptor expression shown here. My initial hypothesize of a lifelong increase in reproductive and growth hormone mRNA expression was partially supported, with target specific differences which are discussed in detail in the following discussion.

3.4.1 Circadian expression of target genes

Conveying and synchronizing a circadian message to tissues throughout the body requires some delivery mechanisms, which are presumably both neural and hormonal. Studies of circadian hormonal expression in fish are often limited to melatonin expression in larger species. The physiological effects of daily variations in circulating melatonin and melatonin receptors expression in different tissues are starting to be reviewed in depth, and are implicated in such diverse processes as reproduction, locomotor activity, feeding and sleep in fish.

The expression of neuroendocrine hormones from the hypothalamus and pituitary can be expressed as a function of circadian timing, with changes reflecting daily environmental cycles of light and dark. In addition to describing the daily rhythms

of the target genes of interest, this circadian data helped to pinpoint the optimal timing of DNA sampling for long-term studies.

3.4.1.1 Per1, Per3 and Cry1a

Samples taken from both the hypothalamus and pituitary show clear circadian oscillations, as illustrated by the rhythmic expression of the classic circadian genes *Per1*, *Per3* and *Cry1a* (fig 3.2a and 3.3a). The expression of *Per1* and *Per3* were strongly circadian in both tissues, with higher peaks during the light period (ZT 3 and ZT 9), over the dark period (ZT 15 and ZT 21). As described in the literature, both *Per1* and *Per3* mRNA rhythms peak at dawn in an LD cycle (Cahill, 2002a), and the early peaks (ZT3 and ZT 9) of *Per1* and *Per3* confirm these findings.

Cry1a expression was also matched between hypothalamus and pituitary samples, with a daily circadian peak at ZT 9, and low expression levels throughout the rest of the light/dark period, with lowest expression at ZT 21 (see fig 3.3a). This light-phase peak at ZT 9 confirms previous findings with z*Cry1a* mRNA rhythms, which peak during the day (Cahill, 2002a).

The relative expression levels *Per1*, *Per3* and *Cry1a* were approximately double in pituitary as compared to hypothalamus samples, suggesting a dramatic shift in light/dark expression in the pituitary for these circadian genes. Overall, these rhythmic expression patterns match timing patterns previously reported in zebrafish tissues (Cahill, 2002a), and clearly confirm the existence of circadian clocks in the zebrafish hypothalamus and pituitary primarily, see fig 3.2a and 3.3a.

3.4.1.2 GnRH and gonadotrophins (LH, FSH, PRL)

Experiments done *in vitro* have demonstrated that circadian clock function acts to regulate the secretion of timed GnRH pulses in cell culture (Chappell et al., 2003). As shown in figure 3.2b, GnRH expression in the zebrafish hypothalamus is clearly circadian, with peak expression at the end of the day (ZT 9), followed by a moderate increase just before dawn (ZT 21).

GnRH (and downstream gonadotrophin) secretion is dynamic, rising in the late afternoon in tandem with peak Cry1a levels (as shown in figure 3.2a). Previous mammalian experiments in over-expressed mCry1 (*in vitro*) have shown significant increases in GnRH pulse amplitude, further suggesting this core clock protein is actively involved in the modulation of neurohormone secretion (Chappell et al., 2003). And in sea bass kept in extended long day photoperiods (18h/6h), a daily rhythm in GnRH expression was noted, with the highest levels of expression during the mid-light period (Bayarri et al., 2004). The results here confirm the circadian expression of GnRH and extend these findings to zebrafish.

Peak GnRH pulses in the late afternoon have also been linked to diurnal changes in gonadotrophins such as LH *in vivo* (Sisk et al., 2001). In teleosts, daily GnRH mRNA and plasma LH peaks are consistency higher in the dark period up to 8 hours before spawning (Gothilf et al., 1997). In zebrafish, a bi-modal peak in expression was noted (fig. 3.3b), with increased expression at both late day and late night, reflecting the circaidan expression of GnRH from the hypothalamus.

Previous experiments on teleost fish indicate the effects of circadian melatonin on neuroendocrine hormone expression are species specific and mixed, depending on age, photoperiod exposure, and local conditions. In masu salmon (*O. masou)*, melatonin administration reduced gonadotrophin releasing hormone (GnRH) in the hypothalamus and downstream luteinizing hormone (LH) in the pituitary while stimulating follicle stimulating hormone (FSH) content (Amano et al., 2003). The current results confirm this pattern, as both GnRH and LH expression profiles are highly synchronized, with a significantly higher expression of FSH at late day. As melatonin expression is expected to be greatest in the dark period, the second peak in GnRH and its corresponding pituitary hormones (LH, FSH, PRL, TSH) is unexpected. This secondary late night bi-modal peak (ZT 21) may be due to sampling transcriptional information (mRNA) rather than plasma protein expression.

In vitro studies from cultured trout pituitary glands show inhibition of prolactin (PRL) release in the presence of physiological doses of melatonin, indicating that

melatonin may lower nocturnal PRL release (Falcon et al., 2003a). As shown in fig 3.3b, nighttime PRL levels are significantly lower than in the day, with the lowest level of PRL expression at ZT 15, 3h into the dark period, thus confirming previous published results in Rainbow Trout (*O. mykiss)*.

The current findings are consistent with previous reports, with downstream expression of the gonadotrophic hormones (LH, FSH, PRL and TSH) following GnRH bi-modal patterns, with peaks in the late day and late night (fig 3.3b), thus the timing and profile of pituitary hormone mRNA resembles that of the releasing hormone, GnRH, as expected by my initial hypotheses.

3.4.1.3 GHRH and GH

In mammals, GH is released in nocturnal pulses from the pituitary gland, linked to the body's circadian cycle (Norris et al., 2003). GH has a number of downstream effects, including the stimulation of bone and muscle growth (Sam & Frohman, 2008). In fish, diurnal variations of GH secretion have been described in Rainbow Trout (*O. mykiss)* (Gomez et al., 1996) and Atlantic Salmon (*S. salar)* (Bjornsson et al., 2000), among others. In Goldfish (*C. auratus)*, diurnal GH expression levels differ between SD and LD photoperiods, with SD groups expressing peak GH levels in the early night, while LD groups have peak GH in the early morning (Marchant & Peter, 1986). The current results extend these findings in zebrafish, and give evidence for a dramatic peak in GH expression 3h after lights on (ZT 3; as shown in fig 3.3b).

Circadian expression of growth hormone releasing hormone (GHRH) in the hypothalamus was highest in the late afternoon (ZT 9) with a shallow 2nd peak at ZT 21 (fig 3.2b), similar to GnRH and gonadotrophic mRNA patterns, yet lower in amplitude. Downstream pituitary GH mRNA is seemingly independent of GHRH, with a significant peak GH at ZT 3 only (a GH specific result, as compared to other pituitary hormones; fig 3.3b). The initial expectation of a clear link between GHRH and GH expression patterns has been overturned. Ideally, further higher resolution analysis of GHRH (and GH) expression in zebrafish hypothalamus will be

performed (hourly timepoints, over a 24h period) to pinpoint detailed changes in this target, and this strategy is recommended for future work.

The expression of GH mRNA shown here may also be based on the circadian expression of melatonin during the light/dark periods. Experiments using cultured adult trout pituitaries showed a bi-modal change in GH release, with picomolar concentrations of melatonin inducing a reduction in GH release, and higher (nanomolar range) concentrations resulting in the stimulation of GH secretion (Falcon et al., 2003a). Further evidence of melatonin modulation of GH secretion from the pituitary comes from pituitary culture experiments, where the addition of luzindol (a melatonin receptor blocker) blocked both the inhibitory and the stimulatory responses of GH to melatonin concentration (Falcon et al., 2003a). These results, while seemingly delayed as compared to predicted expression profiles, may be due to processing delays in melatonin/GH interactions. GH levels are stably expressed from ZT 9 – 21 (late day and throughout the night), with a significant peak 3h after dawn (fig 3.2b). Given the difference between transcription and translation measures it is possible that GH expression follow melatonin secretion, with a consistent 4h-5h delay throughout the circadian cycle.

3.4.1.4 MT1 and MT2

Within the hypothalamus, melatonin receptor 1 (MT1) had a strong circadian profile, with a clear 4-fold peak in expression in the late day (ZT 9), which contrasts sharply with the absence of circadian expression in MT2 in the same tissue (as shown in fig 3.2c). Melatonin receptor expression in the pituitary was markedly different than hypothalamic circadian patterns. Similar to the classical circadian genes *per1* and *per3*, pituitary MT1 and MT2 expression showed a significant peak at dawn (fig 3.3c), followed by a drop in late day and evening levels until late night levels increased slightly.

Analysis reveals that MT1 is the major subtype expressed in the pituitary, with dawn mRNA levels 8.5 fold greater than at dusk, while early morning pituitary MT2 levels are 4 fold higher than at dusk (fig 3.3c). Furthermore, MT1 expression peaks 6h later in the hypothalamus, than in the pituitary (ZT 9 vs. ZT 3,

respectively). These early morning peaks are specific to the pituitary, as the hypothalamus samples showed a single mid-afternoon peak in MT1 expression and no circadian oscillations in MT2 expression. Reports of goldfish melatonin receptor expression have provided evidence of circadian variability in MT1 and MT2 in the optic tectum, with a single concurrent peak at dawn (ZT 0, under 12h/12h lighting), while melatonin binding shows a broad plateau from ZT10 to ZT14 (Ikegami et al., 2009). This suggests that melatonin receptor expression is likely post-transcriptionally regulated, with a 10h–14h of time lag between transcription and appearance of receptor proteins. The transcriptional and post-translational regulation of multiple subtypes of melatonin receptor is considered to be an important molecular basis of melatonin action (Iigo et al., 1994).

In rodents, the expression of MT1 mRNA shows robust circadian rhythms with low levels during the day, and a rapid rise at the beginning of the dark period (ZT 14), coincident with an abrupt increase in levels of circulating melatonin measured by radioimmunoassay When housed in DD (constant dark), peak MT1 expression moved to the middle of the subjective night, approximately 8h before the peak of protein expression (Masana et al., 2000). Using measures of 2-[^{125}I]-Iodomelatonin binding (in the SCN), melatonin receptor activity was highest 2h after lights on, or at the beginning of the subjective day (Masana et al., 2000).

Immunocytochemistry measures of melatonin receptors in the hypothalamus and pituitary would be helpful in describing the protein expression of these targets, but suitable antibodies for zebrafish targets were not available at the time these experiments were undertaken. Future experiments exploring protein expression of melatonin receptors, such as immunochemistry, western blots and 2-D protein gels would be advantageous in comparing transcriptional and translational differences in expression. In the current work, Mel 1c expression levels were sub-threshold for qPCR measurement in the zebrafish hypothalamus and pituitary, and thus not shown. Level of MT1 and MT2 were highly abundant in these structures and figures 3.2c and 3.3c illustrate the circadian expression profiles of MT1 and MT2 in 12h/12h light conditions.

The initial expectation and hypothesis of global MT1, MT2 and Mel1c increases in ZT 15 and 21 were not confirmed. Overall, these results suggests that circadian expression of melatonin receptors is exclusive to the pituitary and the dramatic circadian response of pituitary MT1 at dawn gives evidence a primary role of this receptor (over MT2) in photoperiodic modulation of gonadotrophin release in the zebrafish pituitary. Clearly, transcriptional melatonin receptor expression is rhythmic (fig 3.3c), tissue specific (pituitary, not hypothalamus) and subtype specific (MT1 over MT2). While these rhythms could be expressed differently between RNA and protein, there are daily changes in melatonin responsivity, which are likely involved in circadian and photoperiodic hormonal release.

3.4.1.5 Dio1, Dio2 and Dio3

Circadian deiodinase enzyme expression within the zebrafish hypothalamus is target dependent, with clear Dio2 peaks in the late day (ZT 9), reflecting *Cry1a* expression levels in the same tissue, while Dio1 and Dio3 expression did not show any clear circadian rhymicity (see fig 3.2b). These data are novel, as no published reports on circadian oscillations in teleost Dio expression are currently available and these results confirms reports from photoperiodically entrained rodents where temporal changes of *Dio2* mRNA levels in animals kept under long-day and short-day conditions were monitored (Yasuo et al., 2007). These findings demonstrated that Dio2 mRNA levels are expressed rhythmically in the ependymal cells of LD-entrained hamsters with peak expression in the late day (ZT 9), while Dio2 expression in SD ependymal cells remained low throughout the day (Yasuo et al., 2007).

As far as is known, this is the first demonstration of a diurnal rhythm of Dio2 expression in the zebrafish hypothalamus and this result is important to unravel the molecular basis driving the photoperiodic switch between T_3 and T_4, as has been reported in fish (Morin et al., 1993). As described in the introduction (see chapter 1), T_3 is created in target tissues through the local conversion of T_4 by deiodinase enzymes in hypothalamic tanycyte cells (Hazlerigg & Wagner, 2006). Dio2 converts T_4 to bio-active T_3, while Dio3 inactivates T_3, and the relative

expression of Dio2 and Dio3 determines the levels of biologically active T_3 in the brain (Nakao et al., 2008b). T_3 activity stimulates the release of GnRH by the hypothalamus into the portal blood vessels to pituitary where LH and FSH release is increased (see schematic fig 1.9 for details) (Nakao et al., 2008b). I propose that the clear circadian expression of Dio2, with peak levels in the late day (ZT 9; fig 3.2d) may be associated with the increase in hypothalamic GnRH at the same point (fig 3.2b) stimulating increases in FSH and LH also observed at ZT 9 (see fig 3.3c).

3.4.1.6 TSH co-localizations

As previously reported, TSH receptor expression is co-localized with Dio2 in the hypothalamic tanycytes of photoperiodic animals such as the Syrian Hamster (*M. auratus*) (Revel et al., 2006; Yoshimura et al., 2003) and Quail (*C. japonica)* (Yoshimura et al., 2003) and Dio2 is a key enzyme in the control of thyroid-hormone activity, converting thyroxine (T_4) into tri-iodothyronine (T_3) in the hypothalamus (Hazlerigg & Loudon, 2008). Work by Nakao et al. (2008), has shown that TSH is induced in the Quail PT within 14hours of LD exposure, and Dio2 expression follows 4h later in the neighboring hypothalamic ependymal cells. The current results show paralleled peak expression of Dio2 (in hypothalamus) and TSH (in pituitary) in the late day (ZT 9). As Dio2 is thought to be mediated through TSH receptors (TSH-R) in hypothalamic tanycyte cells (Nakao et al., 2008a), the profile of circadian and photoperiodic expression of these receptors is recommended in future studies.

3.4.2 Photoperiod expression of qPCR targets throughout lifespan

Seasonal photoperiods have been shown to alter spawning and reproductive hormone expression in teleost fish (Zohar et al., 2010). In optimal conditions, zebrafish are able to spawn every 3-4 days, throughout their lives (Westerfield, 1995). Gamete development and maturation are dependent on endocrine factors such as GnRH and pituitary gonadotropes via the HPG axis (Dickey & Swanson, 2000). Differences in hormone and receptor expression between photoperiodically (LD and SD) entrained zebrafish groups were monitored over the course of their lifespan (6mo, 15mo and 24mo) and presented here.

3.4.2.1 GnRH and pituitary reproductive hormones (LH, PRL and FSH)

As demonstrated in figure 3.4, lifespan measures of GnRH were sensitive to photoperiod, with a significant increase in SD GnRH expression (over LD) at 6mo and 15mo. These results were unexpected, countering the expected results hypothesized earlier. In late life, zebrafish SD GnRH levels drop sharply, matching LD levels. In rainbow trout (*O. mykiss*), GnRH levels are highest during March-April (SD), falling from May to July (LD) and are associated with seasonal gonadal maturation (Choi et al., 2010). And previous reports have observed that teleost GnRH receptors (Jodo et al., 2005) are seasonal expressed, with profiles correlating with seasonal changes in gonad size and sex steroid serum levels (Sohn et al., 1999).

As expected, the expression of hypothalamic GnRH (SD>LD) had a similar pattern of expression in the pituitary hormones LH, FSH, and PRL at 6mo and 15mo (fig 3.4). These results confirm similar findings *in vivo* and *in vitro* in goldfish (*C. aruratus*) (Sohn et al., 1999) and gilthead sea bream (*S. aurata*) (Zohar et al., 1995), where GnRH is known to stimulate gonadotrophin release. And in goldfish, short-day photoperiods have been shown to increase TSH mRNA (Sohn et al., 1999) as was shown here in 6mo samples.

Lifespan measures of FSH were sensitive to photoperiod, with lifelong increases in SD>LD groups, and peak SD FSH expression at 6mo, declining gradually at 15mo and 24mo (fig 3.4c). These differences were unexpected, as LD entrained fish are consistently more fertile (as shown in chapter 2, fig 2.5 – 2.8). Previous work using iteroparous species (having multiple reproductive cycles over the lifespan), such as Rainbow Trout (*O. mykiss*) has shown a decrease in plasma FSH after vitellogenesis, suggesting that FSH levels fall and remain at a level sufficient to maintain gamete growth without stimulating further follicular recruitment (Prat et al., 1996). This contrasts with semelparous species (characterized by a single reproductive episode) such as salmon, where FSH levels increase as vitellogenesis proceeds (Swanson et al., 1989). These species produce a single cohort of eggs in a lifetime and compared to zebrafish, do not maintain a store of immature oocytes in their ovaries. In the present study, SD entrained groups had significantly higher

FSH mRNA expression throughout life, as compared with their LD cohort, which had no significant increases over time (see fig 3.4c). It is proposed that the prolonged FSH elevation seen in these animals may result from the need to maximize vitellogenin production and oocyte maturation in reproductively inhibitory conditions (as shown by the low fecundity levels in fig. 2.4).

In rainbow trout (*O. mykiss)*, plasma FSH levels rise prior to ovulation, producing a minor peak at final maturation followed by a subsequent decline, and increase only once the eggs have been stripped from the body (Prat et al., 1996). Given the stimulatory effects of LD photoperiods on zebrafish reproduction, the constant presence of mature oocytes throughout adult life may act to dampen long-term FSH expression. Additionally, FSH levels may be in constant flux, with short-term peaks before weekly egg laying episodes, and these peaks may be overlooked in long-term sampling performed here. LF

3.4.2.2 GHRH

Hypothalamic GHRH levels were significantly different in LD and SD photoperiodic groups in early life. At 6mo, LD GHRH was low, before rising sharply at 15mo, while SD GHRH levels began significantly higher at 6mo before dropping at 15mo (see fig 3.5). Interestingly, these photoperiod differences are almost diametrically opposite the expression of GnRH from the same hypothalamus samples (fig 3.4a), where SD hormone expression dominates at 15mo. As noted in the circadian expression of GHRH and GH, there is no apparent synchronization between these targets and this independence is shown in figure 3.5, where SD GHRH levels drop dramatically from 6mo-15mo, while GH levels from the same population increases at each time point tested, significantly so at each timepoint tested. Unexpectedly, the current results indicate a lifelong increase in pituitary GH expression in SD over LD entrained samples, while LD GH expression is relatively flat throughout life.

GHRH is known to stimulate a dose-dependent release of GH from teleost pituitary cells, suggesting a direct action on pituitary somatotrophs (Vaughan et al., 1992) and GHRH-immunoreactive fibers are present in the proximal pars distalis where

gonadotrophes are located (Zohar et al., 2010). Pituitary cells taken from sexually regressed goldfish (*C. auratus)* are been shown to be more responsive to GHRH than those taken from sexually recrudescent fish (Peng & Peter, 1997). This indicates that sexual maturation and likely sex steroids may alter responsiveness of somatotrophs to GHRH and may result in de-synchrony between hypothalamic GHRH and pituitary GH expression in fish under long-term photoperiodic exposure. The heightened GHRH sensitivity of pituitary explants from sexually regressed (SD entrained) specimens (over LD entrained groups) would be highly recommended for future experiments. Given the dramatic inhibition of SD conditioning on zebrafish fecundity (chapter 2), it would be anticipated that long term SD groups may be more responsive to GHRH expression, through heightened GHRH receptor expression, increased GHRH translation, transcription and/or plasma hormone levels.

In addition to the complicated effects of sexual maturation on GHRH/GH expression, a recent review of GHRH and PACAP (pituitary adenylate cyclase activating polypeptide; a related GH releasing hormone) postulated a reliable role for PACAP as a GH stimulator, over GHRH (Canosa et al., 2007) and is linked with GHRH expression, as these two peptides are encoded together on the same gene (Parker et al., 1997). In *in vitro* experiments, salmon PACAP was shown to release GH from cultured salmon pituitary cells, in a dose-dependent manner, while GHRH governed GH release was less reliable and dose dependency could not be demonstrated (Parker et al., 1997). Due to the limited hypothalamic samples available from each age group, GHRH was selected as a prime candidate for photoperiodic control of GH, based on evidence in goldfish (*C. auratus)*, a teleost species closely related to zebrafish (Rao et al., 1996). The revision of the classic hypothalamic GHRH – pituitary GH relationship may be reflected in the data shown here, as GH expression in any group showed little relationship to GHRH levels in LD and SD samples (as shown in figures 3.2 and 3.5). Unfortunately, limited samples sizes over long experimental phases precluded the monitoring of alternate GH-releasing factors, and given additional resources, measurement of long and short day PACAP levels would be of interest in future experiments.

3.4.2.3 GH

In previous reports, seasonal expression of plasma GH levels have a clear seasonal pattern (high in LD; low in SD) in teleosts species such as goldfish (*C. auratus)* (Marchant & Peter, 1986), and gilthead sea bream (*S. aurata)* (Mingarro et al., 2002). In Atlantic salmon (*S. salar)*, serum GH levels increase in spring and summer during sexual maturation, relating GH to reproductive function (Bjornsson et al., 1994) and GH can stimulate gonadal steroid production (Van der Kraak et al., 1990), gametogenesis and vitellogenesis (Mosconi et al., 2002). The current results are unexpected and counted the hypothesis of a lifelong increase in GH mRNA in LD over SD conditions. GH expression was significantly higher in SD over LD throughout life (fig 3.5b). It has been suggested that GH expression is responsive to food intake and is involved in energy allocation during the pre-spawning season, for later gonadal development and vitellogenesis (Canosa et al., 2005; Mingarro et al., 2002). Given the dramatic increases in LD-associated fertility and fecundity (see Chapter 2), it is a reasonable to hypothesize that GH expression (mRNA and/or protein) may be inhibited in favor of reproductive hormone expression in fecund LD groups, a somewhat ubiquitous evolutionary strategy in fish (Roff, 1983). Further measures of photoperiodic GH, including higher resolution measurements (daily timepoints) to pinpoint detailed changes in GH, and GH receptor expression by the reproductive organs would be necessary to confirm this, and are recommended in future experiments.

The secretion of GH is also affected by melatonin, in a variable manner. It has been shown that *in vitro*, cultured trout pituitary glands alter GH release after melatonin administration, in a dose-dependent manner, with inhibition of GH release at concentrations of daytime circulating melatonin levels, and melatonin-induced increases in GH release with concentrations closer to night-time melatonin levels (Falcon et al., 2003a). This suggests that melatonin contributes to the nocturnal increase and diurnal decrease in plasma GH levels, as reported *in vivo* for Atlantic salmon (*S. salar)* (Bjornsson et al., 2000). Under conditions that stimulate GH secretion, melatonin also induced a sustained inhibition of PRL release (Falcon et al., 2003). GH and PRL are two closely related hormones that often act in an antagonistic manner (Nguyen et al., 2008). The effects of melatonin on growth may

thus result from the differential impact the hormone has on GH and PRL, and perhaps on other pituitary hormones. As reported recently (Falcon et al., 2010), higher melatonin doses can have stimulatory effects on GH release, with bi-modal effects on cultured pituitaries likely mediated by differential expression of melatonin receptors in this region (Falcon et al., 2010). Extending this finding within the present model, the lifelong increase in SD GH expression may indicate the increased rate of circulating melatonin in SD entrained groups. The division between GHRH and GH profiles may be explained through a melatonin-specific action in the gonadotrophins, as facilitated by seasonal and circadian melatonin receptor expression (and action) in the zebrafish pituitary.

3.4.2.4 Melatonin receptor expression

RT-PCR analysis showed that both MT1 and MT2 genes were expressed in the pituitary and hypothalamus, while Mel1c levels were below measurable thresholds. Hypothalamic MT1 and MT2 expression was low (and not significantly different) in both LD and SD groups (6mo and 15mo), with a dramatic increase in MT1 levels at 24mo in SD fish (fig 3.6a) and concurrent drop in MT2 levels in the same group (24mo SD fish; fig 3.6c).

SD pituitary MT1 expression was high at 6mo and 24mo, with a 15mo drop in expression, while pituitary LD MT1 levels were low throughout life; sub-threshold at 6mo (fig 3.6b). Pituitary MT2 levels dropped steadily in SD groups from 6mo to 24mo, but were significantly higher than their LD cohorts at young and middle age (6mo and 15mo; fig 3.6d). Unexpectedly, LD pituitary levels had low expression levels over lifespan (in MT2), or sub threshold to low levels in MT1 (at 6mo; fig 3.6b). In all cases, little seasonal difference (LD vs. SD) was noted till late life (24mo), where expression levels were consistently higher in pituitary than hypothalamus.

Diurnal variations of melatonin receptor expression have been shown in the brain chum salmon brain for MT1 and MT2 (Shi et al., 2004) and in the brain, retina, and pineal gland of golden rabbitfish (*S. guttatus*) for MT1, MT2 and Mel1c (Park et al.,

2007a), suggesting that the alternate expression of melatonin receptor subtypes may account in part for the diurnal variations in the melatonin binding sites in the brain. Interesting links between photoperiod and melatonin receptors have been made, through the regulation of hypothalamic deiodinase expression, and are outlined in the next section.

3.4.2.5 TSH and Dio1, Dio2, Dio3

Reports from mammalian photoperiodic studies have demonstrated increased melatonin receptor expression in the anterior pituitary and pars tuberalis (PT) (Dardente et al., 2003). PT cells derive from thyrotrophs during development, and seasonally express both thyroid-stimulating hormone (TSH) and the common glycoprotein subunit used to form the active heterodimer, thyroid-stimulating hormone (TSH) (Klosen et al., 2002). TSH released from the PT acts on the mediobasal hypothalamus, in the ependymal cell layer surrounding the third ventricle and target tanycyte cells (Hanon et al., 2008). Tanycyte cells may work to modulate hypothalamic-pituitary interactions through the hypophyseal stalk and pituitary portal system and transport melatonin across the blood–brain barrier (Rodriguez et al., 2005). PT cells expressing TSH are melatonin-sensitive and express MT1 receptors yet are blind to TRH (thyrothrophin releasing hormone) suggesting a melatonin specific output (Hazlerigg & Loudon, 2008). As shown in figure 3.3d, lifelong TSH levels (LD and SD) followed similar patterns in pituitary FSH expression, with increased expression in SD samples throughout life, over LD levels. Similarly, pituitary MT1 levels were higher in SD entrained groups at 6mo, and 24mo (over LD groups), but dropped to LD levels at 15mo. Pituitary MT2 levels showed increases in SD > LD at 6mo only, with no significant differences at 15mo between groups, and a LD > SD switch in peak expression at 24mo. While the pattern of LD TSH expression was echoed in the MT2 LD expression pattern, it more closely resembles the overall SD>LD expression of gonadotrophins throughout the ages tested.

As described in mammals, PT-derived TSH acts locally within the mediobasal hypothalamus to control tanycyte Dio gene expression (Hanon et al., 2008) and TSH receptor expression is co-localized with Dio2 in the hypothalamic tanycytes

(Revel et al., 2006). Dio2 is a key enzyme in the control of thyroid-hormone activity, converting thyroxine (T_4) into tri-iodothyronine (T_3) in various target tissues (Hazlerigg & Loudon, 2008).

The expression of Dio1 and Dio2 were similar between LD and SD groups throughout life, with a notable exception in LD 6mo Dio1 (significantly lower than SD and LD aged samples; fig 3.7a). Hypothalamic Dio3 levels were strongly affected by photoperiodic conditioning, with opposite expression peaks throughout life, ending with a significant increase in LD Dio3 at 24mo (fig 3.7c). This result is interesting when compared with circadian expression profiles, where Dio2 is clearly circadian and Dio3 daily levels are flat. These differences suggest a differentiation between circadian (Dio2) and photoperiodic (Dio3) responsiveness in these interactive enzymes.

Dio2 expression did not respond to photoperiodic changes in wild-types, whereas it was strongly induced by LD conditions in Syrian hamsters (Revel et al., 2006; Yasuo et al., 2007), and Japanese quail (Yasuo et al., 2005; Yoshimura et al., 2003). In Djungarian hamsters, *Dio2* expression was induced when animals were transferred from short to long days, but did not change when animals were transferred from long to short days (Barrett et al., 2007; Watanabe et al., 2004; Yasuo et al., 2006). Thus, the effects of photoperiod on gene expression in the ependymal cells (EC) appear to be specific for species, strain, and experimental schedule.

In a recent study using MT1 and MT2 knockout mice, a link between melatonin receptor expression and photoperiodic *Dio3* expression was described, where melatonin injections suppressed *Dio2* and induced *Dio3* expression in wild-types, and this effect was blocked by MT1 disruption (Yasuo et al., 2009). They found photoperiodic melatonin levels affects the expression of *Dio2* and *Dio3* in hypothalamic ependymal cells (EC), acting through MT1 receptors in the pituitary pars tuberalis (PT). This is corroborated by other mammalian studies, showing that the EC itself does not express melatonin receptors (Bartness et al., 2001; Schuster et al., 2000). The PT was considered the target site for seasonal

melatonin signalling due to high levels of MT1 mRNA while lacking MT2 mRNA (Reppert et al., 1995), MT1 mRNA and TSH protein co-localization in the PT (Klosen et al., 2002) and PT produced TSH regulates *Dio2* and *Dio3* expression in the EC in Japanese quail (Nakao et al., 2008b), sheep (Hanon et al., 2008), and mice (Ono et al., 2008).

3.4.2.6 Seasonal vs. constant photoperiods

Fish with short reproductive cycles, such as zebrafish, generally respond positively to exposure of a short period of constant daylengths (Westerfield, 1995), while species with a long gonadal maturation cycles usually require seasonally changing day lengths (Bromage, 2000). Transitional photoperiodic phasing is particularly necessary in setting seasonal reproduction in long-lived species with the capacity for multiple generative cycles (Davies, 2002). Sequential seasonal changes in day length entrain the endogenous circannual rhythms, which ultimately control reproduction (Migaud et al., 2010).

CHAPTER 4 - PHOTOPERIOD ON CELLS AND TISSUES

4.1 Introduction

4.1.1 Core clock mechanisms in zebrafish

As shown by Whitmore et al. (2000), early zebrafish embryos and derived cell lines contain functional circadian clocks. In isolation from other tissues, these cells contain an entrainment pathway (with the ability to see light) and display circadian gene oscillations (Whitmore et al., 2000). A general model of circadian gene regulation has been established in zebrafish, where the transcription–translation auto-regulatory feedback loop forms the core of the circadian clock mechanism, in a very similar manner to that described in mouse and *Drosophila*. The proteins CLOCK (CLK) and brain muscle ARNT-like (BMAL) form a heterodimer, acting to enhance the regulation of the *period* (*per*) and *cryptochrome* (*cry*) genes, initiating their transcription. The repressors PER and CRY interact with the CLK:BMAL heterodimer, thereby down-regulating their own expression (Cahill, 2002a). A significant difference between zebrafish and other model systems lay in the increased number of clock molecules, with zebrafish having at least six *cryptochrome*, three *clock* and three *bmal* genes. The implications of these additional genes are not fully understood at this time and are outside the scope of the current work.

Using their responsive properties to direct light, clock-containing cells offer a novel method to monitor the responsiveness of circadian clock genes to different photoperiodic light regimes, complementing previous findings such as behavioural measures, fertility and growth (discussed in chapters 2 and 3). By coupling a luminescent reporter to core clock genes, it is possible to visualize the molecular responsiveness of individual cells and tissue explants to varying photoperiodic conditions. It is therefore possible to monitor dynamically how the core clock mechanism entrains to differing photoperiods, and possibly obtain clues of how photoperiod may occur from a cellular point of view.

4.1.2 Regular and skeleton photoperiodic entrainment

The entrainment of circadian oscillators to photoperiod was first addressed using *Drosophila* pupae eclosion timing (Pittendrigh, 1964). Pittendrigh demonstrated that single light pulses (or a two pulse "skeleton" photoperiod) could entrain the circadian clock and initiate a set of oscillations that persist in the absence of light. A skeleton photoperiod contains a light and dark phase, similar to a full photoperiod, with each light phase defined by short pulses of light at the beginning and end of the phase, rather than continuous light exposure throughout the day (Pittendrigh, 1964).

In general, two forms of response are likely when cells are exposed to skeleton light regimes. Full entrainment occurs when the observed circadian rhythms between skeleton and full photoperiods are equal (shown in fig 4.1 a+b). If the response to a skeleton regime occurs only during the light pulses, with no sustained peak during the dark phase between the pulses, then no entrainment has occurred, and light is said to have a "masking effect" (shown in fig 4.1c; (Pittendrigh, 1964).

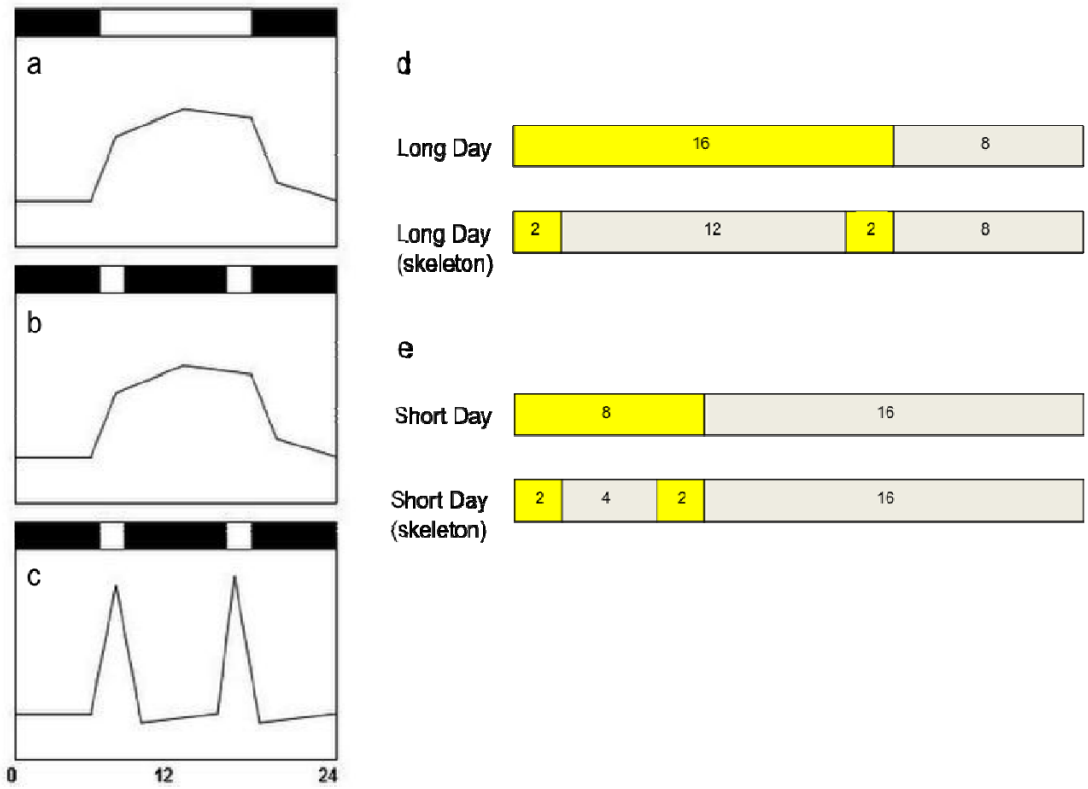

Figure 4.1: Schematic of skeleton photoperiod responsiveness. a) full photoperiod stimulates a circadian response throughout the light period, b) a symmetrical skeleton photoperiod of the same duration elicits a matching response, c) a skeleton photoperiod causing a masking effect or light-driven response, where circadian responsiveness is governed by absolute light exposure and is absent between pulses. d) Long day photoperiod – full duration (16h/8h) vs. LD skeleton photoperiod (2h-12h-2h/8h) and, e) short day photoperiod – full duration (8h/16h) vs. SD skeleton photoperiod (2h-4h-2h/16h). Note that all skeleton light pulses are of matched duration (2h).

4.1.3 Key questions in circadian rhythmicity

Considering the direct light responsiveness of zebrafish cells to a single short pulse of light (Tamai et al., 2007), it was interesting to extend this line of testing to the target tissues employed in the current work (zebrafish hypothalamic and pituitary explants) in either LD or SD (regular and skeleton) light regimes. Figure 4.2 illustrates the proposed entrainment regimes possible for both LD and SD skeleton photoperiods.

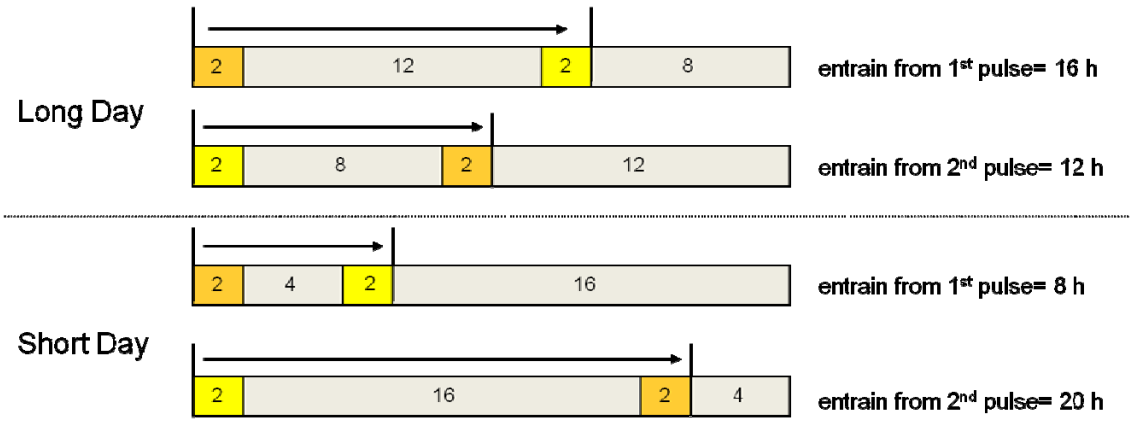

Figure 4.2: Proposed entrainment of peripheral clocks to full and skeleton photoperiods in LD and SD regimes. The leading entrainment pulse for each regime is shown in orange.

Some key issues derived from this line of questioning include:

- Are the entrainment patterns seen in full photoperiods accurately represented by comparable skeleton light/dark cycles?
- Does a LD skeleton photoperiod cause the internal circadian clock to entrain to the first light pulse, thus interpreting a daylength of 16h (2h-12h-2h/8h), or the second pulse, thus responding to a subjective 12h daylength (2h-8h-2h/16h)?
- Conversely, does SD skeleton entrainment cause an oscillation of 8h, with entrainment linked to the first pulse of the light period (2h-4h-2h/16h) or does the clock entrain to the second pulse, with a resulting subjective circadian period of 20h (2h-16h-2h/8h)?

4.1.4 Skeleton photoperiods and circadian models of time

Using the External Coincidence model of photoperiodism (see chapter 1, fig 1.2), an organism does not need to experience a full 12 hours of light to trigger reproductive events, but simply experience a light pulse at dawn and again at dusk, approximately 12 or 14 hours later, with the time between being spent in darkness (a classic skeleton photoperiod); as long as light coincides with a photo-sensitive phase to induce a long day response. In this model, the key photoinducible phase is activated by individual pulses of light exposure, rather than total light duration, and these pulses set the phase of the daily oscillator, initiating a host of downstream effects (see fig 1.2). It is the timing of the light pulses rather than their duration that is critical, as a very short light pulse can operate a photoperiodic "switch" if it falls at a specific phase of the circadian cycle. Brian Follett and Peter Sharp demonstrated this method in the late 1960s by exposing Japanese quail to different lengths of skeleton photoperiods (Follett & Sharp, 1969), as illustrated in figure 1.5 (chapter 1). Starting at dawn, the subjects received 6h of light, with different groups left in extended periods of darkness before being exposed to 15min pulses of light; such as 6h light, followed by 8h of dark before a 15min pulse, compared to other groups of 6h light, 12h dark+pulse, or 6h light, 4h dark+pulse, etc. Results demonstrated that a 2nd "dusk" pulse given between 12h-16h after the "dawn" (lights on) led to reproductive stimulation, as measured by testicular growth and increases in reproductive hormone levels (Follett & Sharp, 1969), clearly demonstrating a 4h photoinducible phase in avian subjects (between CT 12-16).

Skeleton photoperiod experiments in mammals have similarly suggested that a circadian timer sits at the core of photoperiodic time measurement. In a notable set of experiments in rodents, blinded male hamsters were maintained for 11 weeks in LD or SD photoperiods or in constant darkness, with brief (15min) light pulses given at 6h intervals. LD entrained hamsters displayed little to no gonadal atrophy; those maintained in constant darkness showed severe gonadal regression, while subjects in 2h/22h (with brief 15min light pulses at the beginning and end of the light period) did not undergo gonadal atrophy (Rudeen & Reiter, 1980). These experiments suggest that photoperiodic control of

reproduction in these rodents is likely not exclusively linked to light duration, and that the timing of a skeleton light pulse is important to stimulate (or inhibit) mammalian circannual reproductive cycles (Rudeen & Reiter, 1980).

Recalling the Internal Coincidence model of photoperiodism (chapter 1; fig. 1.3), the relative proximity and synchronized phasing of two independent circadian clock elements (linked to dawn and dusk respectively) are used to monitor changes in the external photoperiod. Within the mammalian pars tuberalis, melatonin receptors are abundant and melatonin binding alters gene expression of several clock genes, including *cry* and *per* (Lincoln et al., 2003). Reflecting the internal coincidence model, *cry* gene expression in sheep pituitaries increases as melatonin levels rise in the evening and *per* gene expression drops with declining melatonin at dawn (Lincoln et al., 2003). As shown in figure 4.3, the interval between *per* and *cry* expression varies as the melatonin signal expands and contracts with varying photoperiod (Hazlerigg & Loudon, 2008).

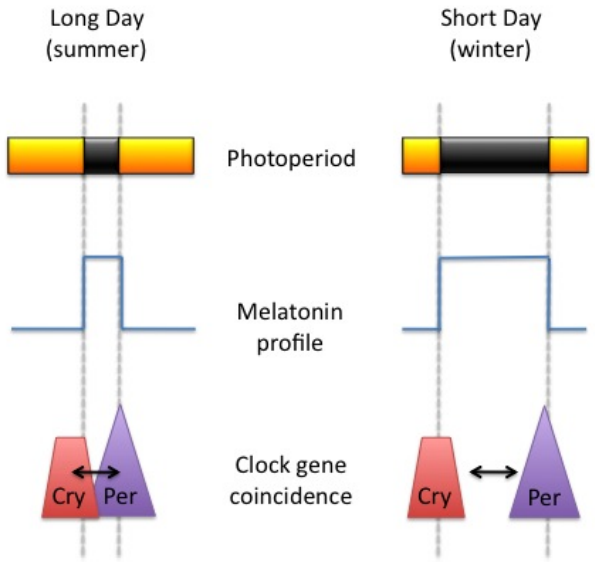

Figure 4.3 - Photoperiod and the internal coincidence of circadian clock gene expression. The length of the dark/night phase is translated into an extended melatonin secretion profile - shorter in summer nights and longer in winter, which leads to altered patterns of circadian clock gene expression in the mammalian PT (pars tuberalis). The coincidence of *per* (dawn) and *cry* (dusk) gene expression changes as the dark period expands and contracts over the annual seasonal cycle. Figure adapted from Hazlerigg & Loudon, 2008.

The synchronization and relative intensity of *cry* and *per* expression is presented here, as this chapter focuses on the direct measurement of circadian responsiveness of luminescent cells and tissue explants to full and skeleton photoperiods using LD and SD regimes. Three types of testing were performed; a) responsiveness of core clock gene expression to photoperiod in clonal cell populations, b) responsiveness of homozygous *Per3-luc* transgenic tissues including circadian-associated targets such as the pituitary, hypothalamus and pineal gland, and fish scales, and c) measurement of fecundity in sexually mature fish raised in LDsk or SDsk photoperiods (complementing "full" photoperiod data shown in chapter 2, figures 2.5-2.8). This data gives insights into the inner workings of peripheral clock mechanisms and is useful in comparing cellular, tissue and behavioural clock responsiveness in zebrafish.

4.2 Methods and Materials

4.2.1 Luminescent zebrafish cell lines

Per1-luc and *Cry1a-luc* cells were provided from established lab stocks, and produced as described previously (Vallone et al., 2004). In the following experiments, all cells were plated at 2.5–5.0 x10^5 cells per milliliter.

4.2.2 Zebrafish *Per3-luciferase* transgenic

Per3-luc transgenic zebrafish were bred and raised in the UCL aquatic facility. This transgenic stock was created with an insertion in the *period* 3 (*Per3*) promoter driving the expression of luciferase (luc) and were a generous gift of the Cahill group (Kaneko et al., 2006).

4.2.3 Bioluminescence assays

Per1-luc and *Cry1a-luc* cells were plated in quadruplicate wells of a 96-well plate in media containing 0.5 mM luciferin (Promega, Madison, Wis.). Cells were placed on a 12h/12h light/dark cycle for 3 days before being transferred into experimental photoperiods, as indicated in results. Bioluminescence was monitored on a Packard TopCount NXT scintillation counter (28°C). The intensity

of bioluminescence (counts per second) correlates with circadian clock gene expression (Carr et al., 2006).

Per3-luc tissue harvesting was performed within minutes of sacrifice and added to a pre-prepared media solution with L15 media with 0.5mM luciferin, Pen/Strep, Gentomycin and 15% Fetal Calf Serum (FCS). For fish scale experiments, scales were taken from anesthetized zebrafish, and cultured in the same manner as Per3-luc tissues; all samples were recorded in triplicate and mean values reported. All recording was performed in a temperature stable environment, with light/dark cycles controlled by LED light arrays illuminating plates with a full spectrum light source (1500 μW/cm^2). Each well was counted for 10s, hourly, for up to 3 weeks.

4.3 Results

4.3.1 *Per1-luc* and *Cry1a-luc* expression in full LD / SD

Initial Packard traces of *Per1-luc* and *Cry1a-luc* cells in full LD (16h/8h) and SD (8h/16h) photoperiods are shown in figure 4.4. *Per1-luc* cells in SD (4.4a; blue points) display a circadian delay during the dark phase of the cycle while maintaining a robust synchronization to light onset. In both LD and SD regimes, *Per1* expression peaks at ZT 3 and shows similar rhythmic amplitudes (fig 4.4a). *Cry1a-luc* cells show strong light responsiveness in LD and SD (fig 4.4b, near vertical peaks at lights on), while SD entrained cells are phase delayed in extended darkness (fig 4.4b; blue points). This figure clearly establishes the differential effect of seasonal photoperiods on the cellular circadian clock.

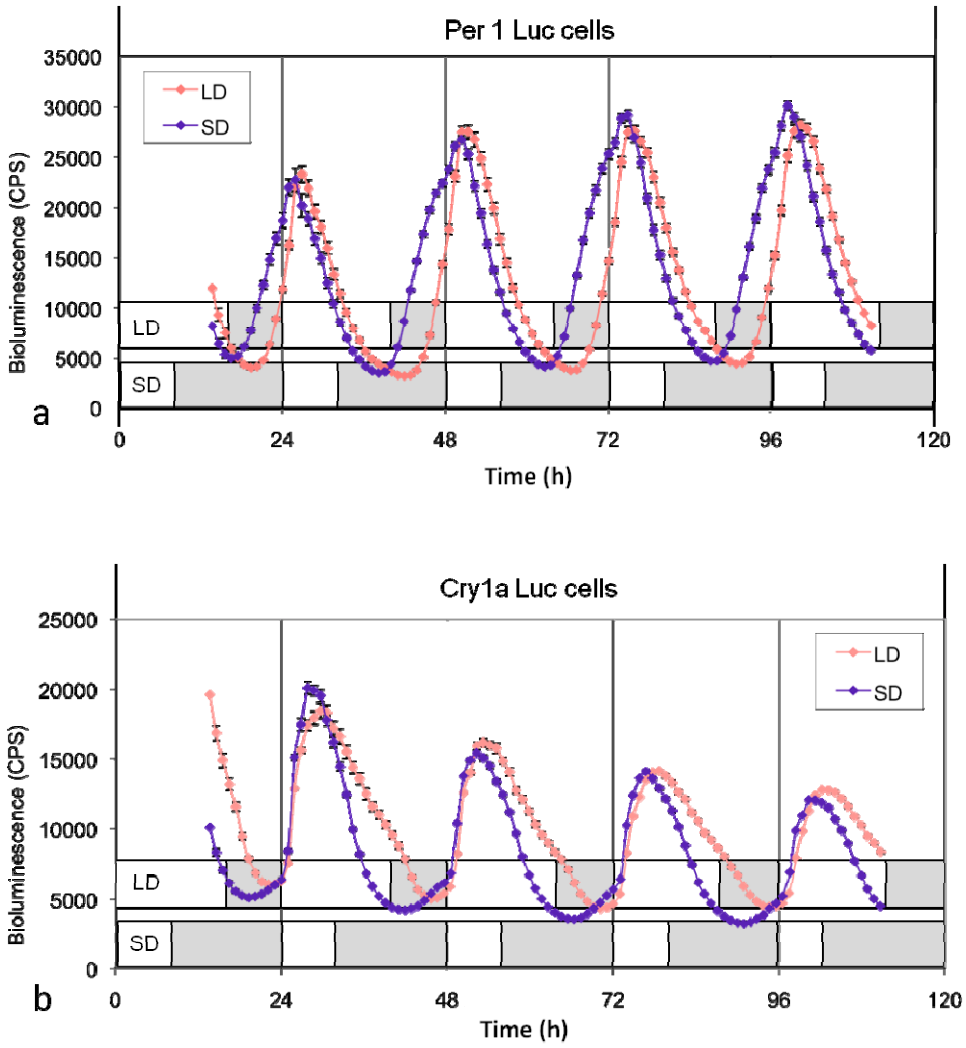

Figure 4.4: *Per1-luc* and *Cry1a-luc* cells exposed to LD (16h/8h) and SD (8h/16h) complete photoperiods. a) *Per1-luc* cells in SD show a phase delay during the extended dark phase, b) *Cry1a-luc* cells show a phase delay during extended periods of darkness (SD cells; blue) yet are strongly synchronized to light onset.

4.3.2 Circadian gene expression in SD skeleton lighting

Figure 4.5 illustrates the entrainment of circadian genes *Per1-luc*, *Per3-luc* and *Cry1a-luc* in peripheral clocks residing within individual body scales and clonal cell lines in a SD skeleton photoperiod (2h-4h-2h/16h). Both *Per1-luc* cells and *Per3-luc* scales entrain to the 1st pulse (dawn) of light (see fig 4.5a), thus entraining preferentially to the shorter subjective daylength (2h-4h-2h, rather than 2h-16h-2h; see 4.2 for schematic of these phases). Within SD skeleton lighting, peak *Per1* expression peaked at ZT 3, while *Per3* peaked at ZT 3-5 (fig 4.5, red and green traces respectively). While *Per1-luc* cells began with a 8-fold increase in oscillatory

amplitude, as compared with *Per3-luc* scales, these levels reached parity by day 8 (fig 4.5a – 192h). Slight responses to the 2nd light pulse were noted in both cells and scales, with no significant effect of circadian phase. It is important to note that recordings taken within the first 24h – 36h of entrainment are subject to phase inhibition, as cells are moved from ambient light phases to experimental conditions.

Figure 4.5b illustrates the responses of *Cry1a* cells to skeleton SD lighting, where the blue traces clearly show a direct response to light on/offset, and display a masked entrainment pattern with short peaks in expression at both dawn and dusk of light pulses. Similar to *Per1-luc* recordings, *Cry1a-luc* cells display dawn pulse entrainment, with the first *Cry1a* peak at ZT 3, the second at ZT 5, with the 4h dark period between pulses being interpreted as "day". The secondary peak in *Cry1a* expression leads to a delay in circadian offset, extending peak *Cry1a* expression into the early dark phase of the SD skeleton lighting. This two peak induction reflects the fact that *cry1a* is directly light inducible, as well as clock controlled.

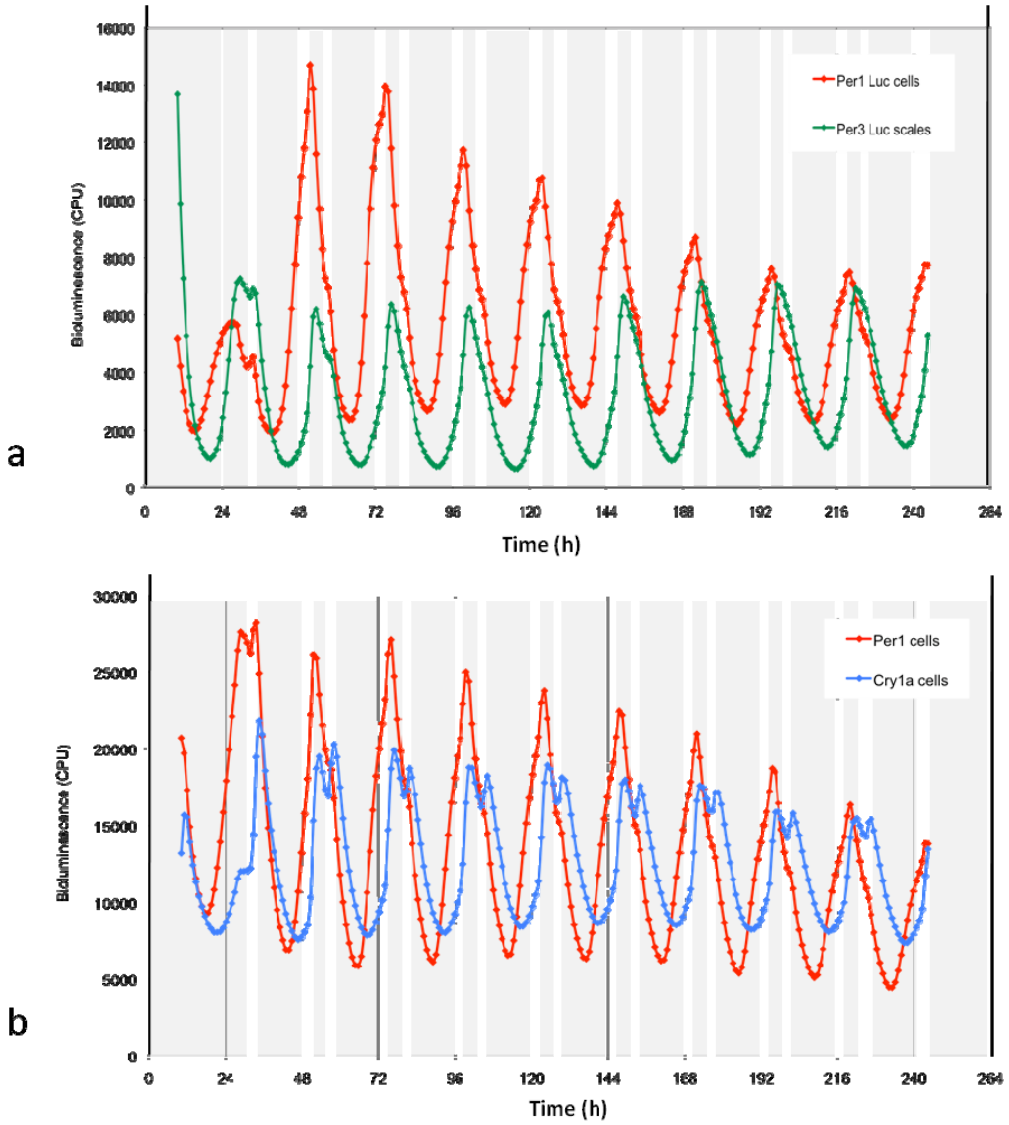

Figure 4.5: Evidence of entrainment to SDsk (2h-4h-2h/16h) photoperiod. a) *Per1-luc* cells (red) and *Per3-luc* fish scales (green) entrain the first pulse (dawn) directly, with little to no activity at dusk; b) *Per1-luc* cells (red) and *Cry1a-luc* cells (blue) entrain to the first (dawn) pulse by day 2 (48h), but *Cry1a-luc* expression is masked by the two pulse skeleton photoperiod.

4.3.3 Clonal cell entrainment to full and skeleton photoperiods

The entrainment of core clock genes were recorded systematically using long-term (up to 3 weeks) TopCount measures of bioluminescence. Figure 4.6a shows the circadian oscillations of *Per1-luc* and *Cry1a-luc* to LD (16h/8h), DD (full dark) and Control (12h/12h) photoperiods. *Per1-luc* expression peaks at ZT 3 after light onset in both the 16h/8h and 12h/12h regimes. In the absence of light (in DD) these oscillations persist with increasingly attenuated amplitudes. In the same

light regimes (LD, DD, 12h/12h), *Cry1a-luc* expression (fig 4.6a; blue trace) peaked directly after light onset and was strongly rhythmic throughout the testing period, displaying a marked compression of oscillatory amplitude in DD and drifting of the dawn peak 1h-2h later by day 9 (DD, 216hrs middle). *Cry1a* cells moved into 12h/12h lighting then displayed clear circadian (day) oscillations, with a phase delay of 1h-2h; peak expression at ZT 5 (midday), rather than ZT 3 (dawn) in LD conditions. Cry1a cells were strongly (and immediately) light responsive in both LD and 12h/12h conditions.

Cell traces shown in figure 4.6b, were exposed to LDsk (2h-12h-2h/8h), DD (full dark) and LD (16h/8h) photoperiods. In LDsk, *Per1-luc* cells show rapid entrainment to the dusk pulse (the 2nd of the 2h-12h-2h light pulses) and have stable oscillations in culture within 24h, with peak expression at the same phase angle seen in LD (16h/8h) entrainment conditions (fig 4.6b; red trace). On the LD skeleton cycle, the "dawn" pulse induced a secondary increase in *Per1-luc* expression, causing a small lag in the 24h oscillation before light-dependent repression occurred. Entrainment to the dusk pulse was maintained after entry into DD (fig 4.6b; red trace at 144 hrs), with peak *Per1-luc* expression at CT 3. Interestingly, the amplitude of *Per1-luc* expression increased 3 fold in DD, suggesting the removal of light-induced repression of *Per1* allowed full expression of the gene, coupled with on-going clonal growth. The end of the DD period shows an experimental issue with an acute drop in *Per1* expression at the end of day 8 (just prior to 216h), which is not repeated, in the following experimental days. In full LD (16h/8h) conditions after LDsk and DD exposure (fig 4.6b, right), *Per1-luc* expression began to rise at lights off (ZT 16); this is in contrast to the results in fig 4.5a (left), where peak entrainment began at dawn, rather than dusk pulses. The different responses between *Per1-luc* expression in fig 4.5a and 4.6b likely reflect prior oscillation patterns, which (in fig 4.6b) were first established in the LDsk regime during the first 6 days of entrainment (fig 4.6b, left; 0 – 144h).

Cry1a-luc cells are entrained to the "dusk" (2nd) pulse and exposure to the dawn pulse resulted in a small secondary peak, suggesting a masking effect during skeleton photoperiod exposure, leading to an extended offset of *Cry1a* expression.

In fig 4.6b (left side, blue), the longest period of darkness is mid-way between the skeleton pulses (2h-12h-2h) rather than the "true" night period (8h dark). *Cry1a-luc* expression entrains to light as though the longest dark period is the night, rather than the day.

During DD, a continuous, 24h *Cry1a-luc* rhythm was shown, based on the dusk peak originally presented in LDsk. Cry1a peaks shifted 1h-2h in the DD phase, based on the entrainment schedule of the previous light conditions (fig 4.5b, middle). A change into LD (16h/8h) reset this rhythm leading to a ZT 5 peak on the 2nd LD day (fig 4.6b – blue trace). *Cry1a* expression in DD showed a drop in oscillatory amplitude, as this gene is a light inducible as well as clock regulated (Tamai et al., 2007). Amplitude was consequently regained immediately upon exposure to a light/dark photoperiod. As noted with *Per1-luc* expression (midway through Day 8; 192 hours) an experimental error caused a minor aberration in *Cry1a* oscillations, likely due to an accidental interruption of the DD entrainment. Shortly thereafter the cells moved to LD (16h/8h) lighting and *Cry1a-luc* oscillations were immediately synchronized by light exposure, as shown by day 10 (240h; fig 4.6b, right side).

Figure 4.6c shows the effects of SD (8h/16h) photoperiodic entrainment, before entering DD (full dark). Light onset led to an increase in *Per1-luc* expression, with a peak at ZT 3, which gradually declined to a nadir point at ZT 11 (3h into the dark phase). At each dawn period, an acute jump in expression was related to light exposure, increasing the peak oscillation briefly between ZT 0-3. In addition, SD entrained *Cry1a-luc* expression peaked at ZT 3, with a strong rhythmic amplitude which persisted in full darkness. A technical problem at 144h caused a brief resetting of this oscillation, accounting for an unequal peak in responsiveness in the DD phase (4.6c- blue trace, right), but did not alter the timing the oscillation.

Finally, exposure to SDsk (2h-4h-2h/16h) led to peak *Per1-luc* expression at ZT 3, associated with the dawn (first) skeleton pulse (fig 4.6d; red trace). A minor expression increase to the dusk pulse led to a small extension in *Per1* decline. *Cry1a-luc* expression showed two peaks, the highest of which was expressed at ZT

3 after the dawn pulse, suggesting entrainment to a 2h-4h-2h subjective daylength (fig 4.6d; blue trace). The 2nd *Cry1a* peak came shortly after the dusk pulse, and is indicative of a directly light stimulated circadian clock element. As shown throughout testing, movement into DD led to a strong drop in circadian amplitude, synchronizing with *Per1* expression levels in this phase (as shown by the oscillation amplitudes on the Y axis; fig 4.6d, right).

The results shown in figure 4.6 a-d confirms peak *Per1-luc* expression at ZT 3 after a dawn pulse (or initial light onset) in all experimental photoperiods except LDsk (in figure 4.6b, left side). *Cry1a* responded to SD skeleton lighting as though the two closest pulses were the "day" phase, and the longest dark period was night, with the first of the light pulses acting as the strongest entrainment factor.

Figure 4.6 (next page): In vitro cell culture of circadian clock rhythms monitored up to 18 days. Per1-luc (red) and Cry1a (blue) expression in a) LD, DD and 12h/12h full photoperiods; b) LDsk, DD, and LD photoperiods; c) SD into DD photoperiods; and d) SDsk into DD photoperiods.

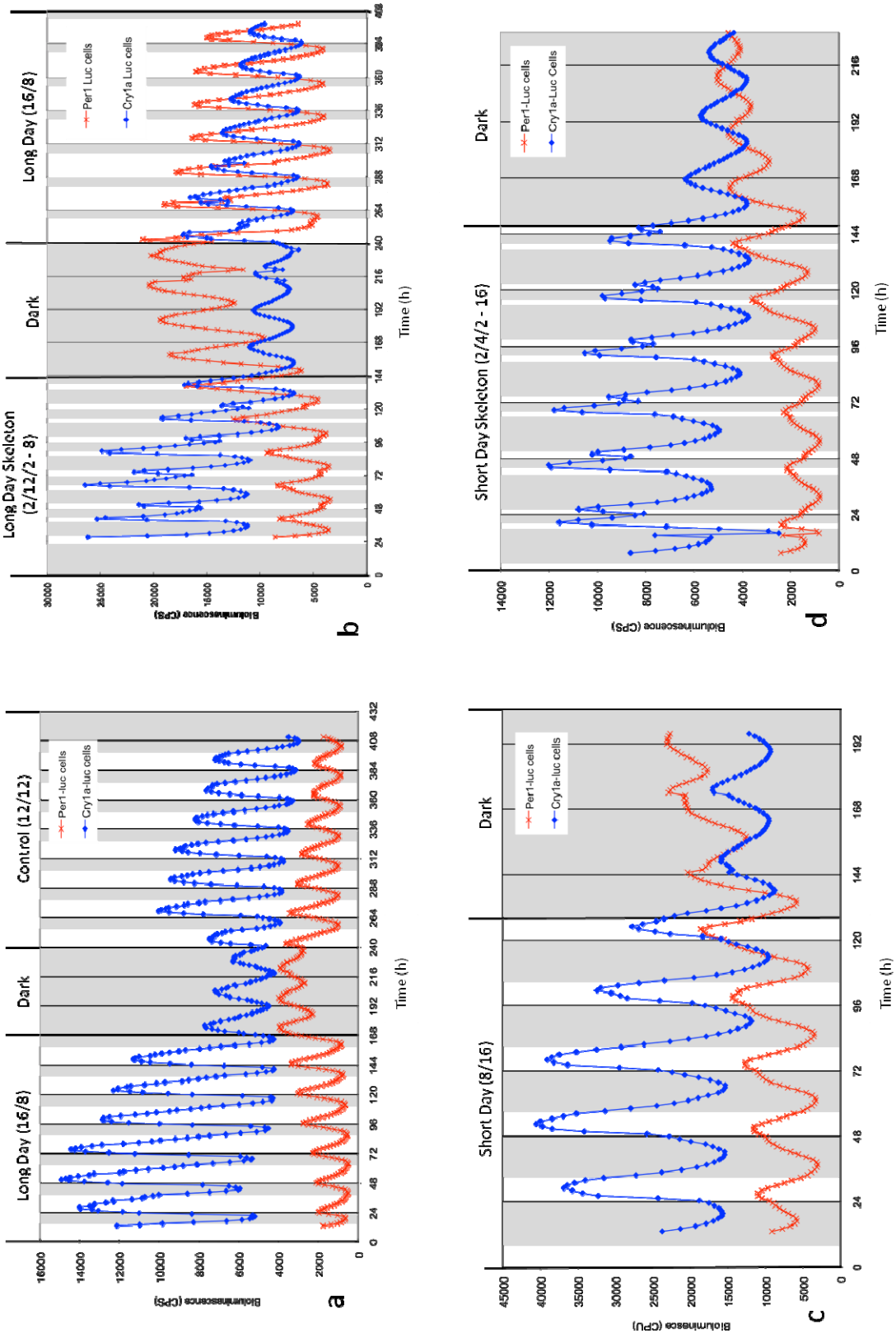
Long Day (16/8)
Dark
Control (12/12)
Per1 -luc cells
Cry1a-luc cells
Bioluminescence (CPS)
Time (h)
a
Long Day Skeleton (2/12/2 - 8)
Dark
Long Day (16/8)
Per1 Luc cells
Cry1a Luc cells
Bioluminescence (CPS)
Time (h)
b
Short Day (8/16)
Dark
Per1-luc cells
Cry1a-luc cells
Bioluminesce (CPU)
Time (h)
c
Short Day Skeleton (2/4/2 - 16)
Dark
Per1-Luc cells
Cry1a-Luc Cells
Bioluminescence (CPS)
Time (h)
d

4.3.4 *Per3-luc* tissue explants - full and skeleton photoperiods

Monitoring of tissue-specific circadian rhythms was undertaken with a focus on *Per3-luc* expression. These tissues were tested in parallel with the cell lines shown in figure 4.6, thus they were exposed to the same photoperiodic lighting regimes. As previously shown (see fig 4.5a), *Per1* and *Per3* expression levels are comparable in a SD skeleton regime, with *Per3* levels peaking 1-2hrs after the expected ZT 3 *Per1* peak. Testing *Per3-luc* tissue explants allows us to measure differences in isolated regions (such as the pituitary, hypothalamus and pineal gland). These tissue-specific responses defined regional responsiveness to seasonal photoperiodic lighting and explored responses to skeleton light regimes (light exposure vs. light duration) in these specific regions.

Figure 4.7a illustrates the periodicity of *Per3-luc* in tissues explants, when exposed to LD (16h/8h), DD (full dark) and 12h/12h (control) lighting conditions. *Per3-luc* rhythms peaked at ZT 3 in both the LD and 12h/12h regimes, with oscillations persisting in DD (fig 4.7a – middle). Long term testing of hypothalamic explants was not sustained after 8days of culture (blue trace), while pituitary samples continued to oscillate well past 17 days (pink trace), without a change in media. The differences in tissue longevity are likely due to explant size and specific tissue perfusion needs.

Per3-luc expression in LDsk (2h-12h-2h/8h), DD and LD (16h/8h) is shown in fig. 4.7b. As with *Per1-luc* cell expression, tissue *Per3-luc* expression peaks at ZT 3. All three tissues types responded to the 2nd light pulse (dusk) as their primary cue for circadian entrainment, suggesting that the tissues treat the longest dark period (12h) as the subjective night and interpret the day phase as consisting of 2h-8h-2h light phase. Interestingly, hypothalamic *Per3-luc* oscillations had a small secondary (dawn) peak while maintaining a clear 24h rhythm in dusk entrainment (fig 4.7b – blue trace). This result was specific to the hypothalamus, while pituitary and pineal explants were unresponsive to dawn light pulses. Hypothalamic oscillations in DD were more quickly attenuated than pituitary and pineal *Per-3luc* rhythms (day 9, 216h, blue trace), but resumed a robust rhythmic amplitude when exposed to a full LD light dark cycle (fig 4.7b, right side, blue trace).

As shown in figure 4.7c, all tissues were exposed to SD (8h/16h) light for 6 days before being moved into full darkness. *Per3-luc* expression was the same in all tissues, peaking at ZT 3 in the SD phase, with continued oscillations in DD. Hypothalamic recordings were significantly higher in amplitude at the start of recording, decreasing over time as the tissues weakened in culture.

Figure 4.7d illustrates the expression of *Per3-luc* tissues in SDsk (2h-4h-2h/16h) before moving to DD. In all cases, *Per3-luc* expression peaks at ZT 3, with the main entrainment pulse at dawn. The second light pulse (dusk) elicited a slight response in hypothalamic and pineal samples, extending the *Per3-luc* period within each 24h cycle slightly. By 240h (day 10), both the pituitary and hypothalamic samples had phase drifted in DD conditions by approximately 1h/day.

Overall, *Per3-luc* expression peaks at ZT 3 (after the dawn pulse) in the majority of photoperiods tested, such as LD (fig. 4.7a) and SD (fig. 4.7c) and SDsk (fig 4.7d). Interestingly, *Per3* expression entrains to the dusk pulse in the LD skeleton photoperiod. Tissues exposed to LD skeleton lighting entrain to a 2h-8h-2h/12h photoperiodic cycle, taking the longest dark period to be the subjective night. Exposure to a SD skeleton photoperiod (2h-4h-2h/16h) caused preferential entrainment to the dawn pulse (2h-4h-2h), again interpreting the (longest) 16h dark phase as the subjective night. When comparing LDsk and SDsk results, it is clear that all three neural tissues tested undergo a phase-shifting effect, as predicted by Pittendrigh and Daan (1976), and consistently interpret the first pulse after the longest dark period as "dawn" and set their circadian oscillations to this cue preferentially.

Figure 4.7 (next page): *In vitro* tissue explant culture of *Per3-luc* rhythms monitored up to 18 days. Pituitary explants (pink), Pineal glands (green) and Hypothalamic samples (blue) from *Per3-luc* mutants were measured in triplicate, with means shown above. *Per3-luc* expression was tested in a) LD, DD and 12h/12h photoperiods; b) LDsk, DD, and LD full photoperiods; c) SD into DD photoperiods; and d) SDsk into DD photoperiod

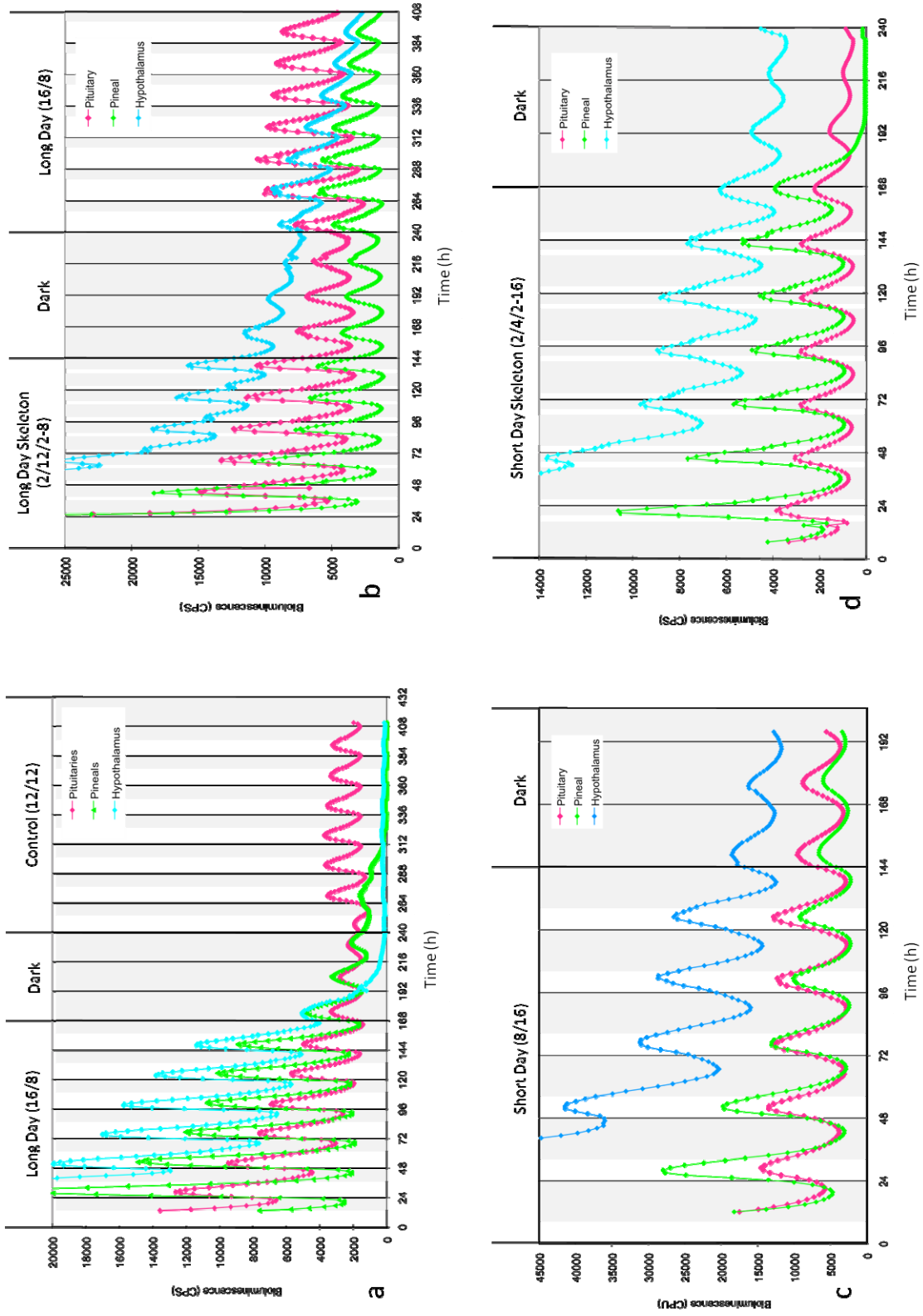
Long Day (16/8)
Dark
Control (12/12)
Pituitaries
Pineals
Hypothalamus
Bioluminescence (CPS)
Time (h)
a
Long Day Skeleton (2/12/2-8)
Dark
Long Day (16/8)
Pituitary
Pineal
Hypothalamus
Bioluminescence (CPS)
Time (h)
b
Short Day (8/16)
Dark
Pituitary
Pineal
Hypothalamus
Bioluminescence (CPU)
Time (h)
c
Short Day Skeleton (2/4/2-16)
Dark
Pituitary
Pineal
Hypothalamus
Bioluminescence (CPS)
Time (h)
d

4.3.5 Skeleton photoperiodic breeding

As first shown in chapter 2, behavioral tests of fecundity were performed under varying photoperiodic conditions. Fecundity results under full LD and SD photoperiods are shown in figures 2.5 (LD vs. SD over 100 consecutive days) and 2.6 (LD vs. SD, followed by a "switch" into opposite regimes, up to 52 days total). Shown here, figure 4.8 illustrates the result of fecundity testing (mean clutch size) in adult zebrafish housed in LDsk (2h-12h-2h/8h) or SDsk (2h-4h-2h/16h) as compared to groups housed in regular UCL fish facility conditions (14h/10h; black trendline).

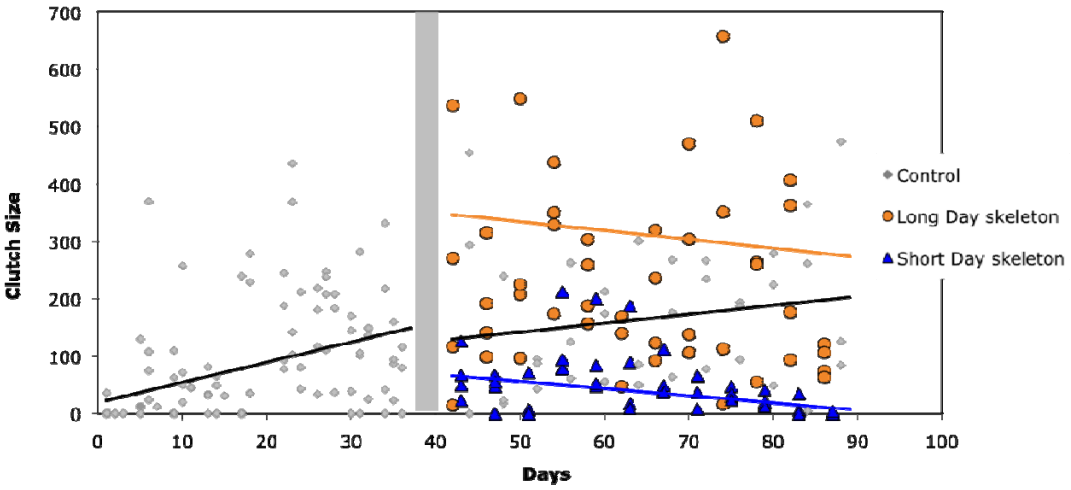

Figure 4.8: Photoperiodic fecundity of adult zebrafish, 8mo old**. a)** Pre-testing in control lighting conditions on days 0-38, followed by breeding either LDsk (2h-12h-2h/8h; orange points) or SD (2h-4h-2h/16h; blue points) from day 41 - 90. Grey bar indicates the switch from control to experimental light regimes, on days 38-41. Grey points indicate clutch sizes of control fish kept in 14h/10h LD conditions.

Photoperiodic fecundity levels changed immediately when moved from control conditions (14h/10h) into experimental light-controlled cabinets. At the start of entrainment, fish exposed to LDsk lighting had a mean breeding level of 404 eggs/clutch, while SDsk exposed fish laid less than 72 eggs/clutch (Control mean = 250 eggs/clutch). Over the course of the experimental phase (days 41-90) LDsk fish had decreasing fecundity levels (LDsk slope = -1.5406), but maintained average level greater than the control (slope = +1.5581) or SDsk (slope = -1.2517) groups. SDsk fish showed an immediate drop in clutch sizes (72 eggs on day 51), down to a single egg laid on day 89.

The difference in skeleton photoperiodic-sensitive fecundity levels was highly significant different between conditions (D = 0.062; p = 0.001). Levels of egg-laying by SDsk fish reached a low of 1 egg laid/day after 50 days of entrainment (Fig 4.8, right side), while LDsk groups had clutches of no less than 98 eggs/day at the same point.

4.4 Discussion

Entrainment of peripheral clocks in zebrafish cell lines and tissues explants have given interesting insights into the role of changing photoperiods on the molecular core components of the clock. The use of skeleton photoperiods allows further investigation of the role of specific clock genes in seasonal responsiveness, exploring the possibility of tissue-specific differences between dawn and dusk sensitivities.

4.4.1 Skeleton and Full Photo-entrainment

The entrainment of zebrafish cellular circadian rhythms to full LD and SD photoperiods shows clear peaks in *Per1* at ZT 3 and Cry1a at ZT 5, in both conditions. SD entrained cells had a clear lag in the declining phase of each cycle as compared to LD cells, but 24h circadian oscillation peaks were maintained throughout the experiment. This demonstrates the importance of the circadian period regardless of daylength in peripheral clocks, and establishes a clear dawn (ZT 3-5) responsiveness in these cells (see fig 4.4).

Key research questions in regards to peripheral clock expression involve the timing of skeleton pulses in defining the subjective "night" or dark period of the entrained circadian period. During a LD skeleton regime (2h-12h-2h/8h), the clock could entrain to either the first 2h light pulse (followed by 12h of dark) or the second pulse (followed by 8h of dark). While the skeleton 2h-12h-2h phasing matches the duration of a full 16h LD light phase, total light exposure is no more than 4h. Conversely, would a SD skeleton photoperiod initiate entrainment to a 2h-4h-2h/16h photoperiod, with cells responding to the dawn pulse primarily, or

would the cellular clock entrain preferentially to the dusk pulse (2nd light pulse; 2h-16h-2h/4h), a subjective "20h day, 4h night" regime?

These questions were addressed in clonal cell populations (expressing *Per1-luc* and *Cry1a-luc*) and in transgenic fish scales (expressing *Per3-luc*). In a SD skeleton photoperiod (2h-4h-2h/16h), both *Per* genes entrained to the first 2h light pulse after 16h of dark, with comparable amplitudes and periodicities. *Cry1a-luc* expression in the same SD skeleton test also entrained to the "dawn" pulse (2h-4h-2h) of the photoperiod, but displayed the masking effect of direct light responsiveness, as both light pulses stimulated *Cry1a* expression. This result confirms previously published findings in 12h/12h skeleton photoperiods, where *Cry1a-luc* cells had dual peaks after light pulses as short as 15min (Tamai et al., 2007).

Testing of clonal populations expressing *Per1-luc* and *Cry1a-luc* indicated peak expression directly after light exposure (approximately ZT 3) in LD, SD, and 12h/12h photoperiods (Fig 4.6a-d). When exposed to a LD skeleton regime (2h-12h-2h/8h) *Per1-luc* cells entrained to the first light pulse (subjective dawn) after the (longest) 12h dark period, followed by a small (masking) peak at the "dusk" light pulse, after the 8h dark period (fig 4.6b; red trace). In LD skeleton exposure, both dawn and dusk pulses stimulated *Cry1a-luc* expression. Peak *Cry1a-luc* expression was recorded 3h after 2nd pulse, suggesting that the cells interpreted longer dark phase of 12h as the subjective "night", and used the alternate 2h-8h-2h/12h regime as their skeleton photoperiod; a model of a 12h/12h light dark cycle rather than the possible 16h/8h cycle interpretation.

As noted by Pittendrigh and Daan (1976), skeleton lighting models predict entrainment patterns will be more stable when activity is focused within the longer pulse interval, over the shorter. In cases of increasing asymmetry, organisms may "phase jump", shifting their active periods from the shorter to the longer interval, in the current model the circadian "dawn" would be interpreted as the first light pulse after the longest period of darkness. This phase shift, called "psi jumping" (Pittendrigh & Daan, 1976), is evidenced between full and skeleton

photoperiods in figure 4.6b, where *Per1-luc* and *Cry1a-luc* expression entrains to the first light exposure after the longest period of darkness, as "dawn", an interpretation based on dark-length, reminiscent of the key role of night length in the External Coincidence Model of Photoperiodism (see figure 1.2, chapter 1 for a review). When comparing LDsk and SDsk *Per3-luc* results, it is clear that all three tissues tested undergo a phase-shifting effect, as predicted by Pittendrigh and Daan (1976), and consistently interpret the first pulse after the longest dark period as "dawn" and set their circadian oscillations to this cue preferentially.

Per1-luc entrainment to a SD skeleton regime resulted in a single peak in expression, followed by a slight lag in phase oscillation, with entrainment linked with the subjective "dawn" pulse; thereby interpreting the 2h-4h-2h/16h cycle as having a 8h "day" period, rather than the extreme 20h "day" possible with a dusk pulse entrainment. In the same SD skeleton conditions, *Cry1-luc* expression peaked just after the 1st light pulse (2h-4h-2h/16h), with a secondary peak at dusk. In this photoperiod, *Cry1a-luc* cells interpreted the two closest pulses as "day", and the longest dark period as "night", as they had in the LD skeleton regime. This reflects and extends previous results, where entraining skeleton photoperiodic pulses of 15min induced peaks in *Cry1a* expression after each exposure (Tamai et al., 2007).

In zebrafish light inhibits CLK:BMAL function (in part) through the transcriptional activation of *cry1a*. The binding of the CRY1a protein to CLK and BMAL (singly) prevents the formation of an active transcriptional complex, leading to the light-dependent repression of *per1* (Tamai *et al*, 2007). This process is thought to be one route by which the core clock mechanism is entrained to photoperiodic cycles in this system. As shown in figure 4.6, this repressive relationship between Cry1a and Per1 is illustrated in period of DD, where Cry1a expression drops immediately, and Per1 levels increase in tandem (as Cry1a repression is removed).

This interaction is further illustrated as light-sensitive *Cry1a* expression is strongly inhibited in full darkness (fig 4.6, middle), which coincides with the strong increase in *Per1* expression, likely due to the release of *Cry1a* repression. The results of LD and SD skeleton entrainment given here reflect classic circadian work

by Colin Pittendrigh (1964) where *Drosophila* eclosion activity "jumps" such that it is timed to occur in the shorter of the two inter-pulse dark intervals.

4.4.2 *Per3-luc* tissue responsiveness

The expression of *Per1* in cell lines is synchronized with *Per3* rhythms in transgenic zebrafish scales (fig 4.5a; green trace). Peaks in both genes are maximal at ZT 3, reflecting published findings *in vivo* and other zebrafish cell lines tested (Cahill, 2002a). *Per3-luc* expression in photoperiod-associated tissues such as the pituitary, pineal and hypothalamus also peaks at ZT 3, a finding also noted in regular LD and SD photoperiods (see fig 4.7a+c). When exposed to skeleton photoperiods, peak *Per3* –luc expression remained locked to ZT 3, and is entrained to the 1st light pulse after the longest period of darkness (dawn in SDsk; dusk in LDsk). These results reflect results in clonal cell responsiveness, in matched experiments (fig 4.6). In both LD and SD skeleton regimes, pineal and pituitary samples responded to a single light pulse while hypothalamic samples in the LD skeleton regime showed a secondary peak with the 2nd pulse exposure (exclusively). This novel finding in hypothalamic tissue explants suggests that some regional sensitivity in neural light responsiveness exists and may be stimulated *in vitro*. Further work using hypothalamic explants would help define the nature of this tissue-specific phenomenon. Ideally, initial tissue explant entrainment, followed by an extended period in DD would explore questions regarding tissue specific free running periods, and comparisons between dispersed hypothalamic cells and intact hypothalamic explant cultures would be of interest.

4.4.3 *Per*/*Cry* Coincidence Theory

The entrainment of peak timing amplitudes and the difference in oscillatory rising/dropping phase entrainment (as shown in fig 4.3) raises the possibility of independent "morning and evening" oscillators within zebrafish cells, with each oscillator sensing light at dawn or dusk specifically. PER and CRY proteins are key components of the negative limb of the circadian clock, rhythmically modulating circadian gene transcription via E-box motifs on target genes (Cahill, 2002a).

Zebrafish *Per1* expression has been shown to peak near dawn, mimicking similar circadian oscillations in seasonally sensitive mammals such as syrian hamsters (*M. auratus)* and soay sheep (*Ovis aries*) (Cahill, 2002a; Hazlerigg & Wagner, 2006). In seasonally breeding hamsters, this increase comes in the early morning as circulating melatonin levels decline and has been localized to the PT (Messager et al., 1999). Using direct injection of melatonin, Dardente and colleagues have shown clear induction of Cry1mRNA and inhibition of *Per1* mRNA in the mammalian PT (Dardente et al., 2003). These findings suggest the amplitude and expression of *Per1* and its repressor *Cry1a*, could be linked with melatonin signaling and could be regulated in a tissue-specific manner, creating a photoperiodic "calendar" model, based on melatonin action on *Per1* and *Cry1* expression in the PT. This model predicts the seasonally changing night length (interval between dusk and dawn light exposure), as represented by the duration of nocturnal melatonin secretion, may be reflected in the temporal coincidence of the per and cry genes in the PT of the mammalian pituitary. Unlike Cry1 in mammals, a key difference in zebrafish Cry1a is its' direct light responsiveness. Currently, no data exist regarding putative responsiveness to melatonin by this gene. Consequently, I was unable to confirm a mammalian style-model in the current work, as tissue constraints in zebrafish did not allow PT specific experimentation. After extensive trials, long-term cultures of isolated pituitaries were performed using transgenic *Per3-luc* samples. These results need to be replicated in *Per1-luc* and *Cry1a-luc* mutants in order to fully examine this model in the current system. My work has proven the feasibility of this approach and established a novel protocol for micro-cultures in a new vertebrate circadian model system.

An alternative interpretation from figure 4.3 fits more with an external coincidence model (see figure 1.2; chapter 1 also). The long photoperiod dramatically increases the duration of expression of *cry1a* in zebrafish cells, as a direct consequence of its light inducibility; long days mean more *cry1a* expression. As *cry1a* is a strong repressor of *per1* expression, the rising phase of *per1* expression is delayed by a duration very similar to the increase in photoperiod. The peak timing is the same, but the *per1* rhythm is delayed, a fact that is very

clear when one examines the trough in expression rather than the peak. If there is a photoinducible phase or window associated with this timing, in the mid or late night, then this change of waveform on a long day would place this photoinducible window now into the light (around dawn) on a long day. It is important to state that we do not yet know if these cell lines show a downstream photoperiodic response. However, the above change in entrained waveform could provide an underlying clock mechanism that could drive photoperiodism in cell culture.

4.4.4 Breeding in Skeleton Photoperiods

After establishing the responsiveness of isolated zebrafish cells and tissue explants to full and skeleton photoperiods, it was useful to record the behavioural effects of such regimes on previously established measures such as fecundity and breeding. Figures 2.5 to 2.8 have illustrated the stimulatory effects of LD light exposure on clutch sizes, and the inhibitory effect of SD regimes on both fertility and fecundity. Would established pairs of breeding zebrafish respond to skeleton photoperiods in similar way to full light regimes, as shown in chapter 2? Figure 4.8 illustrates the mixed results found in the current skeleton breeding model. The LDsk regime did stimulate breeding, with a significant increase in clutch sizes at the beginning of the experimental period, which was sustained above SDsk and control groups throughout the testing period. LDsk clutch sizes were highly variable throughout testing and while clutch sizes remained high, there was a decline in mean fecundity over time, which is not demonstrated by groups in full LD entrainment conditions.

Fecundity rates of SDsk entrained zebrafish were similar to full SD entrained groups. Initial SDsk exposure coincided with an immediate drop in breeding levels, which declined over time. As expected, SDsk entrained pairs had lower clutch sizes than LDsk and Control groups, and displayed less variability in egg laying throughout the experiment.

Exposure to a skeleton LD photoperiod had a positive effect on zebrafish fecundity, and skeleton SD lighting inhibited egg laying, and these effects were significantly

different than controls. These effects were acute, starting on the first day of entrainment and sustained throughout the testing period. Skeleton photoperiods differed from full photoperiodic entrainment, as fecundity levels declined over time, suggesting that absolute light duration is necessary for physiological fitness rather than matched light exposure in the form of skeleton "pulses", as tested here. Further work such as monitoring the light-responsiveness of reproductive tissues is necessary to clearly establish a link between local and systemic control of fecundity in relation to photoperiod. The differences currently observed between LDsk and SDsk reproduction may be due to the limited light exposure duration (4h in both conditions or the need for appropriate phasing of a photo inducible phase, or altered internal coincidence of oscillating genes.

4.4.5 Overall skeleton photoperiod responsiveness

Overall, the work described above has established the similarity between cell and tissue responsiveness in *in vitro* models of skeleton and full LD/SD seasonal photoperiodism. Three fundamental zebrafish circadian genes *Per1*, *Per3* and *Cry1a* were monitored in long term cultures and consistently entrained to light pulses, such that the shortest dark phases were interpreted as part of the subjective day, with the longer dark phase as subjective night. Circadian-associated tissues such as the pituitary, pineal and hypothalamus were cultured individually to monitor the possibility of differential regional rhymicity and responsiveness. Transgenic *Per3-luc* expression in these tissues was expressed as expected, with peaks at ZT 3 in all photoperiods tested. Interestingly, hypothalamic *Per3-luc* explants displayed a clear secondary peak after the dusk pulse in LD skeleton lighting, a result in this tissue specifically. This result suggests a complex interaction with other classic circadian genes such as *Cry1a* and further work using transgenic models would be highly informative. Finally, long-term behavioural testing was undertaken to monitor the effect of seasonal skeleton photoperiods (LD and SD) on zebrafish fecundity. While skeleton LD lighting did have a stimulatory effect of clutch sizes, this effect diminished over time, while full LD entrainment had increasing rates of reproduction throughout the testing period. SD skeleton entrainment inhibited egg laying, as with full SD photoperiodic entrainment (see Chapter 2). These results are mixed, suggesting that light

duration (timing of light pulses) does work to influence whole animal reproductive parameters, but is not maximally stimulatory, as full LD light (16h/8h) exposure increases egg laying sequentially and significantly over time.

CHAPTER 5 – GENERAL DISCUSSION AND FUTURE WORK

The current work was undertaken to gain a better understanding of the photoperiodic regulation of seasonal reproductive physiology and somatic growth in the popular genetic model, zebrafish (*D. rerio*), and determine if this species is a useful new model with which to study the biology of photoperiodism. The results of this study have many applications, most notably to inform industrial aquaculture guidelines for teleost stock growth and maturation, and for use by zebrafish labs worldwide.

This research project had three main paths of study:

1) The effect of photoperiodism on whole organism physiological measures, such as growth and breeding, with a focus on groups housed in seasonal LD (16h/8h; summer) and SD (8h/16h; winter) light conditions.

2) The effect of LD and SD photoperiods on the expression of pituitary and hypothalamic hormones underlying growth and reproduction. These results are later discussed in relation to tissue-specific melatonin receptor expression to determine a relationship between neuroendocrine factors and the circadian system.

3) The responsiveness of isolated zebrafish cells and pituitary/neural explant cultures to seasonal skeleton photoperiods, exploring the effect of total light exposure on circadian rhythmicity in peripheral clock gene expression.

5.1 Photoperiod and Growth

Photoperiodic responsiveness, growth and nutritional status are important to reproductive timing and success, with species-specific thresholds of size, weight and growth to be crossed before sexual maturation can be achieved (Taranger et al., 2010). The data presented in chapter 2 clearly demonstrate the stimulatory effect of LD photoperiods (16h/8h) on adult zebrafish growth, as determined by simple measures of body weight and length (see fig. 2.4). This is reminiscent of

results in salmon, where exposure to increasing photoperiods (spring into summer) triggers early sexual maturation and stimulates growth (Le Bail, 1988). Light-mediated increases in growth were greatest between 11mo to 30mo coincident with the period of peak reproductive activity, and were absent in early adulthood (6mo), which might indicate an early period of photo-insensitivity.

Gonad weight was also significantly different between LD and SD groups, between 6mo to 20mo. Preliminary histological examinations of SD ovaries revealed oocyte atresia, while LD ovaries displayed abundant mature oocytes (data not shown). Interestingly, there were no differences in testis weight between LD and SD, at any age tested. Changes in ovary, but not testis weight indicate a gender-specific effect of photo-stimulation and reproductive capacity, such that successful gonad maturation (and successful reproduction) is dependent on long day photoperiods and may be primarily determined by the photoperiodic-sensitivity of the female zebrafish.

In order to explore the interplay between the external photoperiodic conditions and these physiological results (chapter 2), experimentation focused on pituitary and hypothalamic hormone expression under LD and SD conditions (chapter 3).

5.2 Photoperiod and neurohormone expression

Physiological maturation and growth is governed by the synthesis and release of a number of neurohormones (Holloway et al., 1999), while the individual control of reproductive status and gonadal maturation is governed by the synthesis and release of pituitary gonadotrophins specifically (Davies et al., 1999). Many of these endocrine signals are photoperiodically regulated and responsive to growth rates, thereby providing a link between internal resource/growth cues and the hypothalamic pituitary gonad (HPG) axis in fish (Holloway et al., 1999). Results discussed in chapter 3 focus on the daily and lifelong expression of a host of reproductive and growth related hormones in zebrafish, including the hypothalamic releasing hormones and their downstream pituitary targets, tissue-specific expression of melatonin receptors (circadian and lifelong differences

between LD and SD) and circadian and photoperiodic oscillations of Dio1, Dio2 and Dio3 expression in the zebrafish hypothalamus, never before published.

5.2.1 GnRH and pituitary gonadotrophins

Circadian clock genes are involved in the regulation of timed GnRH (gonadotrophin release hormone) pulses in cell culture (Chappell et al., 2003). In the current work, hypothalamic GnRH expression had dynamic, circadian oscillations; rising in the late afternoon in tandem with peak Cry1a levels (see fig 3.1a), thus confirming similar findings in other (larger) teleosts (Bayarri et al., 2004), and extending these findings to zebrafish. Peak GnRH pulses in the late afternoon have also been linked to diurnal gonadotrophin expression, such as LH *in vivo* (Sisk et al., 2001); also confirmed here, as both GnRH and LH expression profiles are synchronized. At night, (ZT 15; 3hrs into the dark period) pituitary PRL levels are at their lowest, coinciding with the increase in nocturnal melatonin expression. This may reflect similar findings in cultured trout pituitary, where PRL is inhibited in the presence of physiological doses of melatonin (Falcon et al., 2003a). Overall, circadian expression of the pituitary gonadotrophic hormones follows GnRH bi-modal patterns, with peaks in the late day and late night (fig 3.2b), and is consistent with similar patterns reported in larger teleost fish (Bayarri et al., 2004). Though it is not possible to actually measure the levels of circulating hormone in the blood of zebrafish, these results do show that this species might provide a useful and more convenient model system for studying reproductive hormonal changes in larger, commercially important fish species.

Long-term measures of GnRH and pituitary LH, FSH, and PRL levels were significantly higher in SD>LD groups at 6mo and 15mo (fig 3.3). These results are similar to findings in both goldfish (*C. aruratus*) (Sohn et al., 1999) and gilthead sea bream (*S. aurata*) (Zohar et al., 1995), where GnRH is known to stimulate gonadotrophin release, leading to similar expression profiles. At first glance this SD>LD difference may be counter-intuitive, when compared with stimulating effects of LD exposure on growth and reproduction documented in chapter 2. In salmon, FSH expression increases as vitellogenesis (maturation of vitellogenin; an

egg yolk precursor protein) and reproduction proceeds (Swanson et al., 1989), thus LD induced reproduction would be expected to coincide with a rise in FSH, in direct opposition to the findings shown here. These unexpected results may be explained by the breeding strategy used by a given teleost species. Zebrafish are an iteroparous species (having multiple reproductive cycles over their lifespan), similar to Rainbow Trout (*O. mykiss*). In trout, FSH levels oscillate within a given reproductive cycle, decreasing after vitellogenesis and remaining low, while being sufficient to maintain gamete growth without stimulating further follicular recruitment (Prat et al., 1996). I postulate that zebrafish FSH may oscillate in a similar, iteroparous manner, within their shorter reproductive cycle of 3-4 days in zebrafish (Westerfield, 1995), as compared to the extended seasonal cycles of trout. If correct, LD entrained zebrafish would be expected to express FSH in short peaks, 10-12hours before ovulation, dropping to baseline levels immediately after egg laying. Conversely, SD entrained zebrafish with low breeding rates would likely have high baseline FSH levels throughout their reproductively active years, as they struggle to develop mature oocytes and maximize vitellogenin production. Recently, administration of exogenous melatonin (mimicking a SD photoperiod) has been shown to increase egg production and levels of vitellogenin in zebrafish (Carnevali et al., 2011). Zebrafish reproductive hormone levels are likely quite dynamic, with short-lived peaks between spawning periods. These hormonal expression peaks may be overlooked by long-term sampling regime used here, where samples were taken systematically at different ages. Further experiments, expanding the resolution of sampling times, monitoring the expression of FSH receptors in the gonads and incorporating the use of knockout models for GnRH and gonadotrophins may conclusively determine any seasonal sensitivity in this model and are recommended in future testing to confirm the current hypothesis. In essence, the regulation of reproductive hormone gene expression is not as straightforward as initially expected, and more extensive (high resolution) sampling frequencies are planned for future experiments.

5.2.2 GHRH and GH

Measures shown in chapter 3 (fig 3.1 -3.2) demonstrate the circadian rhymicity of hypothalamic GHRH (growth hormone releasing hormone) and pituitary GH

(growth hormone) expression, though their oscillatory profiles are not synchronized. GHRH levels mirrored GnRH and gonadotrophic expression profiles, with lower amplitude. Pituitary GH expression is seemingly independent of GHRH, with a significant peak just after dawn (ZT3). In mammals, GH is released in nocturnal pulses from the pituitary gland and acts to stimulate bone and muscle growth, while in fish GH expression is diurnal (Sam & Frohman, 2008). Experiments using cultured trout pituitaries have shown bi-modal GH release, with picomolar concentrations of melatonin inhibiting GH release, while higher (nanomolar) concentrations increase GH secretion (Falcon et al., 2003a). In the current study, GH transcript levels are stably expressed from ZT 9 – 21 (late day and night), with a single significant peak 3h after dawn. Given the differences between transcription and translation, it is possible that GH expression follows melatonin secretion, with a consistent 4h-5h delay throughout the circadian cycle. Further study is recommended to confirm this hypothesis, including sampling these tissues at higher time resolutions and the use of both protein and mRNA techniques to discern possible differences between expression and secretion. Unfortunately at this time, good antibodies do not exist against these proteins in zebrafish.

Teleost GH is associated with energy allocation during the pre-spawning season, and contributes to the physiological decision to "spawn or wait" (Canosa et al., 2005; Mingarro et al., 2002). As the expression of GH is down-regulated in LD entrained samples (at 6mo, 15mo and 24mo), it is reasonable to hypothesize that these reproductively active groups may inhibit GH synthesis in favour of reproductive hormone expression. Further measures of photoperiodic GH, including higher resolution measurements (daily timepoints) to pinpoint detailed changes in GH, and GH receptor expression (within the reproductive organs) would be necessary to confirm this, and are recommended in future experiments. This could result in de-synchrony between hypothalamic GHRH and pituitary GH expression in fish under long-term photoperiodic exposure, as in the case here. Heightened GHRH sensitivity of pituitary explants from sexually regressed (SD entrained) specimens (over LD entrained groups) would be highly recommended for future *in vitro* experiments. Given the dramatic inhibition of SD exposure on

zebrafish fecundity (chapter 2), I anticipate long-term SD groups would be more responsive to GHRH expression, a hypothesis outside the scope of the current work.

5.2.3 TSH, MT1 and MT2

Mammalian photoperiodic studies have demonstrated increased melatonin receptor expression in the anterior pituitary and pars tuberalis (PT) (Dardente et al., 2003). PT cells derive from thyrotrophs during development, and seasonally express both thyroid-stimulating hormone (TSH) and the common glycoprotein subunit used to form the active heterodimer, thyroid-stimulating hormone (TSH) (Klosen et al., 2002). TSH released from the PT acts on the mediobasal hypothalamus, in the ependymal cell layer surrounding the third ventricle and target tanycyte cells directly (Hanon et al., 2008). Tanycyte cells are thought to modulate hypothalamic-pituitary interactions through the hypophyseal stalk and pituitary portal system, and alter melatonin transport across the blood–brain barrier (Rodriguez et al., 2005). In mammals, the pituitary PT cells expressing TSH are melatonin-sensitive and express MT1 receptors, yet are "blind" to TRH (thyrothrophin releasing hormone), suggesting a melatonin specific interaction (Hazlerigg & Loudon, 2008). In goldfish, short-day photoperiods have been shown to increase TSH mRNA (Sohn et al., 1999) as was shown here in 6mo samples (fig 3.3d).

Melatonin binding assays have pinpointed active sites within the HPG (hypothalamic-pituitary-gonad axis) (Falcon et al., 2010), with seasonal differences in a number of teleost species (Sauzet et al., 2008). As shown in chapter 3, expression of melatonin receptor subtypes MT1 and MT2 is tissue specific, gene specific and age specific with clear differences between LD and SD entrained photoperiodic groups (fig 3.5c). Both TSH and FSH levels were greater in SD>LD samples throughout life, similar to pituitary MT2 levels (in LD only). Interestingly, short-day MT2 levels differed from gonadotrophin expression, at any of the ages tested (fig 3.3 vs fig 3.5d).

Overall, circadian expression of zebrafish MT1 and MT2 is robust within the pituitary, with a dramatic peak in MT1 expression at dawn (compared with pit MT2), similar to the classical circadian genes *Per1* and *Per3* (fig 3.2c). Interestingly, these early peaks were tissue-specific, as hypothalamic samples showed a single (circadian) peak of MT1 expression in the late day and an absence of circadian oscillations in MT2 altogether (see fig 3.1c). Taken together, these results suggest that MT1 has a primary role in photoperiodic modulation of gonadotrophin release (over MT2). These findings are novel and demonstrate that transcriptional melatonin receptor expression is; a) circadian, b) tissue specific (pituitary over hypothalamus) and c) target specific (MT1 over MT2). Mimicking a short day photoperiod through extended melatonin administration has been shown to increase gonadal maturation, but does not trigger a full photoperiodic response from the brain-pituitary-gonadal axis of young LD entrained salmon males (Amano et al., 2000). Interestingly, levels of pituitary GnRH, LH and plasma testosterone were all suppressed by a ten-fold increase in circulating melatonin, suggesting that exposure to increased melatonin levels is involved with gamete maturation specifically (Amano *et al*., 2004). Based on the current findings in differential melatonin receptor expression in the zebrafish pituitary, I propose that MT1 and MT2 act as "gate-keepers" of seasonal reproductive signalling, and are themselves seasonally expressed.

5.2.4 Dio1, Dio2 and Dio3

In mammals, PT-derived TSH acts locally within the mediobasal hypothalamus to control tanycyte Dio gene expression (Hanon et al., 2008) and TSH receptor expression is co-localized with Dio2 in the hypothalamic tanycytes (Revel et al., 2006). Dio2 is a key enzyme in the control of thyroid-hormone activity, converting T_4 into bio-active T_3 in various target tissues (Hazlerigg & Loudon, 2008). Conversely, Dio3 works to inactivate T_3, and together the relative expression of Dio2 and Dio3 determines the levels of biologically active T_3 in the brain (Nakao et al., 2008b). Mammalian T_3 activity stimulates the release of GnRH by the hypothalamus into the portal blood vessels to pituitary, where LH and FSH release is increased (see fig 1.9 for details) (Nakao et al., 2008b).

The interaction of photoperiodic melatonin expression and reproductive activation (specifically within the hypothalamus and pituitary) is more clearly defined in mammalian models than in teleost systems. Using MT1 and MT2 knockout mice, a link between melatonin receptor expression and photoperiodic *Dio3* expression has been described, where melatonin injections suppressed *Dio2* and induced *Dio3* expression in wild-types, and this effect was blocked by MT1 disruption (Yasuo et al., 2009). Researchers have also found photoperiodic melatonin levels affect *Dio2* and *Dio3* expression in hypothalamic ependymal cells (EC), acting through MT1 receptors in the pituitary pars tuberalis (PT). This is corroborated by other mammalian studies, showing that the EC itself does not express melatonin receptors (Bartness et al., 2001; Schuster et al., 2000). The PT is considered a target site for seasonal melatonin signalling due to high levels of MT1 mRNA while lacking MT2 mRNA (Reppert et al., 1995), MT1 mRNA and TSH protein co-localization in the PT (Klosen et al., 2002) and PT produced TSH regulates *Dio2* and *Dio3* expression in the EC in Japanese quail (Nakao et al., 2008b), sheep (Hanon et al., 2008), and mice (Ono et al., 2008).

The zebrafish deiodinase enzyme expression levels reported here are entirely novel, as no published reports on circadian oscillations in teleost Dio expression were available at the time of writing, although Dio enzyme expression in photoperiodically entrained rodents (Yasuo et al., 2007) has been a major topic of circadian research in recent years. In birds, photoperiodic signals are received by deep brain photoreceptors of the medial basal hypothalamus (MBH) and integrated with the endogenous circadian oscillations of the clock-gene system (Yasuo et al., 2005). Daylength cues of light and dark thereby modulate deiodinase expression (Dio2 and Dio3), which stimulate and inhibit GnRH and its target reproductive hormones in the hypothalamus and pituitary, respectively (Yoshimura, 2010). Experiments shown in chapter 3 illustrate that the circadian expression of Dio1, Dio2 and Dio3 in the zebrafish hypothalamus is gene specific, with peak Dio2 levels in the late day. This agrees with rodent data, where circadian Dio2 mRNA levels are rhythmically expressed in the ependymal cells of LD-entrained hamsters and peak at ZT 9, while Dio2 expression in SD ependymal cells remained low throughout the day (Yasuo et al., 2007).

Photoperiodic expression of LD and SD Dio1 and Dio2 were similar throughout life, with a notable exception in LD Dio1 at 6mo, which was significantly lower than 15mo-24mo samples (fig 3.6a). Hypothalamic Dio3 levels were strongly affected by photoperiodic conditions, switching at each timepoint tested; 6mo LD>SD, 15mo SD>LD and 24mos LD>SD. This complex result is interesting when compared with circadian expression profiles, where Dio2 is clearly circadian and Dio3 daily levels are stably expressed from late day throughout the night (ZT 9, 15 and 21). These differences suggest a differentiation between circadian (Dio2) and photoperiodic (Dio3) responsiveness in these interactive enzymes.

As far as is known, this is the first demonstration of a diurnal rhythm of Dio2 expression in the zebrafish hypothalamus and is important in unravelling the molecular basis driving the photoperiodic switch between T_3 and T_4, as reported in fish (Morin et al., 1993). I propose that the circadian expression of Dio2, with peak levels in the late day (ZT 9; fig 3.1d) may be associated with the increase in hypothalamic GnRH at the same time (fig 3.1b) stimulating increases in FSH and LH also observed at ZT 9 (fig 3.2c). The lack of clear photoperiodic impact on Dio expression levels may reflect the frequency, and time-scale of the time points examined. In quail the major photoperiodic changes in Dio levels were seen rapidly, within the first two days of a long day response. It would be very interesting to repeat these studies on Dio expression levels in zebrafish, but under a similar experimental paradigm, following immediate transfer to a long day photoperiod.

5.3 Photoperiod and Breeding

Seasonal photoperiods have been shown to alter spawning and reproductive activity in teleosts (Zohar et al., 2010) and to regulate teleost gonadal maturation and breeding rates in a wide range of marine and freshwater species (Amano et al., 2000; Hansen et al., 2001). In the current study, zebrafish reproduction (fecundity/clutch size and fertility/number of live, successfully fertilized eggs) was significantly different between fish housed in continuous LD or SD lighting. Two sets of experiments were performed, using young (3mo-6mo) and older

(10mo-12mo) zebrafish. When entrained to LD conditions, both groups had greater breeding rates (fig 2.5 and 2.6), and significantly more successfully fertilized eggs (fig 2.7 and 2.8), compare to SD entrained groups. Older, reproductively established fish (experiment 2; 10mo-12mo old) were more sensitive to LD exposure over time, with higher fecundity rates, as measured by trend line analysis, yet laid approximately 30% fewer eggs/clutch at their peak (fig 2.6, phase 1, middle; approx. 550 eggs/clutch) than the younger (3mo-6mo) fish tested (fig 2.5, right; 850 eggs/clutch).

The current breeding results shown in chapter 2, are also reflected in comparable finding in Japanese medaka (*O. latipes*), where embryo production drops dramatically after moving LD (16h/8h) entrained breeders into SD (8h/16h) conditions, ceasing completely after 14 days in SD (Koger et al., 1999). Return to LD conditions resumed embryo production within days, indicating a dual control of photoperiod on medaka embryo production - inhibiting established egg laying rates and re-initiating them after cessation (Koger et al., 1999). In the current study, SD entrained zebrafish took 100 days to cease egg laying (fig 2.5), and return to LD conditions after SD entrainment (fig 2.6) had an immediate but short-lived "rescue" effect, with clutch sizes increasing 10-fold, before dropping to the same breeding rate established in the initial entrainment period (Fig 2.6; middle, blue trend line). These results indicate two time courses for light modulation of reproduction in zebrafish; an immediate effect, shown within 1-2 days and a long-term effect (14-21 days) based on the previously entrained photoperiod. The temporal differences in photoperiodic breeding responsiveness recall comparable results in medaka and illustrate two forms of photoperiodic reproductive control, a) local (immediate) control of egg release mediated by direct responsiveness in the ovaries and b) long-term control of gamete development, likely modulated by reproductive hormones such as LH and FSH expressed by the pituitary. Both zebrafish fecundity and fertility rates (as measured by live/fertilized eggs) were significantly higher in LD>SD, in both young (3.5mo; Fig 2.7) and older (10mo; fig 2.8) groups. Recent results in siamese fighting fish (*Betta splendens*) have also shown increased fertility rates in LD>SD samples (Giannecchini et al., 2012), and tilapia subjected to a 18h/6h photoperiod, have higher fertility rates due to the

modulation of the HPG axis by melatonin, triggering the release of hormones responsible for gametogenesis and gamete maturation (Campos-Mendoza et al., 2004). In species such as rainbow trout, ovarian recrudescence and vitellogenesis is stimulated by long or increasing daylength, while ovulation and later oocyte maturation is synchronized by decreasing or short photoperiod (Bromage & Duston, 1986).

These results suggest specific phases in the reproductive cycle, which can be delayed or advanced by photoperiodic manipulations, under the control of an (photoperiod entrained) endogenous clock mechanism that expresses a phased response to daylength, as has been reported in salmonids (Randall & Bromage, 1998). Importantly, in many female salmonids such as rainbow trout, failure to switch from long to short days after the summer solstice doesn't inhibit spawning, but acts to desynchronize spawning times within the population (Randall & Bromage, 1998). In contrast, male trout (*O. mykiss)* continue to express sperm throughout the spawning season, suggesting that spermatogenesis is less strictly regulated by photoperiod than oogenesis in females (Migaud et al., 2010). In both sets of breeding experiments, moving from LD (or control 14h/10h lighting) conditions into SD lighting reduced clutch sizes (fecundity) and number of fertilized eggs (fertility) (figs 2.4 - 2.7). Coupled with the changes in ovarian weight, these results suggest that gender differences are a significant variable in the expression of zebrafish photoperiodic responsiveness, as shown for the first time in chapter 2.

5.4 Circadian Clock Genes and Skeleton Photoperiods

Cellular circadian rhymicity is based on auto-regulatory transcription–translation feedback loops, where CLOCK (CLK) and brain muscle ARNT-like (BMAL) proteins form a heterodimer, stimulating *period* (*per*) and *cryptochrome* (*cry*) genes, initiating their transcription. The core clock repressor proteins PER and CRY interact with the CLK:BMAL heterodimer, thereby down-regulating their own expression (Cahill, 2002a). By coupling a luminescent reporter to targeted core clock genes, it is possible to visualize the molecular responsiveness of individual

cells and tissue explants to varying photoperiodic conditions. Using skeleton photoperiod protocols (chapter 4) I examined the role of specific clock genes in the measurement of seasonal daylength, exploring the possibility of tissue-specific differences between dawn and dusk responsiveness.

Initial skeleton lighting tests aimed to determine the entrainment of cellular circadian rhythms, as cells could entrain to either the first or second light pulse in a given 24h cycle. Using clonal cell populations and transgenic fish scales in a SD skeleton photoperiod (2h-4h-2h/16h), p*er3, per1* and *cry1a* genes all entrained to the "dawn/first" pulse (2h-4h-2h) of the light regime, following the longest period of darkness (see fig 4.5). Under a LD skeleton regime (2h-12h-2h/8h) *Per1-luc* cells entrained to the first light pulse, while both dawn and dusk pulses stimulated *Cry1a-luc* expression, with *Cry1a-luc* peaking 3h after 2nd pulse, suggesting that the cells interpreted longer dark phase of 12h as the subjective "night". These results confirm predictive models first described by Colin Pittendrigh, which proposed activity (both cellular and behavioural) focused to the longest period between pulse intervals leads to maximally stable entrainment patterns (Pittendrigh & Daan, 1976). In addition, a phenomenon called "psi jumping" or phase shifting can also occur in cases of significant circadian asymmetry, where organisms can shift their active period from the shorter to the longer interval directly (Pittendrigh & Daan, 1976). This is the case when comparing *Per1-luc*, *Per3-luc* and *Cry1a-luc* expression between full and skeleton photoperiods (fig 4.5b), where circadian oscillations were consistently entrained to the first light exposure after the longest period of darkness.

Both p*er1 (*in cell lines) and p*er3* expression from transgenic zebrafish scales were synchronized, peaking at ZT 3 and reflecting published findings *in vivo* and other zebrafish cell lines tested (Cahill, 2002a). *Per3-luc* expression in photoperiod-associated tissues such as the pituitary, pineal and hypothalamus also peaks at ZT 3, a finding also noted in regular LD and SD photoperiods (fig 4.6a+c). When exposed to skeleton photoperiods, peak *Per3* tissue expression remained locked to ZT 3, just after the dawn pulse (during the SD skeleton regime) and after the dusk pulse (during the LD skeleton regime).

In both LD and SD skeleton regimes, pineal and pituitary samples responded to a single light pulse while hypothalamic samples in the LD skeleton regime (exclusively) showed a secondary light response after the dawn pulse. This novel finding in hypothalamic tissue explants suggests that some regional sensitivity in neural light responsiveness exists and may be stimulated *in vitro*. Further work using hypothalamic explants would help define the nature of this tissue-specific phenomenon. Ideally, initial tissue explant entrainment, followed by an extended period in DD would explore questions regarding tissue specific free running periods, and comparisons between dispersed hypothalamic cells and intact hypothalamic explant cultures would be of interest.

In recent years, much research attention has focused on the use of independent morning and evening oscillators, each sensing light at dawn or dusk specifically (see Lincoln et al., 2003 for a comprehensive review). As with many mammalian models tested, zebrafish *Per1* expression peaks near dawn (see chapter 4). In seasonally breeding hamsters this peak coincides with a decline in circulating nocturnal melatonin and has been localized to the PT (Messager et al., 1999). In addition, injection of exogenous melatonin increases Cry1mRNA and decreases *Per1* mRNA in the mammalian PT (Dardente et al., 2003). Together, these findings link *Per1* and its repressor *Cry1a* with melatonin activity within the pituitary, thus combining seasonal/photoperiodic melatonin expression with cellular clock gene oscillations in a key neuroendocrine controller, known to modulate reproductive cues. As zebrafish Cry1a is known to be directly light responsive (unlike mammalian Cry1 homologues), further work is necessary to extend this putative (mammalian) model of seasonal circadian/photoperiodic gene expression here, and was beyond the scope of the current work. Future experiments recording the responsiveness of Cry1a to melatonin and Cry1a knockout testing are recommended to address this line of questioning.

Having established cell and tissue responsiveness to full and skeleton photoperiods, I extended my breeding (fertility/fecundity) tests to monitor skeleton light regimes on reproductive behaviour. As shown in chapter 2, LD photoperiods stimulated fecundity, while SD regimes inhibited both fertility and

fecundity (fig 2.5-2.8). Skeleton photoperiods differed from full photoperiodic entrainment, as fecundity levels declined over time, suggesting that absolute light duration is necessary for physiological fitness rather than matched light exposure in the form of skeleton "pulses", as tested here. Based on these results, I hypothesize that the timing of light pulses/periods is a key factor in the stimulatory effect of LD (and LD skeleton) regimes on zebrafish reproduction, as the absolute duration of light exposure between LDsk and SDsk groups remained equal. This argues for a key role of the clock in the zebrafish photoperiodic response, either by appropriate phasing of a photo inducible phase, or altered internal coincidence of oscillating genes. Further work such as monitoring the light-responsiveness of reproductive tissues is recommended to determine any putative links between local and systemic control of fecundity in relation to photoperiod.

Overall, results from skeleton and full LD/SD photoperiodic testing clearly demonstrated a cellular "interpretation" of the shortest dark phase (between 2 light pulses) as subjective day, with the longer dark phase as subjective night. And while long-term tissue cultures using transgenic pituitary, pineal and hypothalamus explants showed peak *Per3-luc* expression at ZT3, a clear secondary (dusk) peak was noted in hypothalamic samples under LD skeleton lighting exclusively. Finally, long-term behavioural testing was undertaken to monitor the effect of seasonal skeleton photoperiods (LD and SD) on zebrafish reproduction. Both full and skeleton SD entrainment inhibited egg laying, while LD skeleton regimes stimulated breeding rates, with this effect weakening over time. These results show that timing of light phases (through skeleton regimes) influence reproductive behaviour, but increased light duration (through full photoperiod regimes) is necessary to induce maximal LD/Summer stimulatory effects.

5.5 Conclusions

Timely prediction of seasonal change is crucial for many species to survive and reproduce successfully. The changing length of the daily photoperiod is one of the most predictive cues for the seasonal timing of physiology and reproductive

biology. A distinct feature of teleost physiology is their sensitivity to seasonal photoperiodic change, and their use of these light/dark cues to entrain and synchronize their seasonal reproduction. In many organisms short days inhibit and long days stimulate seasonal responses, while experimental paradigms such as skeleton photoperiods have demonstrated that it is not the total amount of light, but the precise timing of a given light pulse that induces the photoperiodic response, thus providing a role for the circadian system in the measurement and interpretation of daylength. After decades of research into the role photoperiod on seasonal breeding, clear molecular pathways have yet to be described in full. The emerging picture of teleost photoperiodism is similar to that of avian species, where non-ocular light receptors and de-centralized oscillators are synchronized to provide the brain-pituitary-gonad axis its necessary cues. Melatonin's role is not necessarily to act as an initiatory messenger, "conducting" an orchestra of individual cellular clocks as in mammals, but to entrain a number of lower level reproductive processes such as gonadal maturation and oocyte recruitment. While the molecular mechanisms of photoperiodism are still hotly debated in mammalian models, the current work demonstrates a clear role for the use of zebrafish, as a new model system for the study of photoperiodic changes in gene expression and physiology.

The ability to synchronize circadian physiology and behavior with the extrinsic light cycle, is governed by the circadian clock, acting at different levels, ranging from the control of rhythmic gene expression, protein degradation and transportation, to the modification of the structure of neuronal circuits and synapses (Elbaz et al., 2013). The current work presents evidence of the circadian control of genes expression, with clear differences in pituitary and hypothalamic rhythmicity patterns in a number of reproductive and growth-associated genes.

Advances in genetic and imaging tools will play a key role in the future application of zebrafish to study circadian rhymicity and clock regulation within the reproductive system. Novel methods for targeting neuronal gene mapping, such as the UAS/Gal4 system, are becoming more commonly used in zebrafish (Vatine et al., 2011). Use of this method in mapping seasonal changes in synaptic networks and ligand/receptor binding will provide a powerful approach in the future. Real-

time imaging of synaptic connectivity in the zebrafish brain during LD and SD will shed light on how circadian and homeostatic processes regulate synaptic plasticity.

The use of zebrafish (*D. rerio*) as a model of circadian and seasonal biology has a number of positive and negative aspects. Due to their small size and short lifespan (2-4years), they are easy housed and many hundreds of fish may be tested in a single experiment. They are ideal for studies of fertility and fecundity, due to their regular spawning cycles and provide 100-500 eggs at each laying. In contrast to other fish models, zebrafish eggs are non-adherent, allowing easy counting and manipulation.

Some challenges are involved when using zebrafish as the main model for photoperiodic research; samples of systemic melatonin and reproductive hormones is limited by insufficient blood samples, the inability to take repeat samples (blood or tissues), and the lack of antibodies available for immunohistochemistry in this species. These issues were faced directly in the course of the work presented here, and are the main reasons for the focus on mRNA, qPCR and gene expression data, rather protein synthesis and activity rates. Interestingly, as a tropical species, zebrafish (*D. rerio*) are not subject to seasonal changes in photoperiodic light specifically. Yet the data presented here used this exogenous variable as the main cue for seasonal change, with dramatic behavioural and genetic results. The photoperiodic sensitivity of the zebrafish pituitary, hypothalamus and reproductive system clearly support my hypothesis that zebrafish are indeed responsive to seasonal light duration and are an excellent model for future vertebrate circadian physiology.CN

To conclude, the work presented in this thesis represents novel research exploring the interactions of photoperiod, reproduction and growth in zebrafish. It provides useful information for the aquaculture, fisheries and scientific communities. In so doing, it is clear that further research remains to be performed to clearly define the underlying physiological mechanisms that regulate photoperiodically regulated reproduction and growth in one of the most popular genetic and scientific animal models in use today.

APPENDIX A: STATISTICAL RESULTS (CHAPTER 2)

Appendix A.1 Effects of Photoperiod on Zebrafish Body Growth

Body Weight (g) – LD vs SD conditions					
Age	**T-test**	**DF**	**P value**		**Significance**
6mo	0.348	101	0.7300	**P > 0.05**	nil
11mo	19.800	78	0.0001	**P < 0.001**	***
15mo	7.350	87	0.0001	**P < 0.001**	***
20mo	3.370	80	0.0012	**P < 0.01**	**
24mo	1.170	80	0.2500	**P > 0.05**	nil
30mo	3.860	37	0.0004	**P < 0.01**	**

Body Length (mm) – LD vs SD conditions					
Age	**T-test**	**DF**	**P value**		**Significance**
6mo	0.91	101	0.3700	**P > 0.05**	nil
11mo	14.40	78	0.0001	**P < 0.001**	***
15mo	12.70	87	0.0001	**P < 0.001**	***
20mo	6.77	80	0.0001	**P < 0.01**	**
24mo	1.33	80	0.1900	**P > 0.05**	nil
30mo	4.04	37	0.0003	**P < 0.01**	**

Appendix A.2 Effects of Photoperiod on Zebrafish Gonad Weight

Ovary Weight (g) – LD vs SD conditions					
Age	**T-test**	**DF**	**P value**		**Significance**
6mo	4.180	29	0.000	**P < 0.001**	***
11mo	0.911	22	0.047	**P < 0.05**	*
15mo	3.500	31	0.001	**P < 0.01**	**
20mo	1.920	44	0.042	**P < 0.05**	*
24mo	0.273	25	0.790	**P > 0.05**	nil
30mo	0.712	11	0.490	**P > 0.05**	nil

Testis Weight (g) – LD vs SD conditions					
Age	**T-test**	**DF**	**P value**		**Significance**
6mo	-1.310	52	0.200	P > 0.05	nil
11mo	-1.660	51	0.100	P > 0.05	nil
15mo	1.280	28	0.210	P > 0.05	nil
20mo	-1.910	39	0.063	P > 0.05	nil
24mo	-1.830	14	0.088	P > 0.05	nil
30mo	1.980	22	0.060	P > 0.05	nil

APPENDIX B: QPCR PRIMERS (CHAPTER 3)

Primer	Accession number	Forward Primer	Reverse Primer	Product Size
GnRH	NM_182887	5' AAATGGAGGCAACATTCAGG 3'	3' CCTTCAGCATCCACCTCATT 5'	118 bp
Ubq	AY394942	5' CTGACCAGCAGAGGTTGATCT 3'	3' TGCTGGTCAGGGGGAATGC 5'	238 bp
GH	AJ937858	5' GGGAAAAGATGAAACGCAAA 3'	3' AAGGTCTGGCTGGGAAACTC 5'	93 bp
LH	NM_205623	5' TACAAGAGCCCGTTTTCCAC 3'	3' AACAGTCGGGCAGGTTAATG 5'	85 bp
FSH	NM_205624	5' TGTGGAGAGCGAAGAATGTG 3'	3' AGACCTTCTGGGTGTGCTGT 5'	119 bp
PRL	NM 181437	5' GGCCTGGAGCACGTCGTA 3'	3' ACGGGAGAGTGGACAGGTTGT 5'	61 bp
MT1	NM_131393	5' CTGGTGATTTTCTCCGTCTACAGA 3'	3' GAGTTTGGCAGTGGCGG 5'	79 bp
MT2	XM_704713	5' TCGGTGTTCAGGAATCGTAAACTG 3'	3' TTTGTGGTCAGTCTGGCCTTC 5'	63 bp
Mel 1c	XM_684351	5' CCGTCTACAGGAACAAGAAACTGA 3'	3' TGAGTCTTTCTGTGGCTGACC 5'	69 bp
GHRH	NM_001080092	5' CATGCAAGTGGGAGTAATTCA 3'	3' CTGGGGAAGATGATGCTGAT 5'	77 bp
TSH	NM_181494	5' GTTATTGGCATGCTGGGACT 3'	3' CTGTCAACACCACCATCTGC 5'	123 bp
Dio1	NM_001007283	5' GTTCAAACAGCTTGTCAAGGACTTC 3'	3' AACTTGGAGGAGAGGCTTGCT 5'	142 bp
Dio2	NM_212789	5' CATCAGCGGTAAGACCCACAA 3'	3' TATAAGCCAGCTGCCGGTCTT 5'	120 bp
Dio3	NC_007131.3	5' GTACGGCCAGAAGCTGGACT 3'	3' GAGGTGTTCCCGCTGGAC 5'	79 bp
Per1	NM_001030183	5' ATCCAGACCCCAATACAAC 3'	5' GGGAGACTCTGCTCCTTCT 3'	
Per3	NM_131584	5' CAGCAACGATTCCTCAGACA 3'	5' CGTTGATCATGCTCCACAGA 3'	
Cry1a	NM_131789	5' TCCAACCCTAATGGAAGCAC 3'	5' ACTCCTCGCTGTGTCGTTTT 3'	

APPENDIX C: TABLE OF QPCR MEAN VALUES (CHAPTER 3)

qPCR Target expression - circadian measures (mean values)				
Hypothalamic Targets	**ZT 3**	**ZT 9**	**ZT 15**	**ZT 21**
Dio1	1.56	1.61	1.51	1.60
Dio2	2.30	3.65	1.83	1.59
Dio3	1.44	2.58	2.54	2.08
GnRH	1.49	2.70	1.41	1.87
GHRH	1.23	1.85	1.25	1.76
MT1	1.89	3.92	2.13	2.00
MT2	1.96	1.70	1.61	2.15
Per1	11.53	9.68	1.56	2.81
Per3	9.21	8.67	1.20	4.57
Cry1a	2.82	7.16	1.84	1.39

Pituitary Targets	**ZT 3**	**ZT 9**	**ZT 15**	**ZT 21**
GH	2.76	1.69	1.70	1.91
LH	1.63	2.13	1.44	2.05
FSH	1.85	2.70	1.65	1.92
TSH	1.49	2.23	1.20	1.67
MT1	8.42	3.93	1.11	1.96
MT2	4.08	1.40	1.53	2.41
Per1	25.46	14.49	3.08	5.15
Per3	16.53	9.74	2.18	2.17
Cry1a	6.62	27.62	4.26	1.67

qPCR Targets - Lifespan measures (mean values)				
Hypothalamic Targets	**Photoperiod**	**6mo**	**15mo**	**24mo**
Dio1	Long Day (16h/8h)	1.08	1.48	1.24
	Short Day (8h/16h)	1.50	1.37	1.28
Dio2	Long Day (16h/8h)	1.16	1.58	1.37
	Short Day (8h/16h)	2.61	1.55	2.45
Dio3	Long Day (16h/8h)	2.11	1.54	3.00
	Short Day (8h/16h)	1.82	1.44	1.85
GnRH	Long Day (16h/8h)	1.32	1.38	1.90
	Short Day (8h/16h)	2.33	2.61	1.69
GHRH	Long Day (16h/8h)	1.30	2.73	1.98
	Short Day (8h/16h)	2.63	1.47	1.85
MT1	Long Day (16h/8h)	1.40	1.34	2.22
	Short Day (8h/16h)	1.34	1.33	1.50
MT2	Long Day (16h/8h)	1.81	1.85	1.07
	Short Day (8h/16h)	1.21	1.51	1.27

Pituitary Targets	Photoperiod	6mo	15mo	24mo
GH	Long Day (16h/8h)	1.43	1.82	1.65
	Short Day (8h/16h)	2.33	2.75	4.67
LH	Long Day (16h/8h)	1.41	1.81	1.73
	Short Day (8h/16h)	2.72	2.09	2.11
FSH	Long Day (16h/8h)	1.57	1.57	1.39
	Short Day (8h/16h)	3.54	2.83	2.49
PRL	Long Day (16h/8h)	1.41	1.62	1.97
	Short Day (8h/16h)	1.91	1.98	1.64
TSH	Long Day (16h/8h)	1.79	1.69	1.42
	Short Day (8h/16h)	2.84	2.19	1.60

MT1	Long Day (16h/8h)	-	2.12	2.34
	Short Day (8h/16h)	4.22	2.45	5.27
MT2	Long Day (16h/8h)	5.51	3.86	1.81
	Short Day (8h/16h)	2.83	1.86	4.82

* values shown are averaged from 5 readings per individual, for a total N of 25 per recording

APPENDIX D: STATISTICAL SUMMARIES (CHAPTER 3)

Statistical Summary of qPCR measures using 1-way Anova and Tukey Post-Hoc testing. Data shown here indicate statistical significance of mean qPCR measures of hormone expression in the Hypothalamus and Pituitary from LD and SD groups.

All samples were analysed F (3, 8); with 3df within groups; 8df between groups.

Appendix D.1 Circadian recordings of Hypothalamus (6mo/15mo/24mo)

Hypothalamic Circadian stats – 1-way Anova			
	F Value	P Value	%
Dio1	0.0709	0.97	3.00
Dio2	9.33	0.0054	99.46
Dio3	4.403	0.042	95.8
GHRH	11.95	0.0025	99.75
GnRH	5.175	0.028	97.2
MT1	16.92	0.0008	99.92
MT2	1.293	0.34	66
Per1	77.4	0.0001	99.99
Per3	37.37	0.0001	99.99
Cry1a	18.07	0.0006	99.94

Hypothalamic Circadian stats – Tukey Post-Hoc Test				
Target	Comparisons	Tukey	p value	Significance
Dio1	no post-hoc testing			-
Dio2	9 vs 3	7.32	P < 0.01	**
	9 vs 15	9.87	P < 0.01	**
	9 vs 21	11.17	P < 0.001	***
	3 vs 15	2.55	P > 0.05	-
	3 vs 21	3.85	P > 0.05	-
	15 vs 21	1.30	P > 0.05	-

Dio3	9 vs 15	0.26	P > 0.05	-
	9 vs 21	3.24	P > 0.05	-
	9 vs 3	7.38	P < 0.01	**
	15 vs 21	2.98	P > 0.05	-
	15 vs 3	7.12	P < 0.01	**
	21 vs 3	4.14	P > 0.05	-
GnRH	9 vs 21	7.96	P < 0.01	**
	9 vs 3	11.60	P < 0.001	***
	9 vs 15	12.37	P < 0.001	***
	21 vs 3	3.64	P > 0.05	-
	21 vs 15	4.41	P > 0.05	-
	3 vs 15	0.77	P > 0.05	-
GHRH	9 vs 21	1.02	P > 0.05	-
	9 vs 15	6.79	P < 0.01	**
	9 vs 3	7.02	P < 0.01	**
	21 vs 15	5.77	P < 0.05	*
	21 vs 3	6.00	P < 0.05	*
	15 vs 3	0.23	P > 0.05	-
MT1	9 vs 15	12.51	P < 0.001	***
	9 vs 21	13.42	P < 0.001	***
	9 vs 3	14.19	P < 0.001	***
	15 vs 21	0.91	P > 0.05	-
	15 vs 3	1.68	P > 0.05	-
	21 vs 3	0.77	P > 0.05	-
MT2	no post-hoc testing			-
Per1	3 vs 9	5.38	P < 0.05	*
	3 vs 21	25.34	P < 0.001	***
	3 vs 15	28.97	P < 0.001	***
	9 vs 21	19.97	P < 0.001	***
	9 vs 15	23.59	P < 0.001	***

	21 vs 15	3.63	P > 0.05	-
Per3	3 vs 9	1.43	P > 0.05	-
	3 vs 21	12.30	P < 0.001	***
	3 vs 15	21.24	P < 0.001	***
	9 vs 21	10.87	P < 0.001	***
	9 vs 15	19.81	P < 0.001	***
	21 vs 15	8.94	P < 0.01	**
Cry1a	9 vs 3	11.27	P < 0.001	***
	9 vs 15	13.82	P < 0.001	***
	9 vs 21	15.32	P < 0.001	***
	3 vs 15	2.55	P > 0.05	-
	3 vs 21	4.05	P > 0.05	-
	15 vs 21	1.51	P > 0.05	-

Appendix D.2 Circadian recordings of Pituitary (6mo/15mo/24mo)

Pituitary Circadian stats – 1-way Anova			
	F Value	P Value	%
GH	6.969	0.112	88.85
LH	4.479	0.058	94.191
FSH	8.798	0.073	92.737
PRL	0.762	0.061	93.890
TSH	26.14	0.021	97.855
MT1	28.06	1.141	99.999
MT2	25.8	0.17	83.00
Per1	62.62	5.013	99.999
Per3	24.780	5.771	99.998
Cry1a	142.3	2.98	99.99

Pituitary Circadian stats – Tukey Post-Hoc Test				
Target	Comparisons	Tukey	p value	Significance
GH	3 vs 21	7.20	P < 0.01	**
	3 vs 15	8.97	P < 0.01	**
	3 vs 9	9.06	P < 0.01	**

	21 vs 15	1.78	P > 0.05	-
	21 vs 9	1.86	P > 0.05	-
	15 vs 9	0.08	P > 0.05	-
LH	9 vs 21	0.94	P > 0.05	-
	9 vs 3	5.87	P < 0.05	*
	9 vs 15	8.10	P < 0.01	**
	21 vs 3	4.93	P < 0.05	*
	21 vs 15	7.16	P < 0.01	**
	3 vs 15	2.23	P > 0.05	-
FSH	9 vs 21	5.01	P < 0.05	*
	9 vs 3	5.46	P < 0.05	*
	9 vs 15	6.75	P < 0.01	**
	21 vs 3	0.45	P > 0.05	-
	21 vs 15	1.74	P > 0.05	-
	3 vs 15	1.29	P > 0.05	-
PRL	9 vs 21	1.37	P > 0.05	-
	9 vs 3	10.99	P < 0.001	***
	9 vs 15	12.01	P < 0.001	***
	21 vs 3	0.92	P > 0.05	-
	21 vs 15	1.95	P > 0.05	-
	3 vs 15	1.03	P > 0.05	-
TSH	9 vs 21	10.83	P < 0.001	***
	9 vs 3	14.31	P < 0.001	***
	9 vs 15	19.91	P < 0.001	***
	21 vs 3	3.48	P > 0.05	-
	21 vs 15	9.09	P < 0.01	**
	3 vs 15	5.61	P < 0.05	*
MT1	3 vs 9	11.89	P < 0.001	***
	3 vs 21	17.11	P < 0.001	***
	3 vs 15	19.36	P < 0.001	***
	9 vs 21	5.22	P < 0.05	*
	9 vs 15	7.47	P < 0.01	**
	21 vs 15	2.25	P > 0.05	-
MT2	3 vs 21	11.27	P < 0.001	***
	3 vs 15	17.14	P < 0.001	***
	3 vs 9	18.02	P < 0.001	***
	21 vs 15	5.92	P < 0.05	*
	21 vs 9	6.79	P < 0.01	**
	15 vs 9	0.87	P > 0.05	-
Per1	3 vs 9	13.86	P < 0.001	***
	3 vs 21	25.66	P < 0.001	***

	3 vs 15	28.27	P < 0.001	***
	9 vs 21	11.80	P < 0.001	***
	9 vs 15	14.41	P < 0.001	***
	21 vs 15	2.61	P > 0.05	-
Per3	3 vs 9	7.99	P < 0.01	**
	3 vs 15	16.90	P < 0.001	***
	3 vs 21	16.91	P < 0.001	***
	9 vs 15	8.90	P < 0.01	**
	9 vs 21	8.91	P < 0.01	**
	15 vs 21	0.01	P > 0.05	-
Cry1a	9 vs 3	34.41	P < 0.001	***
	9 vs 15	38.27	P < 0.001	***
	9 vs 21	42.32	P < 0.001	***
	3 vs 15	3.87	P > 0.05	-
	3 vs 21	8.11	P < 0.01	**
	15 vs 21	4.24	P > 0.05	-

Appendix D.3 Lifespan qPCR: Hypo Targets (Single Age vs Conditions)

Data shown indicates statistical significance of mean qPCR measures of hormone expression in the Hypothalamus from 6mo, 15mo and 24mo samples between LD (16h/8h) and SD (8h/16h) photoperiods.

6mo Hypothalamus – 1-way Anova			
	F Value	P Value	%
Dio1	3.339	0.08689	91.311
Dio2	8.008	0.2725	72.75
Dio3	1.944	0.2697	73.03
GnRH	8.19	0.2213	77.87
GHRH	3.947	0.2069	79.31
MT1	2.78	0.1877	81.23
MT2	1.41	0.2268	77.32

6mo Hypothalamus – Tukey Post-Hoc Test				
Target	Comparisons	Tukey	p value	Significance
Dio1	LD vs SD	4.73	P < 0.05	*

Dio2	LD vs SD	0.25	P > 0.05	-
Dio3	LD vs SD	5.11	P < 0.05	*
GnRH	LD vs SD	7.36	P < 0.01	**
GHRH	LD vs SD	9.38	P < 0.01	**
MT1	LD vs SD	0.46	P > 0.05	-
MT2	LD vs SD	4.18	P < 0.05	*

15mo Hypothalamus – 1-way Anova			
	F Value	P Value	%
Dio1	0.541	0.087	91.252
Dio2	0.002	0.195	80.51
Dio3	3.429	0.244	75.57
GnRH	2.394	0.552	44.82
GHRH	4.428	0.311	68.93
MT1	0.547	0.068	93.169
MT2	0.98	0.299	70.11

15mo Hypothalamus – Tukey Post-Hoc Test				
Target	Comparisons	Tukey	p value	Significance
Dio1	LD vs SD	1.23	P > 0.05	-
Dio2	LD vs SD	0.08	P > 0.05	-
Dio3	LD vs SD	4.90	P < 0.05	*
GnRH	LD vs SD	7.32	P < 0.01	**
GHRH	LD vs SD	5.63	P < 0.01	**
MT1	LD vs SD	0.14	P > 0.05	-
MT2	LD vs SD	2.24	P > 0.05	-

24mo Hypothalamus – 1-way Anova			
	F Value	P Value	%
Dio1	0.247	0.041	95.87
Dio2	4.058	0.286	71.4
Dio3	3.691	0.478	52.10

GnRH	0.862	0.368	63.24
GHRH	0.341	0.265	73.5
MT1	4.041	0.177	82.28
MT2	7.783	0.186	81.44

24mo Hypothalamus – Tukey Post-Hoc Test				
Target	Comparisons	Tukey	p value	Significance
Dio1	LD vs SD	0.68	P > 0.05	-
Dio2	LD vs SD	0.56	P > 0.05	-
Dio3	LD vs SD	6.96	P < 0.01	**
GnRH	LD vs SD	0.74	P > 0.05	-
GHRH	LD vs SD	1.41	P > 0.05	-
MT1	LD vs SD	5.93	P < 0.01	**
MT2	LD vs SD	1.61	P > 0.05	-

Appendix D.4 Lifespan qPCR : Hypo Targets (Photoperiod over Lifespan)

Data shown indicate statistical significance of mean qPCR measures of hormone expression in the hypothalamus from lifespan samples between conditions LD (16h/8h), and SD (8h/16h) photoperiods.

LD Hypothalamic - 1-way Anova			
	F Value	P Value	%
Dio1	2.234	0.0575	94.25
Dio2	8.008	0.2725	72.75
Dio3	1.944	0.2697	73.03
GnRH	4.148	0.299	70.1
GHRH	4.434	0.3718	62.82
MT1	3.873	0.1967	80.33
MT2	1.41	0.2268	77.32

LD Hypothalamic – Tukey Post-Hoc Test				
Target	Comparisons	Tukey	p value	Significance
Dio1	6mo vs 15mo	1.83	P > 0.05	-
	15mo vs 24mo	1.10	P > 0.05	-
	6mo vs 24mo	0.73	P > 0.05	-
Dio2	6mo vs 15mo	2.79	P > 0.05	-
	15mo vs 24mo	1.39	P > 0.05	-
	6mo vs 24mo	1.39	P > 0.05	-
Dio3	6mo vs 15mo	3.80	P < 0.05	*
	15mo vs 24mo	9.74	P < 0.01	**
	6mo vs 24mo	5.94	P < 0.01	**
GHRH	6mo vs 15mo	8.12	P < 0.01	**
	15mo vs 24mo	4.26	P < 0.05	*
	6mo vs 24mo	3.86	P < 0.05	*
GnRH	6mo vs 15mo	0.38	P > 0.05	-
	15mo vs 24mo	3.29	P > 0.05	-
	6mo vs 24mo	3.67	P > 0.05	-

MT1	6mo vs 15mo	0.47	P > 0.05	-
	15mo vs 24mo	6.87	P < 0.01	**
	6mo vs 24mo	6.40	P < 0.01	**
MT2	6mo vs 15mo	0.29	P > 0.05	-
	15mo vs 24mo	5.67	P < 0.01	**
	6mo vs 24mo	5.38	P < 0.01	**

SD Hypothalamic - 1-way Anova			
	F Value	P Value	%
Dio1	0.5412	0.0706	92.94
Dio2	0.9152	0.1613	83.87
Dio3	4.098	0.235	76.5
GnRH	1.94	0.4429	55.71
GHRH	4.434	0.3718	62.82
MT1	0.3966	0.0649	93.511
MT2	1.429	0.0724	92.76

SD Hypothalamic – Tukey Post-Hoc Test				
Target	Comparisons	Tukey	p value	Significance
Dio1	6mo vs 15mo	1.69	P > 0.05	-
	15mo vs 24mo	1.17	P > 0.05	-
	6mo vs 24mo	2.87	P > 0.05	-
Dio2	6mo vs 15mo	3.36	P > 0.05	-
	15mo vs 24mo	1.21	P > 0.05	-
	6mo vs 24mo	2.16	P > 0.05	-
Dio3	6mo vs 15mo	7.14	P < 0.01	**
	15mo vs 24mo	4.91	P < 0.05	*
	6mo vs 24mo	2.23	P > 0.05	-
GHRH	6mo vs 15mo	6.59	P < 0.01	**
	15mo vs 24mo	2.16	P > 0.05	-
	6mo vs 24mo	4.43	P < 0.05	*
GnRH	6mo vs 15mo	1.52	P > 0.05	-
	15mo vs 24mo	4.98	P < 0.01	**

	6mo vs 24mo	3.47	P > 0.05	-
MT1	6mo vs 15mo	0.14	P > 0.05	-
	15mo vs 24mo	2.41	P > 0.05	-
	6mo vs 24mo	2.27	P > 0.05	-
MT2	6mo vs 15mo	4.02	P < 0.05	*
	15mo vs 24mo	3.22	P > 0.05	-
	6mo vs 24mo	0.80	P > 0.05	-

Appendix D.5 Lifespan qPCR : Pituitary Targets (Single Age vs Conditions)

Data shown indicates statistical significance of mean qPCR measures of hormone expression in the Pituitary from 6mo, 15mo and 24mo samples between conditions LD (16h/8h) and SD (8h/16h) photoperiods.

6mo Pituitary - 1-way Anova			
	F Value	P Value	%
GH	0.5701	0.2172	78.28
LH	7.365	0.2569	74.31
FSH	12.97	0.5708	42.92
PRL	2.051	0.1084	89.16
TSH	0.5546	0.2067	79.33
MT1	0.2931	5.989	-
MT2	0.9591	18.87	-

6mo Pituitary – Tukey Post-Hoc Test				
Target	Comparisons	Tukey	p value	Significance
GH	LD vs SD	6.69	P < 0.01	**
LH	LD vs SD	8.95	P < 0.01	**
FSH	LD vs SD	9.03	P < 0.01	**
PRL	LD vs SD	5.26	P < 0.01	**
TSH	LD vs SD	8.00	P < 0.01	**
MT1	LD vs SD	-	P > 0.05	-
MT2	LD vs SD	4.01	P < 0.05	*

15mo Pituitary - 1-way Anova			
	F Value	P Value	%
GH	1.21	0.6139	38.61
LH	4.11	0.2088	79.12
FSH	5.05	0.411	58.9
PRL	0.9562	0.1794	82.06
TSH	1.111	0.2434	75.66
MT1	0.2858	0.6711	32.89

MT2	1.359	3.241	-

15mo Pituitary – Tukey Post-Hoc Test				
Target	Comparisons	Tukey	p value	Significance
GH	LD vs SD	4.11	P < 0.05	*
LH	LD vs SD	2.21	P > 0.05	-
FSH	LD vs SD	7.09	P < 0.01	**
PRL	LD vs SD	3.06	P > 0.05	-
TSH	LD vs SD	3.65	P > 0.05	-
MT1	LD vs SD	1.40	P > 0.05	-
MT2	LD vs SD	4.31	P > 0.05	-

24mo Pituitary - 1-way Anova			
	F Value	P Value	%
GH	5.976	1.346	0.016
LH	0.5013	0.3314	66.86
FSH	1.703	0.5706	42.94
PRL	0.4087	0.2841	71.59
TSH	1.316	0.2263	77.37
MT1	3.262	3.062	0.074
MT2	8.901	1.184	0.0043

24mo Pituitary – Tukey Post-Hoc Test				
Target	Comparisons	Tukey	p value	Significance
GH	LD vs SD	9.02	P < 0.01	**
LH	LD vs SD	2.38	P > 0.05	-
FSH	LD vs SD	5.04	P < 0.05	*
PRL	LD vs SD	2.32	P > 0.05	-
TSH	LD vs SD	1.36	P > 0.05	-
MT1	LD vs SD	5.80	P < 0.01	**
MT2	LD vs SD	9.58	P < 0.01	**

Appendix D.6 Lifespan qPCR : Pituitary Targets (Photoperiod Over Lifespan)

Data shown indicates statistical significance of mean qPCR measures of hormone expression in the Pituitary from lifespan samples between conditions LD (16h/8h) and SD (8h/16h) photoperiods.

LD Pituitary - 1-way Anova			
	F Value	P Value	%
GH	0.5701	0.2172	78.28
LH	0.9724	0.1474	85.26
FSH	6.031	1.006	0.014
PRL	1.175	0.2197	78.03
TSH	0.5546	0.2067	79.33
MT1	0.1768	0.4582	54.18
MT2	0.714	4.392	-

LD Pituitary – Tukey Post-Hoc Test				
Target	Comparisons	Tukey	p value	Significance
GH	6mo vs 15mo	2.90	P > 0.05	-
	15mo vs 24mo	1.26	P > 0.05	-
	6mo vs 24mo	1.64	P > 0.05	-
LH	6mo vs 15mo	3.61	P > 0.05	-
	15mo vs 24mo	0.72	P > 0.05	-
	6mo vs 24mo	2.89	P > 0.05	-
FSH	6mo vs 15mo	0.00	P > 0.05	-
	15mo vs 24mo	0.65	P > 0.05	-
	6mo vs 24mo	0.65	P > 0.05	-
PRL	6mo vs 15mo	1.55	P > 0.05	-
	15mo vs 24mo	2.59	P > 0.05	-
	6mo vs 24mo	4.14	P < 0.01	**
TSH	6mo vs 15mo	0.76	P > 0.05	-
	15mo vs 24mo	2.06	P > 0.05	-

	6mo vs 24mo	2.82	P > 0.05	-
MT1	6mo vs 15mo	-	-	-
	15mo vs 24mo	0.92	P > 0.05	-
	6mo vs 24mo	-	-	-
MT2	6mo vs 15mo	2.23	P > 0.05	-
	15mo vs 24mo	2.77	P > 0.05	-
	6mo vs 24mo	4.99	P < 0.01	**

SD Pituitary - 1-way Anova			
	F Value	P Value	%
GH	3.098	1.618	
LH	0.7204	0.5092	
FSH	0.8997	1.341	
PRL	0.722	0.174	
TSH	2.351	0.6778	
MT1	2.514	3.368	
MT2	5.585	1.371	

SD Pituitary – Tukey Post-Hoc Test				
Target	Comparisons	Tukey	p value	Significance
GH	6mo vs 15mo	1.14	P > 0.05	-
	15mo vs 24mo	5.23	P < 0.01	**
	6mo vs 24mo	6.37	P < 0.01	**
LH	6mo vs 15mo	3.30	P > 0.05	-
	15mo vs 24mo	0.10	P > 0.05	-
	6mo vs 24mo	3.20	P > 0.05	-
FSH	6mo vs 15mo	2.37	P > 0.05	-
	15mo vs 24mo	1.14	P > 0.05	-
	6mo vs 24mo	3.51	P > 0.05	-
PRL	6mo vs 15mo	0.63	P > 0.05	-
	15mo vs 24mo	3.05	P > 0.05	-

	6mo vs 24mo	2.42	P > 0.05	-
TSH	6mo vs 15mo	3.06	P > 0.05	-
	15mo vs 24mo	2.78	P > 0.05	-
	6mo vs 24mo	5.83	P < 0.01	**
MT1	6mo vs 15mo	3.74	P < 0.05	*
	15mo vs 24mo	5.95	P < 0.01	**
	6mo vs 24mo	2.22	P > 0.05	-
MT2	6mo vs 15mo	2.99	P > 0.05	-
	15mo vs 24mo	9.11	P < 0.01	**
	6mo vs 24mo	6.13	P < 0.01	**

Control Pituitary - 1-way Anova			
	F Value	P Value	%
GH	1.41	0.4275	0.28
LH	4.383	0.1146	0.043
FSH	0.9618	0.2972	0.41
PRL	0.1023	0.1879	0.9
TSH	2.418	0.2046	0.13
MT1	2.947	3.658	0.085
MT2	1.673	18.76	0.22

Control Pituitary – Tukey Post-Hoc Test				
Target	Comparisons	Tukey	p value	Significance
GH	6mo vs 15mo	1.64	P > 0.05	-
	15mo vs 24mo	2.91	P > 0.05	-
	6mo vs 24mo	4.56	P < 0.05	*
LH	6mo vs 15mo	1.96	P > 0.05	-
	15mo vs 24mo	8.31	P < 0.01	**
	6mo vs 24mo	6.35	P < 0.01	**
FSH	6mo vs 15mo	2.13	P > 0.05	-
	15mo vs 24mo	1.64	P > 0.05	-
	6mo vs 24mo	3.77	P > 0.05	-

PRL	6mo vs 15mo	1.19	P > 0.05	-
	15mo vs 24mo	1.28	P > 0.05	-
	6mo vs 24mo	0.09	P > 0.05	-
TSH	6mo vs 15mo	4.75	P < 0.05	*
	15mo vs 24mo	0.77	P > 0.05	-
	6mo vs 24mo	5.51	P < 0.01	**
MT1	6mo vs 15mo	2.60	P > 0.05	-
	15mo vs 24mo	6.93	P < 0.01	**
	6mo vs 24mo	4.32	P < 0.05	*
MT2	6mo vs 15mo	2.65	P > 0.05	-
	15mo vs 24mo	1.99	P > 0.05	-
	6mo vs 24mo	4.64	P < 0.05	*

APPENDIX E – CONGRESS BIBLIOGRAPHY AND PRESENTATIONS

Olsen, J. and Whitmore, D. "Seasonal Photoperiodism In Zebrafish – Evidence Of Daylength Effects On Pituitary Hormone Expression." *Society for Light Treatment and Biological Rhythms Conference, Vancouver, Canada, June 2008*. Unpublished conference poster.

Olsen, J. and Whitmore, D. "Seasonal Reproduction - Oscillations in Zebrafish Hormone Expression. "*UCL Graduate School Poster Competition, UCL, London, UK, March 2009.* Unpublished conference poster, winner for Biosciences category.

Olsen, J. "Photoperiodism in Zebrafish - how seasons regulate fertility." *Integrative Physiology Post-Graduate Students Conference, Aberdeen, Scotland, May 2009*. Unpublished conference proceedings.

Olsen, J. "Seasonal and Circadian rhymicity in Zebrafish reproduction." *Paris Interdisciplinary PhD Symposium Conference, Paris, France, June 2011*. Unpublished conference poster.

BIBLIOGRAPHY

Almeida, O.F., & Lincoln, G.A. (1984). Reproductive photorefractoriness in rams and accompanying changes in the patterns of melatonin and prolactin secretion. *Biol Reprod, 30*(1), 143-158.

Amano, M., Iigo, M., Ikuta, K., Kitamura, S., Yamada, H., & Yamamori, K. (2000). Roles of melatonin in gonadal maturation of underyearling precocious male masu salmon. *Gen Comp Endocrinol, 120*(2), 190-197.

Amano, M., Iigo, M., Ikuta, K., Kitamura, S., & Yamamori, K. (2003). Daily variations in melatonin binding sites in the masu salmon brain. *Neurosci Lett, 350*(1), 9-12.

Anderson, G.M., Hardy, S.L., Valent, M., Billings, H.J., Connors, J.M., & Goodman, R.L. (2003). Evidence that thyroid hormones act in the ventromedial preoptic area and the premammillary region of the brain to allow the termination of the breeding season in the ewe. *Endocrinology, 144*(7), 2892-2901.

Aschoff, J. (1960). *Exogenous and endogenous components in circadian rhythms.* Paper presented at the Cold Spring Harbor Symposia on Quantitative Biology.

Bachelot, A., & Binart, N. (2007). Reproductive role of prolactin. *Reproduction, 133*(2), 361-369.

Barrett, P., Ebling, F.J., Schuhler, S., Wilson, D., Ross, A.W., Warner, A., et al. (2007). Hypothalamic thyroid hormone catabolism acts as a gatekeeper for the seasonal control of body weight and reproduction. *Endocrinology, 148*(8), 3608-3617.

Bartness, T.J., Powers, J.B., Hastings, M.H., Bittman, E.L., & Goldman, B.D. (1993). The timed infusion paradigm for melatonin delivery: what has it taught us about the melatonin signal, its reception, and the photoperiodic control of seasonal responses? *J Pineal Res, 15*(4), 161-190.

Bartness, T.J., Song, C.K., & Demas, G.E. (2001). SCN efferents to peripheral tissues: implications for biological rhythms. *J Biol Rhythms, 16*(3), 196-204.

Bayarri, M.J., Rodriguez, L., Zanuy, S., Madrid, J.A., Sanchez-Vazquez, F.J., Kagawa, H., et al. (2004). Effect of photoperiod manipulation on the daily rhythms of melatonin and reproductive hormones in caged European sea bass (Dicentrarchus labrax). *Gen Comp Endocrinol, 136*(1), 72-81.

Bhattacharyya, S., Dey, R., & Maitra, S.K. (2005). Photoperiodic regulation of annual testicular events in the Indian major carp, Catla catla. *Acta Zoologica, 86*, 71-79.

Billings, H.J., Viguie, C., Karsch, F.J., Goodman, R.L., Connors, J.M., & Anderson, G.M. (2002). Temporal requirements of thyroid hormones for seasonal changes in LH secretion. *Endocrinology, 143*(7), 2618-2625.

Bjornsson, B.T., Hemre, G.I., Bjornevik, M., & Hansen, T. (2000). Photoperiod regulation of plasma growth hormone levels during induced smoltification of underyearling Atlantic salmon. *Gen Comp Endocrinol, 119*(1), 17-25.

Bjornsson, B.T., Stefansson, S.O., & Hansen, T. (1995). Photoperiod regulation of plasma growth hormone levels during parr-smolt transformation of Atlantic salmon: implications for hypoosmoregulatory ability and growth. *Gen Comp Endocrinol, 100*(1), 73-82.

Bjornsson, B.T., Taranger, G.L., Hansen, T., Stefansson, S.O., & Haux, C. (1994). The interrelation between photoperiod, growth hormone, and sexual maturation of adult Atlantic salmon (Salmo salar). *Gen Comp Endocrinol, 93*(1), 70-81.

Bobe, J., & Labbe, C. (2010). Egg and sperm quality in fish. *Gen Comp Endocrinol, 165*(3), 535-548.

Boeuf, G. (1993). *Salmonid smolting: a preadaptation to the oceanic environment.* London: Chapman & Hall.

Bole-Feysot, C., Goffin, V., Edery, M., Binart, N., & Kelly, P.A. (1998). Prolactin (PRL) and its receptor: actions, signal transduction pathways and phenotypes observed in PRL receptor knockout mice. *Endocr Rev, 19*(3), 225-268.

Bolliet, V., Ali, M.A., Lapointe, F.J., & Falcon, J. (1996). Rhythmic melatonin secretion in different teleost species: an in vitro study. *J Comp Physiol B, 165*(8), 677-683.

Bradshaw, W.E., & Holzapfel, C.M. (2007). Evolution of Animal Photoperiodism. *Annu. Rev. Ecol. Evol. Syst., 38*, 1-25.

Bromage, N., Porter, M., Randall, C. (2000). The environmental regulation of maturation in farmed finfish with special reference to the role of photoperiod and melatonin. *Aquaculture, 197*, 63–98.

Bromage, N.R., & Duston, J. (1986). Photoperiod mechanisms and rhythms of of reproduction in the female rainbow trout (Salmo gairdineri) using photoperiod techniques. . *Rep. Inst. Freshwater. Res. Drottningholm, 63*, 26 - 35.

Bunning, E. (1932). Uber die Erblichkeit der Tagesperiodizitat bei den Phaseolus Blattern. *Jb wiss Bot, 81*, 411 - 418.

Bunning, E. (1960). Circadian Rhythms and the Time Measurement in Photoperiodism. *Cold Spring Harb Sump Quant Biol, 25*, 249-256.

Bustin, S.A. (2002). Quantification of mRNA using real-time reverse transcription PCR (RT-PCR): trends and problems. *J Mol Endocrinol, 29*(1), 23-39.

Cahill, G.M. (1996). Circadian regulation of melatonin production in cultured zebrafish pineal and retina. *Brain Res, 708*(1-2), 177-181.

Cahill, G.M. (2002a). Clock Mechanisms in Zebrafish. *Cell Tissue Res, 309*, 27-34.

Cahill, G.M. (2002b). Clock mechanisms in zebrafish. *Cell Tissue Res, 309*(1), 27-34.
Cahill, G.M., Hurd, M.W., & Batchelor, M.M. (1998). Circadian rhythmicity in the locomotor activity of larval zebrafish. *Neuroreport, 9*(15), 3445-3449.
Callaghan, T.V., Bjorn, L.O., Chernov, Y., Chapin, T., Christensen, T.R., Huntley, B., et al. (2004). Biodiversity, distributions and adaptations of Arctic species in the context of environmental change. *Ambio, 33*(7), 404-417.
Campos-Mendoza, A., McAndrew, B.J., & Coward, K. (2004). Reproductive response of Nile tilapia (Oreochromis niloticus) to photoperiodic manipulation; effects on spawning periodicity, fecundity and egg size. *Aquaculture, 231*, p.299-314.
Canosa, L.F., Chang, J.P., & Peter, R.E. (2007). Neuroendocrine control of growth hormone in fish. *Gen Comp Endocrinol, 151*(1), 1-26.
Canosa, L.F., Unniappan, S., & Peter, R.E. (2005). Periprandial changes in growth hormone release in goldfish: role of somatostatin, ghrelin, and gastrin-releasing peptide. *Am J Physiol Regul Integr Comp Physiol, 289*(1), R125-133.
Carnevali, O., Gioacchini, G., Maradonna, F., Olivotto, I., & Migliarini, B. (2011). Melatonin induces follicle maturation in Danio rerio. *PLoS One, 6*(5), e19978.
Carr, A.J., Tamai, T.K., Young, L.C., Ferrer, V., Dekens, M.P., & Whitmore, D. (2006). Light reaches the very heart of the zebrafish clock. *Chronobiol Int, 23*(1-2), 91-100.
Carrillo, M., Zanuy, S., Felip, A., Bayarri, M.J., Moles, G., & Gomez, A. (2009). Hormonal and environmental control of puberty in perciform fish: the case of sea bass. *Ann N Y Acad Sci, 1163*, 49-59.
Chappell, P.E. (2005). Clocks and the black box: circadian influences on gonadotropin-releasing hormone secretion. *J Neuroendocrinol, 17*(2), 119-130.
Chappell, P.E., White, R.S., & Mellon, P.L. (2003). Circadian gene expression regulates pulsatile gonadotropin-releasing hormone (GnRH) secretory patterns in the hypothalamic GnRH-secreting GT1-7 cell line. *J Neurosci, 23*(35), 11202-11213.
Chen, W., & Ge, W. (2012). Ontogenic expression profiles of gonadotropins (fshb and lhb) and growth hormone (gh) during sexual differentiation and puberty onset in female zebrafish. *Biol Reprod, 86*(3), 73.
Choi, S., Lee, C.H., Park, W., Kim, D.J., & Sohn, Y.C. (2010). Effects of shortened photoperiod on gonadotropin-releasing hormone, gonadotropin, and vitellogenin gene expression associated with ovarian maturation in rainbow trout. *Zoolog Sci, 27*(1), 24-32.
Comeau, L.A., Campana, S.E., Hanson, J.M., & Chouinard, G.A. (2000). Seasonal changes of thyroid hormones in field-collected Atlantic cod in relation

to condition indices, water temperature and photoperiod. *J. Fish Biol. , 57*, 571-588.
Condon, C.H., Chenoweth, S.F., & Wilson, R.S. (2010). Zebrafish take their cue from temperature but not photoperiod for the seasonal plasticity of thermal performance. *J Exp Biol, 213*(Pt 21), 3705-3709.
Damian, E. (1977). Extra-pineal gland sources of melatonin. *Endocrinologie, 15*(1), 65-66.
Dardente, H., Klosen, P., Pevet, P., & Masson-Pevet, M. (2003). MT1 melatonin receptor mRNA expressing cells in the pars tuberalis of the European hamster: effect of photoperiod. *J Neuroendocrinol, 15*(8), 778-786.
Davie, A., Minghetti, M., & Migaud, H. (2009). Seasonal variations in clock-gene expression in Atlantic salmon (Salmo salar). *Chronobiol Int, 26*(3), 379-395.
Davies, B., Bromage, N., & Swanson, P. (1999). The brain-pituitary-gonadal axis of female rainbow trout Oncorhynchus mykiss: effects of photoperiod manipulation1. *Gen Comp Endocrinol, 115*(1), 155-166.
Davies, B.N. (2002). The effects of fluctuating seasonal and constant water temperatures on the photoperiodic advancement of reproduction in female rainbow trout, Oncorhynchus mykiss. . *Aquaculture, 205*, 183–200.
Dawson, A., & Goldsmith, A.R. (1983). Plasma prolactin and gonadotrophins during gonadal development and the onset of photorefractoriness in male and female starlings (Sturnus vulgaris) on artificial photoperiods. *J Endocrinol, 97*(2), 253-260.
del Pozo, A., Sanchez-Ferez, J.A., & Sanchez-Vazquez, F.J. (2011). Circadian rhythms of self-feeding and locomotor activity in zebrafish (Danio Rerio). *Chronobiol Int, 28*(1), 39-47.
Dickey, J.T., & Swanson, P. (2000). Effects of salmon gonadotropin-releasing hormone on follicle stimulating hormone secretion and subunit gene expression in coho salmon (Oncorhynchus kisutch). *Gen Comp Endocrinol, 118*(3), 436-449.
Dixit, A.S., & Singh, N.S. (2011). Photoperiod as a proximate factor in control of seasonality in the subtropical male Tree Sparrow, Passer montanus. *Front Zool, 8*(1), 1.
Donaldson, E.M., Fagerlund, U.H.M., Higgs, D.A., & McBride, J.R. (1979). Hormonal enhancement of growth. In W. S. Hoar, D. J. Randall & J. R. Brett (Eds.), *Fish Physiology. Bioenergetics and Growth* (Vol. 8). New York: Academic Press.
Eaton, R.C., & Farley, R.D. (1974). Growth and reduction of depensation of the zebrafish Brachydanio rerio, reared in the laboratory. *Copeia*, 204-209.
Ebbesson, L.O.E., Bjornsson, B., Stefansson, S.O., & Ekstrom, P. (1998). Propylthiouracil-induced hypothyroidism in coho salmon, Oncorhynchus kisutch: effects on plasma total thyroxine, total

triiodothyronine, free thyroxine, and growth hormone. . *Fish Physiol. Biochem., 19*(4), 305–313.
Elbaz, I., Foulkes, N.S., Gothilf, Y., & Appelbaum, L. (2013). Circadian clocks, rhythmic synaptic plasticity and the sleep-wake cycle in zebrafish. *Front Neural Circuits, 7*, 9.
Engeszer, R.E., Patterson, L.B., Rao, A.A., & Parichy, D.M. (2007). Zebrafish in the wild: a review of natural history and new notes from the field. *Zebrafish, 4*(1), 21-40.
Falcon, J., Besseau, L., Fazzari, D., Attia, J., Gaildrat, P., Beauchaud, M., et al. (2003a). Melatonin modulates secretion of growth hormone and prolactin by trout pituitary glands and cells in culture. *Endocrinology, 144*(10), 4648-4658.
Falcon, J., Besseau, L., Sauzet, S., & Boeuf, G. (2007). Melatonin effects on the hypothalamo-pituitary axis in fish. *Trends Endocrinol Metab, 18*(2), 81-88.
Falcon, J., Gothilf, Y., Coon, S.L., Boeuf, G., & Klein, D.C. (2003b). Genetic, temporal and developmental differences between melatonin rhythm generating systems in the teleost fish pineal organ and retina. *J Neuroendocrinol, 15*(4), 378-382.
Falcon, J., Marmillon, J.B., Claustrat, B., & Collin, J.P. (1989). Regulation of melatonin secretion in a photoreceptive pineal organ: an in vitro study in the pike. *J Neurosci, 9*(6), 1943-1950.
Falcon, J., Migaud, H., Munoz-Cueto, J.A., & Carrillo, M. (2010). Current knowledge on the melatonin system in teleost fish. *Gen Comp Endocrinol, 165*(3), 469-482.
Follett, B.K., & Nicholls, T.J. (1985). Influences of thyroidectomy and thyroxine replacement on photoperiodically controlled reproduction in quail. *J Endocrinol, 107*(2), 211-221.
Follett, B.K., & Sharp, P.J. (1969). Circadian rhythmicity in photoperiodically induced gonadotrophin release and gonadal growth in the quail. *Nature, 223*(5209), 968-971.
Foster, R.G., & Soni, B.G. (1998). Extraretinal photoreceptors and their regulation of temporal physiology. *Rev Reprod, 3*(3), 145-150.
Fox, S.I. (1984). *Human physiology*. Dubuque, Iowa: W.C. Brown.
Fukada, Y. (2003). Molecular oscillation behind the clockface. *J Biochem, 134*(6), 773-775.
Gahete, M.D., Duran-Prado, M., Luque, R.M., Martinez-Fuentes, A.J., Quintero, A., Gutierrez-Pascual, E., et al. (2009). Understanding the multifactorial control of growth hormone release by somatotropes: lessons from comparative endocrinology. *Ann N Y Acad Sci, 1163*, 137-153.
Gaildrat, P., & Falcon, J. (1999). Expression of melatonin receptors and 2-[125I]iodomelatonin binding sites in the pituitary of a teleost fish. *Adv Exp Med Biol, 460*, 61-72.

Gan, E.H., & Quinton, R. (2010). Physiological significance of the rhythmic secretion of hypothalamic and pituitary hormones. *Prog Brain Res, 181*, 111-126.
Garner, W.W., & Allard, H.A. (1927). Effect of Short Alternating Periods of Light and Darkness on Plant Growth. *Science, 66*(1697), 40-42.
Gern, W.A., Owens, D.W., & Ralph, C.L. (1978). Plasma melatonin in the trout: day-night change demonstrated by radioimmunoassay. *Gen Comp Endocrinol, 34*(4), 453-458.
Ghomi, M.R., Zarei, M., & Sohrabnejad, M. (2011). Effect of photoperiod on growth and feed conversion of juvenile wild carp, Cyprinus carpio. *Acta Biol Hung, 62*(2), 215-218.
Giannecchini, L.G., Massago, H., Batista, J., & Fernandes, K. (2012). Effects of photoperiod on reproduction of Siamese fighting fish Betta splendens. *Aquaculture, 41*(4).
Gomez, J.M., Boujard, T., Fostier, A., & Le Bail, P.Y. (1996). Characterization of growth hormone nycthemeral plasma profiles in catheterized rainbow trout (Oncorhynchus mykiss). *J Exp Zool, 274*(3), 171-180.
Gothilf, Y., Meiri, I., Elizur, A., & Zohar, Y. (1997). Preovulatory changes in the levels of three gonadotropin-releasing hormone-encoding messenger ribonucleic acids (mRNAs), gonadotropin beta-subunit mRNAs, plasma gonadotropin, and steroids in the female gilthead seabream, Sparus aurata. *Biol Reprod, 57*(5), 1145-1154.
Granados-Fuentes, D., & Herzog, E.D. (2013). The clock shop: coupled circadian oscillators. *Exp Neurol, 243*, 21-27.
Grey, C.L., & Chang, J.P. (2013). Growth hormone-releasing hormone stimulates GH release while inhibiting ghrelin- and sGnRH-induced LH release from goldfish pituitary cells. *Gen Comp Endocrinol, 186*, 150-156.
Hamner, K.C., & Bonner, J. (1938). Photoperiodism in Relation to Hormones as Factors in floral initiation and development. *The Botanical Gazette, 100*(2).
Hanon, E.A., Lincoln, G.A., Fustin, J.M., Dardente, H., Masson-Pevet, M., Morgan, P.J., et al. (2008). Ancestral TSH mechanism signals summer in a photoperiodic mammal. *Curr Biol, 18*(15), 1147-1152.
Hansen, T., Karlsen, O., Taranger, G.L., Hemre, G.I., Holm, J.C., & Kjesbu, O.S. (2001). Growth, gonadal development and spawning time of Atlantic cod (Gadus morhua) reared under different photoperiods. *Aquaculture, 203*, 51-67.
Hastings, M.H., & Follett, B.K. (2001). Toward a molecular biological calendar? *J Biol Rhythms, 16*(4), 424-430.
Hazlerigg, D. (2012). The evolutionary physiology of photoperiodism in vertebrates. *Prog Brain Res, 199*, 413-422.
Hazlerigg, D., & Loudon, A. (2008). New insights into ancient seasonal life timers. *Curr Biol, 18*(17), R795-R804.

Hazlerigg, D.G., & Wagner, G.C. (2006). Seasonal photoperiodism in vertebrates: from coincidence to amplitude. *Trends Endocrinol Metab, 17*(3), 83-91.

Hellqvist, A., Schmitz, M., Mayer, I., & Borg, B. (2006). Seasonal changes in expression of LH-beta and FSH-beta in male and female three-spined stickleback, Gasterosteus aculeatus. *Gen Comp Endocrinol, 145*(3), 263-269.

Holloway, A.C., Sheridan, M.A., Van Der Kraak, G., & Leatherland, J.F. (1999). Correlations of plasma growth hormone with somatostatin, gonadal steroid hormones and thyroid hormones in rainbow trout during sexual recrudescence. *Comparative Biochemistry and Physiolology, 123*, 251-260.

Hoover, E.E. (1937). Experimental Modification of the Sexual Cycle in Trout by Control of Light. *Science, 86*(2236), 425-426.

Huether, G. (1993). The contribution of extrapineal sites of melatonin synthesis to circulating melatonin levels in higher vertebrates. *Experientia, 49*(8), 665-670.

Iigo, M., Kezuka, H., Suzuki, T., Tabata, M., & Aida, K. (1994). Melatonin signal transduction in the goldfish, Carassius auratus. *Neurosci Biobehav Rev, 18*(4), 563-569.

Ikegami, T., Azuma, K., Nakamura, M., Suzuki, N., Hattori, A., & Ando, H. (2009). Diurnal expressions of four subtypes of melatonin receptor genes in the optic tectum and retina of goldfish. *Comp Biochem Physiol A Mol Integr Physiol, 152*(2), 219-224.

Jackson, S.D. (2009). Plant responses to photoperiod. *New Phytol, 181*(3), 517-531.

Jodo, A., Kitahashi, T., Taniyama, S., Bhandari, R.K., Ueda, H., Urano, A., et al. (2005). Seasonal variation in the expression of five subtypes of gonadotropin-releasing hormone receptor genes in the brain of masu salmon from immaturity to spawning. *Zoolog Sci, 22*(12), 1331-1338.

Johnston, J.D. (2004). Photoperiodic regulation of prolactin secretion: changes in intra-pituitary signalling and lactotroph heterogeneity. *J Endocrinol, 180*(3), 351-356.

Kaneko, M., Hernandez-Borsetti, N., & Cahill, G.M. (2006). Diversity of zebrafish peripheral oscillators revealed by luciferase reporting. *Proc Natl Acad Sci U S A, 103*(39), 14614-14619.

Karsch, F.J., Bittman, E.L., Foster, D.L., Goodman, R.L., Legan, S.J., & Robinson, J.E. (1984). Neuroendocrine basis of seasonal reproduction. *Recent Prog Horm Res, 40*, 185-232.

Kezuka, H., Furukawa, K., Aida, K., & Hanyu, I. (1988). Daily cycles in plasma melatonin levels under long or short photoperiod in the common carp, Cyprinus carpio. *Gen Comp Endocrinol, 72*(2), 296-302.

Kirkman, T.W. (1996). Statistics to Use. Retrieved Nov, 2010, from http://www.physics.csbsju.edu/stats/KS-test.html

Klein, D.C., Smoot, R., Weller, J.L., Higa, S., Markey, S.P., Creed, G.J., et al. (1983). Lesions of the paraventricular nucleus area of the hypothalamus disrupt the suprachiasmatic leads to spinal cord circuit in the melatonin rhythm generating system. *Brain Res Bull, 10*(5), 647-652.

Klosen, P., Bienvenu, C., Demarteau, O., Dardente, H., Guerrero, H., Pevet, P., et al. (2002). The mt1 melatonin receptor and RORbeta receptor are co-localized in specific TSH-immunoreactive cells in the pars tuberalis of the rat pituitary. *J Histochem Cytochem, 50*(12), 1647-1657.

Koger, C.S., Teh, S.J., & Hinton, D.E. (1999). Variations of light and temperature regimes and resulting effects on reproductive parameters in medaka (Oryzias latipes). *Biol Reprod, 61*(5), 1287-1293.

Konopka, R.J., & Benzer, S. (1971). Clock mutants of Drosophila melanogaster. *Proc Natl Acad Sci U S A, 68*(9), 2112-2116.

Kuo, M.W., Lou, S.W., Postlethwait, J., & Chung, B.C. (2005). Chromosomal organization, evolutionary relationship, and expression of zebrafish GnRH family members. *J Biomed Sci, 12*(4), 629-639.

Kwok, H.F., So, W.K., Wang, Y., & Ge, W. (2005). Zebrafish gonadotropins and their receptors: I. Cloning and characterization of zebrafish follicle-stimulating hormone and luteinizing hormone receptors--evidence for their distinct functions in follicle development. *Biol Reprod, 72*(6), 1370-1381.

Laale, H.W. (1977). Culture and preliminary observations of follicular isolates from adult zebra fish, Brachydanio rerio. *Can J Zool, 55*(2), 304-309.

Le Bail, P.Y. (1988). *Growth-reproduction interaction in salmonids*.

Lechan, R.M., & Fekete, C. (2005). Role of thyroid hormone deiodination in the hypothalamus. *Thyroid, 15*(8), 883-897.

Lee, L.T., Siu, F.K., Tam, J.K., Lau, I.T., Wong, A.O., Lin, M.C., et al. (2007). Discovery of growth hormone-releasing hormones and receptors in nonmammalian vertebrates. *Proc Natl Acad Sci U S A, 104*(7), 2133-2138.

Lees, A.D. (1952). The Significance of the Light and Dark Phases in Photoperiodic Control of Daipause in Metatetranychus Ulmi Koch. *Agricultural Research Council Unit of Insect Physiology*, 487-497.

Lethimonier, C., Madigou, T., Munoz-Cueto, J.A., Lareyre, J.J., & Kah, O. (2004). Evolutionary aspects of GnRHs, GnRH neuronal systems and GnRH receptors in teleost fish. *Gen Comp Endocrinol, 135*(1), 1-16.

Lincoln, G. (1999). Melatonin modulation of prolactin and gonadotrophin secretion. Systems ancient and modern. *Adv Exp Med Biol, 460*, 137-153.

Lincoln, G.A., Andersson, H., & Loudon, A. (2003). Clock genes in calendar cells as the basis of annual timekeeping in mammals--a unifying hypothesis. *J Endocrinol, 179*(1), 1-13.

Lumsden, P.J. (2002). *Biological Rhythms*. New Delhi, India: Springer-Verlag.
Majewski, P., Adamska, I., Pawlak, J., Baranska, A., & Skwarlo-Sonta, K. (2005). Seasonality of pineal gland activity and immune functions in chickens. *J Pineal Res, 39*(1), 66-72.
Malpaux, B., Migaud, M., Tricoire, H., & Chemineau, P. (2001). Biology of mammalian photoperiodism and the critical role of the pineal gland and melatonin. *J Biol Rhythms, 16*(4), 336-347.
Marchant, T.A., Chang, J.P., Nahorniak, C.S., & Peter, R.E. (1989). Evidence that gonadotropin-releasing hormone also functions as a growth hormone-releasing factor in the goldfish. *Endocrinology, 124*(5), 2509-2518.
Marchant, T.A., & Peter, R.E. (1986). Seasonal variations in body growth rates and circulating levels of growth hormone in the goldfish, Carassius auratus. *J Exp Zool, 237*(2), 231-239.
Masana, M.I., Benloucif, S., & Dubocovich, M.L. (2000). Circadian rhythm of mt1 melatonin receptor expression in the suprachiasmatic nucleus of the C3H/HeN mouse. *J Pineal Res, 28*(3), 185-192.
Mayer, I., Bornestaf, C., Wetterberg, L., & Borg, B. (1997). Melatonin does not prevent long photoperiod stimulation of secondary sexual characters in the male three-spined stickleback Gasterosteus aculeatus. *Gen Comp Endocrinol, 108*(3), 386-394.
Menaker, M. (1968). Extraretinal light perception in the sparrow. I. Entrainment of the biological clock. *Proc Natl Acad Sci U S A, 59*(2), 414-421.
Messager, S., Ross, A.W., Barrett, P., & Morgan, P.J. (1999). Decoding photoperiodic time through Per1 and ICER gene amplitude. *Proc Natl Acad Sci U S A, 96*(17), 9938-9943.
Migaud, H., Davie, A., & Taylor, J.F. (2010). Current knowledge on the photoneuroendocrine regulation of reproduction in temperate fish species. *J Fish Biol, 76*(1), 27-68.
Migaud, H., Fontaine, P., Kestemont, P., Wang, N., & Brun-Bellut, J. (2004). Influence of photoperiod on the onset of gonadogenesis in Eurasian perch Perca fluviatilis. *Aquaculture, 241*, 561–574.
Mingarro, M., Vega-Rubin de Celis, S., Astola, A., Pendon, C., Valdivia, M.M., & Perez-Sanchez, J. (2002). Endocrine mediators of seasonal growth in gilthead sea bream (Sparus aurata): the growth hormone and somatolactin paradigm. *Gen Comp Endocrinol, 128*(2), 102-111.
Morin, P.P., Hara, T.J., & Eales, J.G. (1993). Thyroid hormone deiodination in brain, liver, gill, heart and muscle of Atlantic salmon (Salmo salar) during photoperiodically-induced parr-smolt transformation. I. Outer- and inner-ring thyroxine deiodination. *Gen Comp Endocrinol, 90*(2), 142-156.
Morris, C.J., Aeschbach, D., & Scheer, F.A. (2012). Circadian system, sleep and endocrinology. *Mol Cell Endocrinol, 349*(1), 91-104.

Mosconi, G., Carnevali, O., Habibi, H.R., Sanyal, R., & Polzonetti-Magni, A.M. (2002). Hormonal mechanisms regulating hepatic vitellogenin synthesis in the gilthead sea bream, Sparus aurata. *Am J Physiol Cell Physiol, 283*(3), C673-678.

Mylonas, C.C., Fostier, A., & Zanuy, S. (2010). Broodstock management and hormonal manipulations of fish reproduction. *Gen Comp Endocrinol, 165*(3), 516-534.

Nakao, N., Ono, H., Yamamura, T., Anraku, T., Takagi, T., Higashi, K., et al. (2008a). Thyrotrophin in the pars tuberalis triggers photoperiodic response. *Nature, 452*(7185), 317-322.

Nakao, N., Ono, H., & Yoshimura, T. (2008b). Thyroid hormones and seasonal reproductive neuroendocrine interactions. *Reproduction, 136*(1), 1-8.

Nanda, K.K., & Hamner, K.C. (1958). Studies on the nature of the endogenous rhythm affectingphotoperiodic response of Biloxi soybean. *Botan.Gaz., 120*, 14-25.

Nett, T.M., Turzillo, A.M., Baratta, M., & Rispoli, L.A. (2002). Pituitary effects of steroid hormones on secretion of follicle-stimulating hormone and luteinizing hormone. *Domest Anim Endocrinol, 23*(1-2), 33-42.

Nica, G., Herzog, W., Sonntag, C., Nowak, M., Schwarz, H., Zapata, A.G., et al. (2006). Eya1 is required for lineage-specific differentiation, but not for cell survival in the zebrafish adenohypophysis. *Dev Biol, 292*(1), 189-204.

Norberg, B., Brown, C.L., Halldorsson, O., Stensland, K., & Björnsson, B.T. (2004). Photoperiod regulates the timing of sexual maturation, spawning, sex steroid and thyroidhormone profiles in the Atlantic cod (Gadus morhua). *Aquaculture*
, 229(Issues 1–4), pages 451–467.

Norris, A.J., Stirland, J.A., McFerran, D.W., Seymour, Z.C., Spiller, D.G., Loudon, A.S., et al. (2003). Dynamic patterns of growth hormone gene transcription in individual living pituitary cells. *Mol Endocrinol, 17*(2), 193-202.

O'Donovan-Lockard, P., Sagil, G., Villcock, W., Hilge, V., & Abraham, M. (1987). *Stimulation and inhibition of gonadal development in fish.* Paper presented at the Research in Modern Aquaculture. Proceedings of the Third Status Seminar.

Ono, H., Hoshino, Y., Yasuo, S., Watanabe, M., Nakane, Y., Murai, A., et al. (2008). Involvement of thyrotropin in photoperiodic signal transduction in mice. *Proc Natl Acad Sci U S A, 105*(47), 18238-18242.

Oppedal, F., Taranger, G.L., Juell, J.E., & Hansen, T. (1999). Growth, osmoregulation and sexual maturation of underyearling Atlantic salmon smolt Salmo salar L. exposed to different intensities of continuous light in sea cages. *Aquacult. Res. , 30*, 491- 499.

Park, Y.J., Park, J.G., Hiyakawa, N., Lee, Y.D., Kim, S.J., & Takemura, A. (2007a). Diurnal and circadian regulation of a melatonin receptor, MT1, in the

golden rabbitfish, Siganus guttatus. *Gen Comp Endocrinol, 150*(2), 253-262.
Park, Y.J., Park, J.G., Jeong, H.B., Takeuchi, Y., Kim, S.J., Lee, Y.D., et al. (2007b). Expression of the melatonin receptor Mel(1c) in neural tissues of the reef fish Siganus guttatus. *Comp Biochem Physiol A Mol Integr Physiol, 147*(1), 103-111.
Parker, D.B., Power, M.E., Swanson, P., Rivier, J., & Sherwood, N.M. (1997). Exon skipping in the gene encoding pituitary adenylate cyclase-activating polypeptide in salmon alters the expression of two hormones that stimulate growth hormone release. *Endocrinology, 138*(1), 414-423.
Parker, M.W., Hendricks, S.B., Borthwick, H.A., & Scully, N.J. (1945). Action Spectrum for the Photoperiodic Control of Floral Initiation in Biloxi Soybean. *Science, 102*(2641), 152-155.
Paul, M.J., George, N.T., Zucker, I., & Butler, M.P. (2007). Photoperiodic and hormonal influences on fur density and regrowth in two hamster species. *Am J Physiol Regul Integr Comp Physiol, 293*(6), R2363-2369.
Peng, C., & Peter, R.E. (1997). Neuroendocrine regulation of growth hormone secretion and growth in fish. *Zool. Stud., 36*, 79-89.
Piesiewicz, A., Kedzierska, U., Podobas, E., Adamska, I., Zuzewicz, K., & Majewski, P.M. (2012). Season-dependent postembryonic maturation of the diurnal rhythm of melatonin biosynthesis in the chicken pineal gland. *Chronobiol Int, 29*(9), 1227-1238.
Pitcher, T.J. (1986). *The Behavior of teleost fishes*. Baltimore, Md.: Johns Hopkins University Press.
Pittendrigh, C.S. (1964). The Entrainment of Circadian Oscillations by Skeleton Photoperiods. *Science, 144*(3618), 565.
Pittendrigh, C.S. (1966). The circadian oscillation in Drosophila pseudoobscura pupae: A model for the photoperiodic clock. *Z Pflanzenphysiol, 54*, 275-307.
Pittendrigh, C.S. (1972). Circadian surfaces and the diversity of possible roles of circadian organization in photoperiodic induction. *Proc Natl Acad Sci U S A, 69*, 2734 - 2737.
Pittendrigh, C.S., Bruce, V.G., & Kaus, P. (1958). On the significance of transients in daily rhythms. *Proc Natl Acad Sci U S A, 44*, 965-973.
Pittendrigh, C.S., & Daan, S. (1976). A Functional Analysis of Circadian Pacemakers in Nocturnal Rodents IV. Entrainment: Pacemaker as Clock. *J. comp. Physiol., 106*, 291 - 331.
Porterfield, S.P., & Hendrich, C.E. (1993). The role of thyroid hormones in prenatal and neonatal neurological development--current perspectives. *Endocr Rev, 14*(1), 94-106.
Power, D.M., Llewellyn, L., Faustino, M., Nowell, M.A., Bjornsson, B.T., Einarsdottir, I.E., et al. (2001). Thyroid hormones in growth and development of fish. *Comp Biochem Physiol C Toxicol Pharmacol, 130*(4), 447-459.

Prat, F., Sumpter, J.P., & Tyler, C.R. (1996). Validation of radioimmunoassays for two salmon gonadotropins (GTH I and GTH II) and their plasma concentrations throughout the reproductivecycle in male and female rainbow trout (Oncorhynchus mykiss). *Biol Reprod, 54*(6), 1375-1382.

Randall, C.F., & Bromage, N.R. (1998). Photoperiodic history determines the reproductive response of rainbow trout to changes in daylength. *Comp. Physiol., 183*, 651–661.

Rao, S.D., Rao, P.D., & Peter, R.E. (1996). Growth hormone-releasing hormone immunoreactivity in the brain, pituitary, and pineal of the goldfish, Carassius auratus. *Gen Comp Endocrinol, 102*(2), 210-220.

Reiter, R.J. (1975). Changes in pituitary prolactin levels of female hamsters as a function of age, photoperiod, and pinealectomy. *Acta Endocrinol (Copenh), 79*(1), 43-50.

Reppert, S.M., Godson, C., Mahle, C.D., Weaver, D.R., Slaugenhaupt, S.A., & Gusella, J.F. (1995). Molecular characterization of a second melatonin receptor expressed in human retina and brain: the Mel1b melatonin receptor. *Proc Natl Acad Sci U S A, 92*(19), 8734-8738.

Reppert, S.M., Perlow, M.J., Ungerleider, L.G., Mishkin, M., Tamarkin, L., Orloff, D.G., et al. (1981). Effects of damage to the suprachiasmatic area of the anterior hypothalamus on the daily melatonin and cortisol rhythms in the rhesus monkey. *J Neurosci, 1*(12), 1414-1425.

Reppert, S.M., & Weaver, D.R. (2002). Coordination of circadian timing in mammals. *Nature, 418*(6901), 935-941.

Reppert, S.M., Weaver, D.R., & Ebisawa, T. (1994). Cloning and characterization of a mammalian melatonin receptor that mediates reproductive and circadian responses. *Neuron, 13*(5), 1177-1185.

Reppert, S.M., Weaver, D.R., & Godson, C. (1996). Melatonin receptors step into the light: cloning and classification of subtypes. *Trends Pharmacol Sci, 17*(3), 100-102.

Revel, F.G., Saboureau, M., Pevet, P., Mikkelsen, J.D., & Simonneaux, V. (2006). Melatonin regulates type 2 deiodinase gene expression in the Syrian hamster. *Endocrinology, 147*(10), 4680-4687.

Roche, J.F., Karsch, F.J., Foster, D.L., Takagi, S., & Dziuk, P.J. (1970). Effect of pinealectomy on estrus, ovulation and luteinizing hormone in ewes. *Biol Reprod, 2*(2), 251-254.

Rodriguez, E.M., Blazquez, J.L., Pastor, F.E., Pelaez, B., Pena, P., Peruzzo, B., et al. (2005). Hypothalamic tanycytes: a key component of brain-endocrine interaction. *Int Rev Cytol, 247*, 89-164.

Rodriguez, L., Carrillo, M., Sorbera, L.A., Zohar, Y., & Zanuy, S. (2004). Effects of photoperiod on pituitary levels of three forms of GnRH and reproductive hormones in the male European sea bass (Dicentrarchus labrax, L.) during testicular differentiation and first testicular recrudescence. *Gen Comp Endocrinol, 136*(1), 37-48.

Roff, D.A. (1983). An allocation model of growth and reproduction in fish. *Can. J. Fish. Aquat. Sci., 40*, 1395-1404.

Romer, A.S., & Parsons, T.S. (1977). *The Vertebrate Body*. Philadelphia, PA: Holt-Saunders International.
Rudeen, P.K., & Reiter, R.J. (1980). Influence of a skeleton photoperiod on reproductive organ atrophy in the male golden hamster. *J Reprod Fertil, 60*(2), 279-283.
Sam, S., & Frohman, L.A. (2008). Normal physiology of hypothalamic pituitary regulation. *Endocrinol Metab Clin North Am, 37*(1), 1-22.
Santos, C.R., Ingleton, P.M., Cavaco, J.E., Kelly, P.A., Edery, M., & Power, D.M. (2001). Cloning, characterization, and tissue distribution of prolactin receptor in the sea bream (Sparus aurata). *Gen Comp Endocrinol, 121*(1), 32-47.
Sauzet, S., Besseau, L., Herrera Perez, P., Coves, D., Chatain, B., Peyric, E., et al. (2008). Cloning and retinal expression of melatonin receptors in the European sea bass, Dicentrarchus labrax. *Gen Comp Endocrinol, 157*(2), 186-195.
Schuster, C., Gauer, F., Guerrero, H., Lakhdar-Ghazal, N., Pevet, P., & Masson-Pevet, M. (2000). Photic regulation of mt1 melatonin receptors in the Siberian hamster pars tuberalis and suprachiasmatic nuclei: involvement of the circadian clock and intergeniculate leaflet. *J Neuroendocrinol, 12*(3), 207-216.
Shao, Y.T., Arvidsson, M., Trombley, S., Schulz, R.W., Schmitz, M., & Borg, B. (2013). Androgen feedback effects on LH and FSH, and photoperiodic control of reproduction in male three-spined sticklebacks, Gasterosteus aculeatus. *Gen Comp Endocrinol, 182*, 16-23.
Sharp, P.J. (1996). Strategies in avian breeding cycle. *Animal Reproduction Science, 42*, 505-513.
Sharp, P.J., & Follett, B.K. (1969). The effect of hypothalamic lesions on gonadotrophin release in Japanese quail (Coturnix coturnix japonica). *Neuroendocrinology, 5*(3), 205-218.
Shi, Q., Ando, H., Coon, S.L., Sato, S., Ban, M., & Urano, A. (2004). Embryonic and post-embryonic expression of arylalkylamine N-acetyltransferase and melatonin receptor genes in the eye and brain of chum salmon (Oncorhynchus keta). *Gen Comp Endocrinol, 136*(3), 311-321.
Sisk, C.L., Richardson, H.N., Chappell, P.E., & Levine, J.E. (2001). In vivo gonadotropin-releasing hormone secretion in female rats during peripubertal development and on proestrus. *Endocrinology, 142*(7), 2929-2936.
Skliar, E.F., Amiragov, M.S., Bobe, L.S., Gavrilov, L.I., Kurochkin, M.G., Solntseva, D.P., et al. (2006). [Development of salt concentrates for mineralization of recycled water aboard the space station]. *Aviakosm Ekolog Med, 40*(4), 35-40.
Sohn, Y.C., Yoshiura, Y., Kobayashi, M., & Aida, K. (1999). Seasonal changes in mRNA levels of gonadotropin and thyrotropin subunits in the goldfish, Carassius auratus. *Gen Comp Endocrinol, 113*(3), 436-444.

Spence, R., Fatema, M.K., Ellis, S., Ahmed, Z.F., & Smith, C. (2007). The diet, growth and recruitment of wild zebrafish (Danio rerio) in Bangladesh. *Journal of Fish Biology, 71*, 304-309.

Spence, R., Gerlach, G., Lawrence, C., & Smith, C. (2008). The behaviour and ecology of the zebrafish, Danio rerio. *Biol Rev Camb Philos Soc, 83*(1), 13-34.

Sumova, A., Travnickova, Z., Peters, R., Schwartz, W.J., & Illnerova, H. (1995). The rat suprachiasmatic nucleus is a clock for all seasons. *Proc Natl Acad Sci U S A, 92*(17), 7754-7758.

Sundararaj, B.I., & Sehgal, A. (1970). Effects of a long or an increasing photoperiod on the initiation of ovarian recrudescence during the preparatory period in the catfish, Heteropneustes fossilis (Bloch). *Biol Reprod, 2*(3), 413-424.

Swanson, P., Bernard, M., Nozaki, M., Suzuki, H., Kawauchi, H., & Dickhoff, W.W. (1989). Gonadotropins I and II in juvenile coho salmon. *Fish Physiol. Biochem., 7*, 169-176.

Tagawa, M., & Brown, C.L. (2001). Entry of thyroid hormones into tilapia oocytes. *Comp Biochem Physiol B Biochem Mol Biol., 129*(2-3), 605 - 611.

Takahashi. (1995). Molecular neurobiology and genetics of circadian rhythms in mammals. *Annu Rev Neurosci, 18*, 531-553.

Takahashi, & Menaker, M. (1982). Role of the suprachiasmatic nuclei in the circadian system of the house sparrow, Passer domesticus. *J Neurosci, 2*(6), 815-828.

Takahashi, H. (1977). Juvenile hermaphroditism in the zebrafish, Brachydanio rerio. *Bull. Fac. Fish., 28*, 57 - 65.

Takahashi, J.S., DeCoursey, P.J., Bauman, L., & Menaker, M. (1984). Spectral sensitivity of a novel photoreceptive system mediating entrainment of mammalian circadian rhythms. *Nature, 308*(5955), 186-188.

Tamai, T.K., Young, L.C., & Whitmore, D. (2007). Light signaling to the zebrafish circadian clock by Cryptochrome 1a. *Proc Natl Acad Sci U S A, 104*(37), 14712-14717.

Taranger, G.L., Carrillo, M., Schulz, R.W., Fontaine, P., Zanuy, S., Felip, A., et al. (2010). Control of puberty in farmed fish. *Gen Comp Endocrinol, 165*(3), 483-515.

Taylor, J.F., North, B.P., Porter, M.J.R., Bromage, N.R., & Migaud, H. (2006). Photoperiod can be used to enhance growth and improve feeding efficiency in farmed rainbow trout, Oncorhynchus mykiss. *Aquaculture, 256*, 216–234.

Tello, J.A., Wu, S., Rivier, J.E., & Sherwood, N.M. (2008). Four functional GnRH receptors in zebrafish: analysis of structure, signaling, synteny and phylogeny. *Integr Comp Biol, 48*(5), 570-587.

Tse, D.L., Chow, B.K., Chan, C.B., Lee, L.T., & Cheng, C.H. (2000). Molecular cloning and expression studies of a prolactin receptor in goldfish (Carassius auratus). *Life Sci, 66*(7), 593-605.

Underwood, H. (1990). The pineal and melatonin: regulators of circadian function in lower vertebrates. *Experientia, 46*(1), 120-128.
Vallone, D., Gondi, S.B., Whitmore, D., & Foulkes, N.S. (2004). E-box function in a period gene repressed by light. *Proc Natl Acad Sci U S A, 101*(12), 4106-4111.
Van der Kraak, G., Rosenblum, P.M., & Peter, R.E. (1990). Growth hormone-dependent potentiation of gonadotropin-stimulated steroid production by ovarian follicles of the goldfish. *Gen Comp Endocrinol, 79*(2), 233-239.
Vatine, G., Vallone, D., Gothilf, Y., & Foulkes, N.S. (2011). It's time to swim! Zebrafish and the circadian clock. *FEBS Lett, 585*(10), 1485-1494.
Vaughan, J.M., Rivier, J., Spiess, J., Peng, C., Chang, J.P., Peter, R.E., et al. (1992). Isolation and characterization of hypothalamic growth-hormone releasing factor from common carp, Cyprinus carpio. *Neuroendocrinology, 56*(4), 539-549.
Vaz Nunes, M., & Saunders, D. (1999). Photoperiodic time measurement in insects: a review of clock models. *J Biol Rhythms, 14*(2), 84-104.
Watanabe, M., Yasuo, S., Watanabe, T., Yamamura, T., Nakao, N., Ebihara, S., et al. (2004). Photoperiodic regulation of type 2 deiodinase gene in Djungarian hamster: possible homologies between avian and mammalian photoperiodic regulation of reproduction. *Endocrinology, 4*, 1546 - 1549.
Wayne, N.L., Malpaux, B., & Karsch, F.J. (1988). How does melatonin code for day length in the ewe: duration of nocturnal melatonin release or coincidence of melatonin with a light-entrained sensitive period? *Biol Reprod, 39*(1), 66-75.
Weber, G.M., Powell, J.F., Park, M., Fischer, W.H., Craig, A.G., Rivier, J.E., et al. (1997). Evidence that gonadotropin-releasing hormone (GnRH) functions as a prolactin-releasing factor in a teleost fish (Oreochromis mossambicus) and primary structures for three native GnRH molecules. *J Endocrinol, 155*(1), 121-132.
Westerfield, M. (1995). *The zebrafish book : a guide for the laboratory use of zebrafish (Danio rerio)* (Ed. 3. ed.). Eugene, OR: M. Westerfield.
Whitmore, D., Foulkes, N.S., & Sassone-Corsi, P. (2000). Light acts directly on organs and cells in culture to set the vertebrate circadian clock. *Nature, 404*(6773), 87-91.
Whitmore, D., Foulkes, N.S., Strahle, U., & Sassone-Corsi, P. (1998a). Zebrafish Clock rhythmic expression reveals independent peripheral circadian oscillators. *Nat Neurosci, 1*(8), 701-707.
Whitmore, D., Sassone-Corsi, P., & Foulkes, N.S. (1998b). PASting together the mammalian clock. *Curr Opin Neurobiol, 8*(5), 635-641.
Wittbrodt, J., Shima, A., & Schartl, M. (2002). Medaka--a model organism from the far East. *Nat Rev Genet, 3*(1), 53-64.

Yamazaki, S., Numano, R., Abe, M., Hida, A., Takahashi, R., Ueda, M., et al. (2000). Resetting central and peripheral circadian oscillators in transgenic rats. *Science, 288*(5466), 682-685.

Yasuo, S., Watanabe, M., Iigo, M., Nakamura, T.J., Watanabe, T., Takagi, T., et al. (2006). Differential response of type 2 deiodinase gene expression to photoperiod between photoperiodic Fischer 344 and nonphotoperiodic Wistar rats. *Am J Physiol Regul Integr Comp Physiol*.

Yasuo, S., Watanabe, M., Nakao, N., Takagi, T., Follett, B.K., Ebihara, S., et al. (2005). The reciprocal switching of two thyroid hormone-activating and -inactivating enzyme genes is involved in the photoperiodic gonadal response of Japanese quail. *Endocrinology, 146*(6), 2551-2554.

Yasuo, S., Yoshimura, T., Ebihara, S., & Korf, H.W. (2007). Temporal dynamics of type 2 deiodinase expression after melatonin injections in Syrian hamsters. *Endocrinology, 148*(9), 4385-4392.

Yasuo, S., Yoshimura, T., Ebihara, S., & Korf, H.W. (2009). Melatonin transmits photoperiodic signals through the MT1 melatonin receptor. *J Neurosci, 29*(9), 2885-2889.

Yoshimura, T. (2010). Neuroendocrine mechanism of seasonal reproduction in birds and mammals. *Anim Sci J, 81*(4), 403-410.

Yoshimura, T., Yasuo, S., Watanabe, M., Iigo, M., Yamamura, T., Hirunagi, K., et al. (2003). Light-induced hormone conversion of T4 to T3 regulates photoperiodic response of gonads in birds. *Nature, 426*(6963), 178-181.

Zimmerman, N.H., & Menaker, M. (1979). The pineal gland: a pacemaker within the circadian system of the house sparrow. *Proc Natl Acad Sci U S A, 76*(2), 999-1003.

Zohar, Y., Elizur, A., Sherwood, N.M., Powell, J.F., Rivier, J.E., & Zmora, N. (1995). Gonadotropin-releasing activities of the three native forms of gonadotropin-releasing hormone present in the brain of gilthead seabream, Sparus aurata. *Gen Comp Endocrinol, 97*(3), 289-299.

Zohar, Y., Munoz-Cueto, J.A., Elizur, A., & Kah, O. (2010). Neuroendocrinology of reproduction in teleost fish. *Gen Comp Endocrinol, 165*(3), 438-455.